Papers of Ship Research Instute Vol.27 No.4 July 1990

Nonlinear Response of Moored Floating Structures in Random Waves and its Stochastic Analysis
Part 1. Theory and Model Experiments

Shunji KATO [1]
Takeshi KINOSHITA [2]

[1] Ship Research Institute
[2] Institute of Industrial Science of University of Tokyo

Contents

ABSTRACT

This paper deals with stochastic analysis of slow drift responses(forces and motions) of floating structures moored in random seas and their statistical predictions. First the study review for slow drift forces causing the slow drift motion is described, and four problems which must be solved in future are discussed. Second it is shown that nonlinear responses (total second order responses) including the slow drift responses can be represented by a two term Volterra functional series. Physical meanings of kernel functions in the functional series are investigated from a viewpoint of transfer functions(or frequency response functions). It is shown that the kernel functions can be estimated not only from bispectral analyses of experimental data but also by numerical calculations based on the potential theory. Furthermore on the basis of the mathematical fact that the second term in the Volterra functional series can be expressed by an equivalent linear process of instantaneous wave power in stochastic sense, new functional model is developed. This is based on the Wiener filter theory. This model is used to solve the problems excluded in the investigations obtained up to now. The problems are as folows: a) Hydrodynamic forces of slow drift motion in still water are modified in waves; b) Newman- Pinkster's approximation for slowly varying drift forces does not satisfy the condition of physical causality. Comparisons between simulated results and experimental ones have been conducted in both frequency and time domains. Main results are as follows: 1) Viscous drift force exists in addition to the drift force driven from the potential theory and it becomes significant compared with the potential drift force for large wave height. It is shown that the approximate method which takes into account the viscous drift force; 2) The hydrodynamic forces of slow drift motions are modified in waves and this phenomenon is caused not only by the wave drift damping (speed dependence of added resistance in waves) but also by increase of viscous damping force in waves. The ratio between the damping force in waves and that in still water was not more than 1.6 in the experiments which we carried out during this research project. But the problem why the hydrodynamic forces in still water are modified in waves remains completely unsolved; 3) It has been confirmed that the experimental and simulated results are in good agreement with each other provided we know how much the added mass and the damping forces in still water are modified in waves.

Finally a theory of probability density functions (p.d.f.'s) is developed for an instantaneous total second order response and its maxima, in order to predict 1/n th highest mean amplitudes and extreme statistics of total second order responses. New formula for the total second order p.d.f.'s which include not only quadratic but also linear responses are derived. These p.d.f.'s can be represented by the generalized Laguerre polynomials of which the first term is a Gamma p.d.f. consisting of three parameters. Assuming that the response and its time derivative processes are mutually independent, the 1/n th highest

mean amplitude can be evaluated numerically from the derivative of the instantaneous response p.d.f.. This method is first applied to the sway motions of moored floating semi-circular and rectangular two dimensional cylinders, and the applicability of the method is studied by comparisons with Naess' exact solution. The variation of the 1/n th highest mean amplitude of the total second order response is then investigated following increases in damping and restoring forces. And comparisons between the experimental results and the estimated ones obtained from the present theory are carried out. The applicability of the present theory has been confirmed. The results are as follows: 1) It is confirmed through comparisons with Naess' exact solution that the present method is an accurate approximation for pure second order responses(slow drift responses); 2) The p.d.f. of the total second order response differs from that of the pure second order response. In fact it becomes a widely-banded distribution with an increase in the damping coefficient. Additionally it significantly deviates from Gaussian p.d.f.; 3) It is confirmed that the usual prediction method based on the Longuet-Higgns' method significantly underestimates the measured results while the present method estimates them very well. And it is shown that the extreme response of the total second order response is greater than that based on the assumption of the pure second order response.

Chapter 1

Introduction

A floating city and a floating airport interest people more than before, and floating drilling rigs are forced to operate under severe environmental conditions. The accurate estimation of motions and wave forces acting on these structures is important for economical and safety design of these structures[1),2),3),4)]. For instance, an accurate motion prediction is required to evaluate the workability of the structure and the predictions of mooring forces and horizontal excursions are needed to design the safety mooring system. Since all of these responses are random variables, these evaluations must be conducted by extreme values of the responses. In order to obtain the extreme statistics of these random responses, instantaneous and peak probability density functions are required. If the probability density functions (p.d.f.'s) are obtained, short term and long term predictions of the responses of the structure become possible[5)].

There are two methods for obtaining peak p.d.f.'s[6)]. The one is deterministic, and the other is nondeterministic. For both methods, frequency response functions of exciting forces to incident waves and hydrodynamic forces (i.e. added mass and damping force coefficients) are required. In the case of ships, many studies have already been reported for these hydrodynamic problems. For example, there is the strip method[7),8)] as a popular calculation method, and detail investigations[9),10)] for the accuracy of the strip method have sufficiently been made. There is the three dimensional source distribution method[11)] to get an exact solution for ideal fluid flow. (But the validation is still required)

The deterministic manner is summarized as follows:

The wave force time history in random seas is obtained from the wave force frequency response function and the random wave time history and the motion time series is numerically calculated by solving a motion equation in time domain. By the statistical analysis of the motion time history, a histogram corresponding to a peak p.d.f. is obtained. The merits of this manner are that the motion time history can be obtained even if the motion equation is nonlinear and that the peak p.d.f. can be found out without calculating the motion fre-

quency response function. However since the statistical values obtained in this way are nothing but one sample in statistical sense, numerous calculations are required to get stable statistical values. Namely, in order to reduce a scatter of statistical values, it is necessary to get ensemble of sample statistical values obtained from many calculations of motion time histories. Even if the Ergodicity is assumed, statistical analysis of a motion time history with an infinite duration is required to get ensemble statistical values. Thus it is remarkably difficult to get ensemble statistical values by using the deterministic manner.

Another problem in the deterministic manner is a frequency dependency of hydrodynamic coefficients in the motion equation. Since the hydrodynamic coefficients of the motion equation is a function of wave frequencies in general, exactly speaking, the motion equation becomes a differential-integral equation. It is very difficult to solve the equation in time domain since the hydrodynamic coefficient in an infinite frequency is required.

While, on the nondeterministic manner, Cartwright and Longuet-Higgins[12] have shown that the peak p.d.f. for linear responses can be represented by a response variance and a band width parameter. Thus in the case of linear responses, the peak p.d.f. can be obtained analytically if a frequency response function is found out.

In the field of ship and ocean engineering, most responses can be regarded as linear, but some can not, of which nonlinear components become significant. Nonlinearities of wave excitations or a motion response functions to external forces should be considered. For floating offshore structures, it is usual that both nonlinear phenomena happen. As an example of the former phenomenon, wave drift forces in regular waves and slowly varying drift forces in irregular waves must be considered, and as an example of the latter viscous damping forces and mooring forces must be considered.

It has been considered that the slowly varying drift forces in irregular waves occur by the following reason:

Because of the nonlinearity of the wave drift force, the existence of two waves of different frequencies always implies the existence of wave excitations at the sum and difference frequencies. The latter frequency may occur near the resonance frequency of the floating structure moored in horizontal motions. And if the damping is low(as it is usually in such motions), a highly tuned resonance motion must be expected even though the low-frequency force is generally small in magnitude. Accordingly, the motion of a floating structure moored in irregular waves consists of sum of a slowly varying component and a component oscillating at wave frequencies. The spectrum of this time history has two peaks. The one peak occurs within the wave frequency range and the other occurs below the lowest frequency (close to resonance frequency) at which there is any significant energy in the incident waves. For the combined responses with a low and wave frequency components (i.e. total second order response), in general, maxima and minima are not equal, so the probabilities of them are different. Thus in order to analyze statistically such nonlinear responses, new approach is

required.

The application of probability theory to this problem was accomplished by Neal[13]. He assumed that a nonlinear response could be represented by a two term Volterra functional series, and he provided a closed form for a characteristic function(c.f.) of the response by using the Kac and Siegert method[14] (K-S method). According to K-S method, the problem of obtaining a c.f. for a random variable, which is represented by the sum of linear and quadratic forms of Gaussian random variables with mutual independence, can be reduced to a problem of solving eigenvalues and eigenfunctions of an integral equation. Since a probability density function (p.d.f.) of the response corresponds to an inverse Fourier transform of the c.f., Neal's method gives important information to estimate the p.d.f. of the nonlinear response to second order. This p.d.f., however, cannot be generally expressed in a closed form.

Naess[15),16),17] introduced a slow drift approximation and a pure quadratic response approximation to obtain the second order response p.d.f., and showed that the resulting eigenvalue problem generated a set of equal double eigenvalues. The p.d.f. of the response can be obtained by his approximations except when the equal double eigenvalues exist. Equal double eigenvalues may occur because a large number of eigenvalues are needed to describe a highly tuned response as shown by the authors et al[18]. Included are many nearly zero eigenvalues, thus caution is required. The Naess' method requires a pure quadratic response.

Vinje[19] assumed that the considered nonlinear response is weakly nonlinear and the p.d.f. is close to a Gaussian p.d.f., and he provided the series form of the p.d.f. from Taylor expansions of cumulants. His method is a kind of the approximate method called the Gram-Charlier expansion(or Edgeworth expansion).

Naess' method can be applied to obtain the instantaneous p.d.f. of the nonlinear response, but cannot be applied to get the peak p.d.f. while the Vinje's method can. In order to get the peak p.d.f. of the nonlinear response, a joint p.d.f. of response acceleration, velocity, and displacement is needed. But it is very difficult to exactly obtain this p.d.f. and some approximation is required. Hineno[20] applied the Vinje's method to the peak p.d.f. of nonlinear responses and obtained a series form(Hermite polynomial series). Recently Naess[21] developed the SRSS (Square Root form of Sum of Squares) method, which is the method that the extreme statistical values can be represented by the square root form of sum of squares of stochastic variables, and applied it to get the extreme response of the nonlinear response. But theoretical background is not clear.

Besides these studies, Yamanouchi[22] studied on nonlinear roll spectrum, and he investigated the relationship between the degree of nonlinearity and roll spectrum. And Roberts[23),24] obtained the approximate steady p.d.f.'s by means of Fokker-Planck equation method (or stochastic differential equation method). This is a promising method in future, but has the defects that the external force

is limited only to white noise and it is difficult to solve numerically because of infinite boundary conditions.

In this way, the consistent method to get the statistics of the nonlinear response has not yet been developed. As things are, the deterministic manner is the main current[25),26)]. As indicated earlier, this deterministic manner has many demerits, thus a new probability method may be required.

The objective of the present study is to develop a simulation model for total second order response of floating structures moored in random seas and its stochastic analysis method.

In Chapter 2, the study review for slow drift force(second order force) is described, and four problems which must be solved infuture are discussed. As the most important problem in them, the following problems are treated in this paper.

a) Hydrodynamic forces of slow drift motion in still water are modified in waves.

b) The Newman-Pinkster's approximation[25)] for the slowly varying drift force does not satisfy the condition of physical causality.

In Chapter 3, it is shown that the total second order force including slow drift forces can be represented by a two term Volterra functional series. Physical meanings of the kernel functions in the functional series are investigated from a viewpoint of frequency response functions (or transfer functions) and a method estimating the kernel ones from experimental data is also studied, which is the method using the bispectrum (a kind of higher order spectra). Furthermore a new functional model such that the second term of the Volterra functional series can be represented by the equivalent linear process of instantaneous wave power is developed. The new model is based on the Wiener filter theory[27)].

Several kinds of experiments have been carried out. Relation between the kernel function and the frequency response function of the slow drift force is investigated through comparisons between the experimetal results and numerical calculations. And the applicability of the present functional model is studied by comparing between the experimental data and numerical simulations. Furthermore the unsolved problems a)(i.e. how much the hydrodynamic forces in still water are modified in waves) and b) are investigated by using the new functional model.

The main results obtained in this Chapter are as follows:

(1) The kernel functions in the Volterra series correspond to the linear and quadratic transfer functions in frequency domain. The quadratic transfer function expresses a frequency characteristic of slowly varying drift force. The quadratic transfer function estimated by using the bispectral analysis from the experimental results does not agree with the numerical result based on the potential theory, viscous drift force exists in addition to the drift force due to the potential theory and it becomes more significant

than the potential drift force when the wave amplitude has a finite amplitude. If the viscous drift force is taken into account to the quadratic transfer function obtained from the numerical calculations even though it is approximately evaluated, the corrected numerical result is in good agreement with the experimental one.

(2) The hydrodynamic forces of slow drift motions are modified in waves. This phenomenon is caused not only by the wave drift damping proposed by Wichers et al.[28] and but also by increase of viscous damping force in waves newly suggested by the authors[29]. Recently other causes have also been found (e.g. one of the authors and Takaiwa[30]).

When the slow drift motion is dominant compared with the linear motion, the damping force at the slow drift motion increases by 1.6 times as large as one in still water whereas the added mass force becomes smaller than that in still water within limit of our experiment. However the problem how much and why the hydrodynamic forces in still water are modified in waves remains completely unsolved.

(3) Comparison between time domain simulations taking into account the viscous drift force in addition to the potential drift force and measured data is conducted. It has been confirmed that both results are in good agreement if we know how much the added mass and the damping forces in still water are modified in waves.

In Chapter 4, on the basis of the results obtained in Chapter 3 a theory of probability density functions(p.d.f.'s) is developed for an instantaneous total second order response and its maxima, in order to predict 1/n th highest mean amplitudes and extreme responses. New formulas for the total second order p.d.f.'s which include not only quadratic but also linear responses are derived. These new p.d.f.'s can be represented by the generalized Laguerre polynomials of which the first term is a Gamma p.d.f. consisting of three parameters. Assuming that the response and its time derivative processes are mutually independent, the 1/n th highest mean amplitude can be evaluated numerically from the derivative of the instantaneous response p.d.f.. This method is first applied to the sway motion of moored floating semi-circular and rectangular two dimensional cylinders, and the applicability of the method is studied by comparisons with Naess' exact solution. The variation of the 1/n th highest mean amplitude of the total second order response is then investigated following increases in damping and restoring forces. And comparisons between the experimental results in Chapter 3 and the calculated ones obtained from the present theory are carried out. The applicability of the present theory is confirmed.

The main results obtained in this Chapter are as follows:

(1) In the case of pure second order response (slow drift response) the instantaneous p.d.f. and the extreme responses estimated from the present method are in good agreement with the exact results shown by Naess.

(2) Using the present method, an investigation to determine the statistical interference between the first and second order responses was conducted for a system with a linear damping and a linear restoring forces. The p.d.f. of the total second order response differs from that of the pure second order response. In fact it becomes a widely-banded distribution with an increase in the damping coefficient. Additionally it significantly deviates from Gaussian p.d.f..

(3) As to the extreme response, comparison between the result obtained from the present method and one from the model test during long duration has been carried out. It is confirmed that the usual prediction method based on the Longuet-Higgins' method significantly underestimates the measured results while the present method estimates them very well. And it is shown that the extreme response of the total second order response is greater than that based on the assumption of the pure second order response.

REFERENCES IN INTRODUCTION

[1] American Bureau of Shipping: Rules for Building and Classing of mobile Offshore Drilling Units, 1968, 1973, and 1985 (ABS).

[2] Det norske Veritas : Rules for Classification of Mobile Offshore Units, 1985,(DNV).

[3] Lloyd's Register of Shipping : Rules and Regulations for the Classification of Mobile Offshore Units, 1984(LR).

[4] International Maritime Organization : Res A414(XI) Code for the Construction and Equipment of Mobile Offshore Drilling Units, 1979(IMO).

[5] Fukuda, J: Statistical estimations of responses, Symposium on Seakeeping, the Soc. of Nav. Archit. of Japan, 1969.

[6] Yamanouchi, Y: Responses in sea waves, Symposium on Seakeeping , ibid.

[7] Korvin-Krowkovsky, B.V. : Investigation of ship motions in regular waves, SNAME, 1955.

[8] Salvessen, N., Tuck, E.O., and Faltinsen, O. : Ship motions and sea loads, SNAME, vol.78, 1970.

[9] Seakeeping Committee : Comparison of Results Obtained with Computer Programs to Predict Ship Motions in Six Degrees of Freedom, Proc. 15th ITTC, 1978.

[10] Seakeeping Committee :Comparison of Results Obtained with Computer Programs to Predict Ship Motion in Six Degrees of Freedom and Associated Responses, Proc. 16th ITTC, 1981.

[11] Newman, J.N. : The Theory of Ship Motions, Adv. Appl. Mech., vol.18, 1978.

[12] Cartwright, D.E. and Longuet-Higgins, M.S.: The Statistical Distribution of the Maxima of a Random Function, Proc. of the Royal Society, vol.237, 1956.

[13] Neal, E. : Second-Order Hydrodynamic Forces Due to Stochastic Excitation, Proc. 10th ONR Symposium, Cambridge, Mass., 1974.

[14] Kac, M. and Siegert, A.J.F. : On the Theory of Noise in Radio Recievers with Square Law Detector, Jour. of Appl. Phys., vol.18, 1947.

[15] Naess, A.: Statistical Analysis of Second-Order Response of Marine Structures, Jour. of Ship Research, vol.29, 1985.

[16] Naess, A.: The Statistical Distribution of Second-Order Slowly-Varying Forces and Motions, Appl. Ocean Research, vol.8, 1986.

[17] Naess, A.: On the Statistical Analysis of Slow-Drift Forces and Motions of Floating Offshore Structure, 5th OMAE Symposium, vol.1, 1986.

[18] Kinoshita, T., Kato, S. and Takase, S.: Non-normality of Probability Density Function of Total Second Order Responses of Moored Vessels in Random Seas, J. Soc. Nav. Arch. Japan, vol.164, 1988.

[19] Vinje, T.: On the Calculation of Maxima of Nonlinear Waveforces and Wave Induced Motions, I.S.P., vol.23, 1976.

[20] Hineno, M.: The calculation of the Statistical Distribution of the Maxima of Nonlinear Responses in Irregular Waves, Jour. of the Soc. of Nav. Archit. of Japan, vol.156, 1984.

[21] Naess, A.: Prediction of extremes of combined first-order and slow-drift of offshore structures, Appl. Ocean Res., vol.11, No.2, 1989.

[22] Yamanouchi, Y. and Ohtsu, K.: On the non-linearity of Ship's Response and the Higher Order Spectrum - Application of the Bispectrum - , Jour. of the Soc. of Nav. Archit. of Japan, vol.131, 1972.

[23] Roberts, J.B.: Nonlinear Analysis of Slow Drift Oscillations of Moored Vessels in Random Seas, Jour. Ship Res., vol.25, 1981.

[24] Roberts, J.B.: A Stochastic Theory for Nonlinear Ship Rolling in Irregular Seas, J. S. R., vol.26, 1982.

[25] Pinkster, J.A. and Hujismans, R.H.M.: The Low Frequency Motion of a Semi-submersible in Waves, BOSS'82, 1982.

[26] Naess, A. and Hoft, J.R.: Time Simulation of the Dynamic Response of Heavily Listed Semi-submersible Platform in Seaways, Norwegian Maritime Research, 1984.

[27] Wiener, N.: Nonlinear Problems in Random Theory, M.I.T. Press and John Wiley & Sons, 1958.

[28] Wichers, J.E.W.: On the Low-Frequency Surge Motion of Vessels Moored in High Sea, OTC paper, No.4437, 1982.

[29] Kato, S. and Kinoshita, T.: On the Effect of Exciting Short Period Disturbance on Free and Forced Oscillation for the System with Nonlinear Damping, 36th Performance Subcommittee of Ocean Engineering Committee, the Soc. of Nav. Archit. of Japan, 1983.

[30] Kinoshita, T. and Takaiwa, K.: Slow Motion Forced Oscillation Test of Floating Body in Waves (2nd Report), J. Soc. Nav. Arch. Japan, No164.

Chapter 2

Review and some Problems of Second order forces

In this section, first we shall describe the state of the art of studies of the slowly varying second order forces. Second, we discuss some problems. The coordinates used in this section are shown in Fig.A.1 in Appendix A.

If the static restoring force by mooring lines is very small, a highly tuned resonance generally occurs at a very low natural frequency in horizontal plane for a moored floating structure. It is important in practice to predict the magnitude of the low frequency horizontal excursions of a platform and to ensure that they are kept within acceptable bounds. This is one of the most important hydrodynamic problems that must be solved in designing ocean platforms. This phenomenon was first reported by Verhagen and Sluijs[1]. They explained the phenomenon as:

Because of the nonlinearity of the free-surface conditions, the existence of two waves with different frequencies always implies the existence of waves at the sum and difference (beat) frequencies. The latter may occur near the resonance frequency of the moored platform in horizontal motion, i.e. sway, surge, or yaw motions. If the incident wave system consists of a continuous spectrum of waves, one is assured that there is always some disturbance at any very low frequency, and, if the damping is small (as it usually is in such motions), a highly tuned resonant motion must be expected.

On a basis of a physical investigation, Hsu and Blenkarn[2] suggested an estimation method of slowly varying nonlinear forces causing the slow drift motion as follows:

In any small time interval, consider the incident waves approximately as if they were simple sinusoidal waves, that is, fit the time history over a very short time interval by a sinusoidal curve with a specific amplitude and the period, and compute the steady force as if these sinusoidal waves existed for all time. At a

slightly later time, the waves will have changed, and so the process is repeated with a new sinusoidal wave of different amplitude and period, to which there corresponds a new value of the "*steady force*". And so on. In this way, a slowly varying second order force is predicted, its amplitude varying roughly with the square of the wave envelope.

This argument seems reasonable if the incident waves constitute a narrow band process.

Marthinsen[3] has recently provided a mathematical ground for the method of Hsu and Blenkarn. First, note that, if the incident wave system consists of a single frequency wave, the steady drift force can be expressed:

$$\overline{F}^{(2)} = F_d(\omega)a_1^2 \tag{2.1}$$

whereF_d is a transfer function that depends on the frequency of the primary wave(but not on its amplitude). and a_1 is a primary wave amplitude.

Now suppose that the incident waves contain many frequency components:

$$\zeta_1(x,t) = \sum a_i \cos(\omega_i t - \kappa_i x + \delta_i) \tag{2.2}$$

where a_i is the real amplitude and δ_i is an arbitrary phase constant.

He rewrites (2.2) in the following way:

$$\zeta_1(x,t) = \Re\{A(x,t)\exp[i(\omega_p t - \kappa_p x)]\} \tag{2.3}$$

where

$$A(x,t) = \sum a_i \exp\{i[(\omega_i - \omega_p)t - (\kappa_i - \kappa_p)x + \delta_i]\} \tag{2.4}$$

and ω_p is some frequency at or near the peak of the wave spectrum, with κ_p the corresponding wave number. The quantity $A(x,t)$ is clearly slowly varying in both space and time, if the wave spectrum is narrow banded. So by using a slowly varying function $a(x,t)$ can be represented as:

$$\zeta_1(x,t) = a(x,t)\cos(\omega_p t - \kappa_p x + \psi(x,t)) \tag{2.5}$$

where $a(x,t)$ is the slowly varying amplitude and ψ the slowly varying phase function. They are represented as:

$$\begin{aligned} a(x,t) \quad &= [(\sum a_i \cos\{(\omega_i - \omega_p)t - (\kappa_i - \kappa_p)x + \delta_i\})^2 \\ &+(\sum a_i \sin\{(\omega_i - \omega_p)t - (\kappa_i - \kappa_p)x + \delta_i\})^2]^{1/2} \end{aligned}$$

$$\psi(x,t) = \tan^{-1}[\frac{\sum a_i \sin\{(\omega_i - \omega_p)t - (\kappa_i - \kappa_p)x + \delta_i\}}{\sum a_i \cos\{(\omega_i - \omega_p)t - (\kappa_i - \kappa_p)x + \delta_i\}}]$$

If the **local frequency** ω_L and **local wave number** κ_L are introduced as

$$\omega_L = \omega_p + \frac{\partial \psi}{\partial t}$$
$$\kappa_L = \kappa_p - \frac{\partial \psi}{\partial t} \tag{2.6}$$

finally the following representation can be obtained.

$$F^{(2)}(t) = \overline{F}^{(2)} + \tilde{F}^{(2)}(t) = F_d(\omega_L) a^2(x_0, t) \tag{2.7}$$

where x_0 is a fixed point, which is typically the location of the centre of gravity of the body, or possibly just the origin of the coordinates used for analyzing the body motion. And $\tilde{F}^{(2)}$ is a slowly varying drift force.

Equation (2.7) represents essentially the method prescribed by Hsu and Blenkarn. This method is justified only if the wave spectrum is narrow banded. Because if the wave spectrum is of wide band, the concept of local frequency can no longer be used.

Robert[4] developed a formula like (2.7). His formula is $\omega_L = \omega_p$, i.e. $\psi_t = 0$. Marthinsen shows that this method gives valid results if $\frac{dF_d}{d\omega} \ll 1$, that is, the transfer function of steady drift force is flat for wave frequencies, and invalid results if $\frac{dF_d}{d\omega} \gg 1$.

Newman[5] followed a different formulation but derived a similar result. His approach has been used by many subsequent investigators. His argument is as follows:

Let the wave elevation at some x be represented by

$$\zeta_1(t) = \Re\{\sum a_i \exp(i\omega_i t)\} \tag{2.8}$$

where a_i is the complex wave amplitude of frequency ω_i. The first order force caused by these waves can be represented as:

$$F^{(1)}(t) = \Re\{\sum f_{1i} a_i \exp(i\omega_i t)\} \tag{2.9}$$

where $f_{1i} = f_1(\omega_i)$ is a first order transfer function relating force amplitude and phase to the wave amplitude and phase.

We expect that the second order force components will depend on the square of the wave amplitude. Thus, noting that the products of two wave components can be written:

$$\Re\{a_i \exp(i\omega_i t)\} \times \Re\{a_j \exp(i\omega_j t)\} =$$

$$\frac{1}{2}\Re\{a_i a_j \exp[i(\omega_i + \omega_j)t] + a_i a_j^* \exp[i(\omega_i - \omega_j)t]\}$$

where the asterisk denotes a complex conjugate.

The second order force components should then take the form:

$$F^{(2)}(t) = \Re\{\sum_i \sum_j f_{2ij}^{(+)} a_i a_j \exp[i(\omega_i + \omega_j)t]\}$$
$$+\Re\{\sum_i \sum_j f_{2ij}^{(-)} a_i a_j^* \exp[i(\omega_i - \omega_j)t]\} \tag{2.10}$$

The (+) and (−) notations distinguish between the second order transfer functions relating to the sum frequency and the difference frequency, respectively. We are interested only in the second order zero- and beat-frequency force, and so we neglect the first sum and delete the subscript 2 and (−) notation. So we have simply:

$$F^{(2)}(t) = \Re\{\sum_i \sum_j f_{ij} a_i a_j^* \exp[i(\omega_i - \omega_j)t]\} \tag{2.11}$$

Note that $f_{ij} = f_2(\omega_i, \omega_j)$. The time average of $\overline{F}^{(2)}$ is

$$\overline{F}^{(2)} = \Re\{\sum_i f_{ij} a_i a_j^*\} \tag{2.12}$$

Since $\overline{F}$ and the products $a_i a_j^*$ are real, $\Im f_{ii}$ is of no interest. Thus,

$$f_{ii} = F_d(\omega_i)$$

The coefficients, f_{ij} with $i = j$, are generally complex. Since the force expression in (2.11) does not depend on the choice of i and j (which are arbitrary), we require that

$$f_{ij} = f_{ji}^*$$

that is, the second order force matrix must be a Hermitian matrix. f_{ij} can be viewed as a surface in a three dimensional space with coordinates ω_i, ω_j, and f_{ij}. For each pair of frequencies, which define a point with coordinates (ω_i, ω_j) in the $\omega_i - \omega_j$ plane, the height of the surface is given by $\Re f_{ij}$ or by $\Im f_{ij}$. The height of the surface is known along the 45° line in the base plane: The real part is just f_{ii}, and the imaginary part is zero. Newman assumes that these surfaces are smooth and that their tangent planes make small angles with the base plane.

If this assumption is valid, then

$$f_{ij} = f_{ii} + O(\omega_i - \omega_j) \tag{2.13}$$

for frequency pairs lying near the 45° line.Then the off diagonal terms in f_{ij} can be approximated, the following formula is given for the slowly varying force

$$F^{(2)}(t) = \Re\{\sum_i \sum_j f_{ii} a_i a_j \exp[i(\omega_i - \omega_j)t]\}$$
$$\times\{1 + O(\omega_i - \omega_j)\} \quad as \quad \omega_i - \omega_j \to 0 \tag{2.14}$$

Triantafylou[6] has pointed out that the Newman's approximation might be valid unless the second order waves could be considered as shallow water waves.

Pinkster[7] has developed the same formula as Newman's. He indicated that if F_d can be represented by a linear function, f_{ij} in (2.11) can be approximated as:

$$f_{ij} = f_{\frac{i+j}{2},\frac{i+j}{2}}$$

And he gave a slow drift force spectrum in the following form:

$$S_F(\omega) = 2\rho^2 g^2 \int S_\zeta(\omega') S_\zeta(\omega' + \omega) F_d^2(\omega + \frac{\omega'}{2})\, d\omega' \tag{2.15}$$

where S_ζ is a incident wave spectrum. All of these analyses are approximate solutions.

Recently Pinkster[8),9)] and Ogilvie[10)] have shown the exact expressions for the second order forces and moments within the potential theory, those expressions were obtained based on the method of direct integration of fluid pressure acting on the instantaneous wetted surface of a body.

Their expressions of the second order force can be represented as the sum of the following components (see Appendix A):

(1) : Component caused by fluid pressure between mean and instantaneous wave surfaces:

$$\vec{F}_1^{(2)} = -\frac{\rho g}{2} \oint_C \vec{n}(\zeta_1 - \xi_{31} - y\xi_{41} + x\xi_{51})^2\, ds \tag{2.16}$$

(2) : Component due to quadratic pressure term in Bernoulli equation :

$$\vec{F}_2^{(2)} = \frac{\rho}{2} \iint_{S_m} \vec{n} \mid \nabla\varphi_1 \mid^2 dS \tag{2.17}$$

(3) : Component caused by variation of the acting point of fluid pressure:

$$\vec{F}_3^{(2)} = \rho \iint_{S_m} \vec{n}\{(\vec{\xi}^{(1)} + \vec{\alpha}^{(1)} \times \vec{x}) \cdot \nabla\varphi_{1t}\}\, dS \tag{2.18}$$

(4) : Component caused by variation of direction of first order wave force with respect to rotation of a body:

$$\vec{F}_4^{(2)} = \vec{\alpha}^{(1)} \times \vec{F}^{(1)} \tag{2.19}$$

(5) : Component due to second order potentials:

$$\vec{F}_5^{(2)} = \rho \iint_{S_m} \vec{n}(\varphi_{2t}^I + \varphi_{2t}^d)\, dS \tag{2.20}$$

where ζ_1 is the first order surface elevation, and $\vec{\alpha}^{(1)} = (\xi_{41}, \xi_{51}, \xi_{61})$, which is the first order rotational motion vector, and ξ_{31} is the first order heave motion In addition, there exists a term $\rho g A_{wp}(x_f \xi_{41} + y_f \xi_{51})$ in the vertical second order forces, which term is caused by the product of first order rotational motions.

If the instantaneous wave surface elevation is expressed by (2.8), the second order forces can be represented like (2.10). The components (1) through (4) are caused by the product of first order quantities, the component (5) is only caused by second order potentials, that is, it can be obtained only by solving the boundary value problem of second order potentials.

Although the Pinkster-Ogilvie theory has become popular, there are several problems that can not be determined by the theory. They are as follows:

[1] Contribution of second order potentials to the drift force

The component (5) depends on the second order velocity potential φ_2 , which is very difficult to compute. There are several different ways in which to approach this problem. For example, Lighthill[11] has shown that the second order force can be expressed wholly in terms of first order quantities by use of reciprocal relationships. His expressions, however, require the evaluation of an integral of second order pressures over the entire free surface, which is called a free surface integral. The amount of numerical work required to achieve this is likely to become vast unless some approximation will be found to represent an asymptotic behavior of second order potential away from the body. The purpose of evaluating this term is not to obtain an accurate prediction of slowly varying drift force but rather than to find out if the term is important.

Pinkster[9], Standing et al.[12], and Matsui[13] have obtained the following conclusion by evaluating the total slowly varying drift force without calculating the free surface integral.

The contribution of term (5) to the total slowly varying drift force can be negligible at high wave frequencies, at which the first order diffraction effect is significant, but it can be of great importance at low frequencies.

Faltinsen and Løken[14] formulated the problem precisely to second order, expressed the drift force in terms of first and second order potentials, and then used Green's theorem to eliminate the explicit dependence on the second order potentials. They obtained the same conclusion. They treated only the two

dimensional problem, but it certainly is possible that the same conclusion will be obtained in the three dimensional case.

However there is one case in which the second order potential may be important. It is the case that the second order waves may be shallow even though the first order waves are still deep water waves. It is possible for this phenomenon to occur, because the second order waves have the very low frequency component.

[2] Necessity of singular perturbation

One defect of the usual perturbation analysis (regular perturbation analysis) is that it is based on the assumption that motions of the structure are small compared with the dimensions of the structure itself. Since it is well known that the low frequency resonance response of a moored floating structure often involves very large horizontal excursions, then it is clear that this usual perturbation approach becomes invalid.

Triantafyllou[6] developed a mathematical model that involves only linear hydrodynamic problems, even while it permits large excursions of the platform in the horizontal plane. He used a kind of multi-scale expansion theory, and assumed that the motion response consists of two motions:

1) The one is the usual motion response to the incident waves; the amplitude, velocity, and acceleration are small, and considered to be $O(\varepsilon)$, where ε is the usual perturbation parameter.

2) The other is the low frequency motion having the velocity that is $O(\varepsilon)$, whereas its amplitude is $O(1)$.

If t is the time variable that is normally used, he used a new time variable, $t = \varepsilon t$, for analyzing the low frequency motion. Thus his method is a kind of derivative perturbation analysis, i.e. singular perturbation.

[3] Effect of wave drift damping etc.

It is observed that the damping force on a moored floating structure during low frequency motion in waves becomes greater than the one in still water. Wichers et al.[15),16)] explained that this phenomenon is caused by a kind of added damping force due to the drifting of a structure in waves. They called it **wave drift damping** in order to distinguish it from the linear radiation wave damping. The authors et al.[17] and Standing et al.[18)] examined a simple method , which is called "*drift force gradient method*", for approximating the additional damping due to the presence of waves, based on drift forces in regular waves at zero forward speed, using the analytical relationship between forward speed and wave encounter frequency together with wave frequency gradients of the drift forces. Wichers et al.[19)] proposed a different way using added resistance gradient and Hearn et al.[20)] computed by so called "*added resistance method*" that models the low frequency motion by steady forward speed of the structure

in the fluid structure interaction analysis. Hearn et al. concluded that the drift force gradient method seems to predict the correct trend but not the correct magnitude, and that the subject of theoretically predicting wave drift damping is not fully resolved and more research is required.

On the other hand , the authors[21] showed an increase of the decay of low frequency motion coupled with the wave induced motion due to the nonlinear viscous damping force (**nonlinear coupled viscous damping**). The explanation of this phenomenon is indicated in Appendix D.

Saito and Takagi[22] demonstrated from comparisons between simulations and model experiments that drift forces based on potential theory as well as the nonlinear coupled viscous damping have an influence on the increase of low frequency damping in sway motion. One of the authors and Takaiwa[23] showed that the increase of the viscous damping force due to waves is sometimes much larger than the nonlinear coupled viscous damping even taking off the wave drift damping for a semisubmersible and it depends on the ratio between wave particle velocity and motion velocity. They called it as **drag coefficient change due to waves.** Furthermore they indicated that the low frequency added mass in still water is also modified in waves. But theoretical backgrounds of these phenomena are still not clear yet.

[4] Physical causality of Newman approximation

In general, the slowly varying drift force can be represented by a Volterra system function, which will be stated in the next sections.

$$F^{(2)}(t) = \int_{\tau_1}\int_{\tau_2} g_2^f(\tau_1,\tau_2)\zeta(t-\tau_1)\zeta(t-\tau_2)\,d\tau_1\,d\tau_2 \tag{2.21}$$

where

$$g_2^f(\tau_1,\tau_2) = \frac{1}{4\pi^2}\int_{\omega_1}\int_{\omega_2} G_f^2(\omega_1,\omega_2)\exp\{i(\omega_1\tau_1+\omega_2\tau_2)\}\,d\omega_1\,d\omega_2 \tag{2.22}$$

As stated earlier, Newman[24] introduced the approximation for the quadratic transfer function G_2^f. His approximation is that $G_2^f(\omega_1,\omega_2)$ is estimated by its values along the diagonal $\omega_2 = -\omega_1$ as follows:

$$G_2^f(\omega_1,\omega_2) = \begin{cases} G_2^f(\omega_1,-\omega_1) & \text{as } \omega_1\cdot\omega_2 \le 0 \\ 0 & \text{otherwise} \end{cases} \tag{2.23}$$

then Eq.(2.22) becomes

$$g_2^f(\tau_1,\tau_2) = h_2^f(\tau_1)\delta(\tau_2) \tag{2.24}$$

where $\delta(\tau)$ is the Dirac's delta function and

$$h_2^f = \begin{cases} \frac{1}{2\pi}\int_\omega G_2^f(\omega,-\omega)\exp(i\omega\tau)\,d\omega \\ \frac{2}{\pi}\int_0^\infty \Re\{G_2^f(\omega,-\omega)\}\cos(\omega\tau)\,d\omega \\ \frac{2}{\pi}\int_0^\infty -\Im\{G_2^f(\omega,-\omega)\}\sin(\omega\tau)\,d\omega \quad \text{for } \tau \ge 0 \end{cases} \tag{2.25}$$

Substituting (2.24) into (2.21) yields:

$$F^{(2)}(t) = \zeta(t) \cdot \int_{\tau} h_2^f(\tau)\zeta(t-\tau)d\tau \tag{2.26}$$

and since $G_2^f(\omega, -\omega)$ represents the steady drift force, it must be real; i.e. $\Im\{G_2^f(\omega, -\omega)\} \equiv 0$. Eq.(2.26) means that $F^{(2)}(t)$ is approximately written as the product of two Gaussian random processes (which are not statistically independent). However, from (2.25) we must note that $h_2^f(t)$ does not satisfy the physical causality unless $G_2^f(\omega, -\omega)$ takes a constant value. It is physically inconsistent that $G_2^f(\omega, -\omega)$ is constant, i.e. the steady drift force does not depend on wave frequencies. This inconsistency is caused by the lack of the phase information of $G_2^f(\omega, -\omega)$.

In this way, there exist many problems which must be solved on the slow drift phenomenon. This paper treats the slowly varying drift force from a viewpoint of system functional theory in order to solve the problem of physical causality of Newman's approximation. Then there will be a discussion along this approach on the third problem, i.e. how the wave drift damping affects the slow drift motion can also be investigated by this approach. But we will not discuss on the first and second problems in this paper since they require lots of additional research.

REFERENCES IN CAPTER 2

[1] Verhagen, J.G.H., van Sluijs, M.F.: The Low Frequency Drifting Force on a Floating Body in Waves, I.S.P., vol.17, 1970.

[2] Hsu, F.H. and Blenkarn, K.A.: Analysis of Peak Mooring Forces caused by Slow Vessel Drift Oscillation in Random Waves, Proc. 2nd OTC, 1970.

[3] Marthinsen, T.: Calculation of Slowly Varying Drift Forces, Appl. Ocean Res., vol.5, 1983.

[4] Roberts, J.B.: Nonlinear Analysis of Slow Drift Oscillations of Moored Vessels in Random Seas, Jorn. Ship Res., vol.25, 1981.

[5] Newman, J.N.: Second-Oreder Slowly Varying Forces on Vessels in Irregular Waves, Proc. Internat. Symp. on Dynamics of Marine Vehicles and S tructures in Waves, Univ. Coll. London, 1974.

[6] Triantafylou, M.S.: A Cocsistent Hydrodynamic Theory for Moored and Positioned Vessels, Jour. Ship Res., vol.26, 1982.

[7] Pinkster, J.A.: Low Frequency Phenomena Associated with Vessels Moored at Sea, Soc. of Petroleum Engineers of AIME, SPE paper No.4837, 1974

[8] Pinkster, J.A.: Low Frequency Second Order Wave Exciting Forces on Floating Structures, Neth. Ship Model Basin Pub., No.650, 1980.

[9] Pinkster, J.A.: Low Frequency Second Order Wave Forces on Vessels Moored at Sea, Proc. 11th Symp. on Naval Hydrodynamics, Univ. Coll. London, 1976.

[10] Ogilvie, T.F.: Second Order Hydrodynamic Effects on Ocean Platforms, Proc. International Workshop on Ship and Platform Motions, 1983.

[11] Lighthill, J: Waves and Hydrodynamic Loading, Proc. Symp. on BOSS, Univ. Coll. London, 1979.

[12] Standing, R.G., Dacunha, N.M.C. and Matten, R.B.: Slow- Varying Second Order Wave Forces : Theory and Experiment, NMI R138, 1981.

[13] Matsui, T.: Analysis of Slowly Varying Wave Drift Forces on Compliant Structures, Proc. of 5th OMAE Symp. vol.1, 1986.

[14] Faltinsen, O.M. and Løken, A.E.: Slow Drift Oscillations of a Ship in Irregular Waves, Appl. Ocean Res., vol.1, 1979.

[15] Wichers, J.E.W. and van Sluijs, M.F.: The Influence of Waves on the Low-Frequency Hydrodynamic Coefficients of Moored Vessels, OTC paper, No.3625, 1979.

[16] Wichers, J.E.W.: On the Low-Frequency Surge Motion of Vessels Moored in High Sea, OTC paper, No.4437, 1982.

[17] Kinoshita, T., Takaiwa, K., Masuda, K. and Kato, W.: Performance of Multi-Body-Type Floating Breakwater, Proc. of 5th OMAE symposium, Tokyo, vol.1, 1986.

[18] Standing, R.G., Brendling, W.J. and Wilson, D.: Recent developments in the analysis of wave drift forces, low-frequency damping and response, Proc. OTC, Houston, 1987, Paper No. 5456.

[19] Wichers, J.E.W. and Huijsmans, R.M.H.: On the lowfrequency hydrodynamic damping forces acting on offshore moored vessels, OTC paper No.4813, 1984.

[20] Hearn, G.E. and Tong, K. C.: Added resistance gradient versus drift force gradient-based predictions of wave drift damping, Int. Shipbuilding Progress, 1988, vol.35, No.402.

[21] Kato, S. and Kinoshita, T.: On the Effect of Exciting Short Period Disturbance on Free and Forced Oscillation for the System with Nonlinear Damping, 36th Performance Subcommittee of Ocean Engineering Committee, the Soc. of Nav. Archit. of Japan,1983.

[22] Saito, K. and Takagi, M.: On the increased damping for a moored semisubmersible platform during low-frequency motions in waves, Proc. 7th Int. OMAE symp., ASME, Newyork, 1988, Vol.II.

[23] Kinoshita, T. and Takaiwa, K.: Slow Motion Forced Oscillation Test of Floating Body in Waves (2nd Report), J. Soc. Nav. Arch. Japan, No.164.

Chapter 3

Formulation of second order forces due to Volterra functional series and Application of Wiener's filter theory

3.1 Relationship between Volterra functional series and second order force system

Let $\vec{F}(t)$ denote the nonlinear total second order force vector of a floating structure to a random excitation $\{\zeta(t) \mid t \in R\}$. Since $\vec{\mathbf{F}}(t)$ is the response vector to the entire time history of $\zeta(t)$, we call $\vec{\mathbf{F}}(t)$ a functional vector defined on a class of excitation $\zeta(t)$ as

$$\vec{F}(t) = \vec{\mathbf{F}}[\zeta(t)] \tag{3.1}$$

If $\vec{\mathbf{F}}[\zeta(t)]$ is a continuous functional vector of $\zeta(t)$ in the function space sense, then $\vec{F}(t)$ can be expanded in a functional vector power series such that

$$\begin{aligned}\vec{F}(t) &= \vec{F}_0 + \int \vec{h}_1(t,t_1)\zeta(t_1)dt_1 + \cdots \\ &\quad + \int \cdots \int \vec{h}_n(t,t_1,\cdots,t_n)\zeta(t_1)\cdots\zeta(t_n)dt_1\cdots dt_n + \cdots\end{aligned} \tag{3.2}$$

If this series represents a causal physical system, then the kernel function vectors satisfy

$$\vec{h}_n(t, t_1, \cdots, t_n) = \vec{0} \qquad t_i > t \tag{3.3}$$

Series satisfying this property were studied by Volterra[1], and series of the form (3.1) that satisfy Eq.(3.3) are called Volterra functional vector series.

If the nonlinear system is time invariant, then kernel function vectors in Eq.(3.2) depend only on time difference. Thus,

$$\begin{aligned}\vec{F}(t) &= \vec{F}_0 + \int \vec{g}_1'(\tau)\zeta(t-\tau)d\tau + \cdots \\ &+ \int\int \vec{g}_2'(\tau_1, \tau_2)\zeta(t-\tau_1)\zeta(t-t_2)d\tau_1\tau_2 + \cdots\end{aligned} \tag{3.4}$$

where $\vec{F}_0$ is a constant vector. In general, the kernel function vectors in Eq.(3.4) may not be symmetric for their arguments. However, a permutation of indices in any kernel vectors only affects the order in which the integration is carried out but does not affect the response. Thus, for the purpose of analysis, symmetric kernel vector may be assumed without loss of generality; i.e.

$$\vec{g}_n(\tau_1, \tau_2, \cdots, \tau_n) = \frac{1}{n!}\sum_{[i]} \vec{g}_n'(\tau_{i1}, \cdots, \tau_{in}) \tag{3.5}$$

If the kernels are continuous and absolutely integrable and if the input is bounded and the contribution from terms of order n in Eq.(3.4) decreases to zero as $n \to \infty$, then it can be proved that the functional power series (3.4) converge uniformly.

We shall limit our analysis to excitation effects through second order and $\vec{F}_0 = 0$. Then Eq.(3.4) is truncated at n=2 and takes the following form:

$$\vec{F}(t) = \int \vec{g}_1^f(\tau)\zeta(t-\tau)d\tau + \int\int \vec{g}_2^f(\tau_1, \tau_2)\zeta(t-\tau_1)\zeta(t-\tau_2)d\tau_1 d\tau_2 \tag{3.6}$$

And we will treat the vector function as the scalar function hereinafter for simplicity. If $\zeta(t)$ is a wave excitation, this series can be used to analyze the response that is proportional to both the wave height and the squared wave height. There exist the time and spatial dependencies in the incident wave system. But since the wave system have a dispersivity, it is not necessary to consider the spatial dependency as indicated by Hasselmann[2] . It may also be mentioned that the adopted formulation is consistent with second order corrections to a linear wave field, in the sense that such corrections may be incorporated in Eq.(3.6) where $\zeta(t)$ then denotes the linear part of the wave field. Consequently, the assumption that $\zeta(t)$ is a linear, Gaussian wave process is consistent with the second order model in Eq.(3.6). If the kernels in Eq.(3.6)

are continuous and absolutely integrable, then the kernels possess the Fourier transform. The transform pairs are defined as follows:

$$\begin{aligned} g_1^f(t) &= \tfrac{1}{2\pi}\int_\tau G_2^f(\omega)\exp(i\omega\tau)d\omega \\ G_1^f(\omega) &= \int_\omega g_1^f(\tau)\exp(-i\omega\tau)d\tau \\ g_2^f(\tau_1,\tau_2) &= \tfrac{1}{4\pi^2}\int_{\omega_1}\int_{\omega_2} G_2^f(\omega_1,\omega_2)\exp\{i(\omega_1\tau_1+\omega_2\tau_2)\}d\omega_1 d\omega_2 \\ G_2^f(\omega_1,\omega_2) &= \int_{\tau_1}\int_{\tau_2} g_2^f(\tau_1,\tau_2)\exp\{-i(\omega_1\tau_1+\omega_2\tau_2)\}d\tau_1 d\tau_2 \end{aligned} \tag{3.7}$$

In Eq.(3.7) the kernel g_1^f is a linear impulse response function, and its transform, G_1^f, is a linear transfer function. The kernel g_2^f is analogous to the linear impulse response function and is called "*quadratic impulse response function*". Its transform, G_2^f, is called "*quadratic transfer function*". Since the kernel $g_2^f(\tau_1,\tau_2)$ can be assumed to be symmetrical in its arguments; i.e.

$$g_2^f(\tau_1,\tau_2) = g_2^f(\tau_2,\tau_1) \tag{3.8}$$

thus

$$G_2^f(\omega_1,\omega_2) = G_2^f(\omega_2,\omega_1) \tag{3.9}$$

Consequently, the quadratic transfer function is symmetrical about the line $\omega_1 = \omega_2$ in the (ω_1,ω_2) plane.

If $\zeta(t)$ is a Gaussian random wave with one-sided spectrum U, Rice[3] has shown that it is represented in the following stochastic integral:

$$\zeta(t) = \int \cos(\omega t - \mu(\omega))\sqrt{2U(\omega)d\omega} \tag{3.10}$$

where μ is a random phase distributed uniformly over 0° to 360°. This representation means the stochastic integral, and it converges in the sense of stochastic quadratic mean.

Substituting (3.10) into (3.6) we have:

$$F^{(1)}(t) = \int \cos(\omega t - \mu(\omega) + \theta_1(\omega))\sqrt{2\mid G_1^f(\omega)\mid^2 U(\omega)d\omega} \tag{3.11}$$

$$\begin{aligned} F^{(2)}(t) &= \iint \cos\{(\omega_1+\omega_2)t - (\mu(\omega_1)+\mu(\omega_2)) + \theta_2(\omega_1,\omega_2)\} \\ &\quad \times\sqrt{\mid G_2^f(\omega_1,\omega_2)\mid^2 U(\omega_1)U(\omega_2)d\omega_1 d\omega_2} \\ &\quad + \iint \cos\{(\omega_1-\omega_2)t - (\mu(\omega_1)-\mu(\omega_2)) + \theta_2(\omega_1,-\omega_2)\} \\ &\quad \times\sqrt{\mid G_2^f(\omega_1,-\omega_2)\mid^2 U(\omega_1)U(\omega_2)d\omega_1 d\omega_2} \end{aligned} \tag{3.12}$$

where

$$G_1^f(\omega) = \mid G_1^f(\omega) \mid \exp(i\theta_1(\omega))$$
$$G_2^f(\omega_1, \omega_2) = \mid G_2^f(\omega_1, \omega_2) \mid \exp\{i\theta(\omega_1, \omega_2)\}$$

It is clear that the first term on right hand side of (3.12) shows the sum component of second order force and the second term indicates the difference component. Taking the ensemble average of Eq.(3.12), and taking into account a statistical independence of the random phases, we get:

$$E[F^{(2)}] = \int G_2^f(\omega, -\omega) U(\omega) d\omega \tag{3.13}$$

While the time average of $\overline{F}^{(2)}(t)$ is represented in the following form:

$$\overline{F}^{(2)} = \sum_i F_d(\omega_i) \mid a_i \mid^2 \tag{3.14}$$

By using the relationship as;

$$a_i = \sqrt{2U(\omega_i)d\omega_i}$$

Eq.(3.14) can be expressed in the following integral:

$$\overline{F}^{(2)} = \int 2F_d(\omega) U(\omega) d\omega \tag{3.15}$$

If (3.13) is equal to (3.15), the following relationship holds:

$$G_2^f(\omega, -\omega) = 2F_d(\omega) \tag{3.16}$$

Similarly, from comparison between (3.12) and (2.11) the system function G_2^f can be related to the transfer function of slowly varying drift force like:

$$G_2^f(\omega_1, -\omega_2) = 2f_2(\omega_1, -\omega_2) \tag{3.17}$$

3.2 Application of Wiener's filter theory to slowly varying drift force

It is clear from (3.12) that the slowly varying drift force can be expressed by a quadratic form of random processes. So we expect that the quadratic impulse response function may reveal a kind of filter function in the field of communication engineering. Thus if the system considered is Ergodic, it is possible from the Wiener's theory to replace g_2^f by a optimum linear filter, i.e.:

$$F^{(2)}(t) = \int w_2(\tau) \zeta^2(t - \tau) d\tau \tag{3.18}$$

where w_2 is an optimum linear impulse response function.

The Wiener's theory[4] provides an optimum filter function w_2 under the following three conditions:

(1) The input process must be an Ergodic process and its spectral density can be resolved into factors.

(2) A criterion of error minimizes the least mean square of error.

(3) A filter function is linear and causal.

The criterion of error between the second term of Eq.(3.6) and Eq.(3.18), that is, J can be obtained from the conditions (1) and (3) as follows:

$$J = E[\{\iint g_2^f(\tau_1, \tau_2)\zeta(t-\tau_1)\zeta(t-\tau_2)d\tau_1 d\tau_2 - \int w_2(\tau)\zeta^2(t-\tau)dt\}^2] \quad (3.19)$$

The problem minimizes J in (3.19) with respect to an arbitrary function w_2, i.e. a kind of stationary value problems in calculus of variation.

Let $J[w_2]$ be a functional.

Now, assuming that w_2^0 is a function minimizing J, then the necessary condition for w_2^0 to be a optimum Wiener filter is given by:

$$\lim_{\varepsilon \to \infty} \frac{\partial J[w_2^0 + \varepsilon w_2]}{\partial \varepsilon} = 0 \quad (3.20)$$

This representation is equivalent to the following equation:

$$\int_{\tau_1}\int_{\tau_2} [R_\zeta(0)R_\zeta(\tau_2 - \tau_1) + 2R_\zeta(\tau - \tau_2)R_\zeta(\tau - \tau_2)]$$

$$\times\{g_2^f(\tau_1, \tau_2) - w_2(\tau_1)\delta(\tau_2 - \tau_1)\}d\tau_1 d\tau_2 = 0 \quad (3.21)$$

where R_ζ is the auto correlation function of $\zeta(t)$.

Thus we have:

$$g_2^f(\tau_1, \tau_2) = w_2(\tau_1)\delta(\tau_2 - \tau_1) \quad (3.22)$$

If the Fourier transform of w_2 is given by W_2, the following relation is satisfied.

$$G_2^f(\omega_1, \omega_2) = W_2(\omega_1 + \omega_2) \quad (3.23)$$

Multiplying the incident wave spectrum in both sides of (3.23) and integrating in frequency domain, a concrete form of W_2 is given by:

$$W_2(\omega) = \frac{1}{\sigma_\zeta^2}\int G_2^f(\omega - \omega', \omega')S_\zeta(\omega')d\omega' \quad (3.24)$$

Now, we assume that $G_2^f(\omega_i, -\omega_j)$ is smooth with respect to ω_i and ω_j and that $\frac{\partial G_2^f}{\partial \omega_j} = \upsilon G_2^f(\omega_i, -\omega_j), i \neq j$ and υ is any small quantity; that is, the tangent planes of $G_2^f(\omega_i, -\omega_j)$ makes small angles with $G_2^f(\omega_i, -\omega_j)$.

Triantafylou[5] has pointed out that this assumption is valid only for the case that the second order waves need not be considered as shallow water waves. If this is valid, then from Taylor expansion we get:

$$\frac{G_2^f(\omega-\omega',\omega')-G_2^f(\omega',-\omega')}{G_2^f(\omega',-\omega')} \sim \sum \frac{v^n}{n!}\omega^n \quad [\omega \to \infty]$$

From definition of asymptotic series

$$G_2^f(\omega-\omega',\omega') \sim G_2^f(\omega',-\omega')\cdot\vartheta(\omega) \quad [\omega \to \infty] \tag{3.25}$$

where $\vartheta(\omega)$ is a response function, of which amplitude exponentially decreases with an increase of ω. This expression is equivalent to the approximation suggested by Newman(see Eq.(2.13)).

Substituting (3.25) into (3.24) we get:

$$W_2(\omega) = \frac{\overline{F}^{(2)}}{\sigma_\zeta^2}\cdot\vartheta(\omega) \tag{3.26}$$

where $\overline{F}^{(2)}$ is the steady drift force in irregular waves (see Eq.(3.13)). Thus, the impulse response function can be expressed as:

$$w_2(\tau) = \frac{1}{2\pi\sigma_\zeta^2}\overline{F}^{(2)}\int\vartheta(\omega)\exp(i\omega\tau)d\tau \tag{3.27}$$

Taking into account that $\vartheta(\omega)$ is a exponential decaying function , it means that w_2 represents a low pass filter function. That is, we can generate the slowly varying drift force by passing $\frac{\overline{F}^{(2)}}{\sigma_\zeta^2}\cdot\zeta^2(t)$ through a low pass filter.

3.3 Estimation of transfer functions of first and second order forces

This section shows the method to estimate transfer functions of first and second order responses from experiments.

If a surface elevation $\zeta(t)$ is expressed by a Gaussian random process with zero mean, the cross correlation function between second order force F and ζ can be represented in the following form:

$$\begin{aligned} R_{F\zeta}(t) &= E[(F(t)-\overline{F})\zeta(t-\tau)] \\ &= \int g_1^f(t_1)R_\zeta(t_1-t)dt_1 \end{aligned} \tag{3.28}$$

And from Wiener-Khintchine relationship the cross spectrum is given by:

$$S_{F\zeta}(\omega) = G_1^f(\omega)S_\zeta(\omega) \tag{3.29}$$

where S_ζ is a two sided wave spectrum.

This result means that the cross spectrum involves only the first term of the functional polynomials, and the linear transfer function G_1^f is derived by standard cross spectral technique.

Next, we consider a third order moment function as follows:

$$R_{\zeta\zeta F}(\tau_1, \tau_2) = E[\zeta(t+\tau_1)\zeta(t-\tau_1)\{F(t-\tau_2) - \overline{F}\}] \tag{3.30}$$

Substituting (3.6) and taking into account of the symmetry of the quadratic impulse response function g_2^f, Eq.(3.30) becomes:

$$R_{\zeta\zeta F}(\tau_1, \tau_2) = 2\iint g_2^f(t_1, t_2) R_\zeta(t_1 + \tau_1 + \tau_2) R_\zeta(t_2 - \tau_1 + \tau_2) dt_1 dt_2 \tag{3.31}$$

And utilizing Parseval's formula, the representation in frequency domain is obtained in the following form:

$$R_{\zeta\zeta F}(\tau_1, \tau_2) = 2\iint G_2^{f*}(\omega_1, \omega_2) S_\zeta(\omega_1) S_\zeta(\omega_2) \times \exp[i\{(\omega_1 - \omega_2)\tau_1) + (\omega_1 + \omega_2)\tau_2\}] d\omega_1 d\omega_2 \tag{3.32}$$

Tick[6] has defined a cross bispectrum $C_{\zeta\zeta F}$ as a two dimensional Fourier transform of a third order moment function $R_{\zeta\zeta F}$ as follows:

$$R_{\zeta\zeta F}(\tau_1, \tau_2) = \iint \exp\{i(\Omega_1\tau_1 + \Omega_2\tau_2)\} C_{\zeta\zeta F}(\Omega_1, \Omega_2) d\Omega_1 d\Omega_2 \tag{3.33}$$

$$C_{\zeta\zeta F}(\Omega_1, \Omega_2) = \frac{1}{4\pi^2}\iint \exp\{-i(\Omega_1\tau_1 + \Omega_2\tau_2)\} R_{\zeta\zeta F}(\tau_1, \tau_2) d\tau_1 d\tau_2 \tag{3.34}$$

From (3.32) and (3.34) we can find the relationship between the cross bispectrum and the quadratic transfer function in the following form:

$$G_2^f(\omega_1, \omega_2) = \frac{C_{\zeta\zeta F}^*(\omega_1 - \omega_2, \omega_1 + \omega_2)}{S_\zeta(\omega_1) S_\zeta(\omega_2)} \tag{3.35}$$

The method for estimating the cross bispectrum by using experimental data is indicated in Appendix B.

3.4 Comparisons between experimental results and numerical simulations

3.4.1 Model tests

(1) Model

In the experiments an offshore floating structure model supported by twelve legs with footing was used. The configuration of the model and the direction

of incident waves are shown in Fig.3.1. The principal dimensions are indicated in Table 3.1. This is the 1/14.3 scale model of the structure used in the at-sea experiment being carried out in Yura port of Yamagata prefecture.

(2) Test set-up and Measuring items

The model experiments were carried out at the Mitaka No.2 Tank (Length is 400m, the breadth 18m, and the depth 8m) in Ship Research Institute. The model set-up is shown in Fig.3.2. As shown in this figure, the model was restrained by two soft springs through the device which restricted the yaw motion. The spring constant of them was 1.683 kg/m, (0.663 ton/m for the actual structure.).

The measured items are as follows:

(i) Surge and heave motion measured by a non-contact optical motion measuring system;

(ii) Pitch motion measured by a vertical gyroscope;

(iii) Surface elevation measured by a servo needle wave probe fixed at a position, the x coordinate of which is equal to that of the centre of gravity of the model in still water.

(3) Kinds and methods of model tests

(a) Free oscillation test in still water

The natural periods and equivalent damping coefficients in surge motion was obtained from this test. Two kinds of spring coefficients were used. The one was 1.683 kg/m, and the other 5.09 kg/m.

(b) Forced surge sinusoidal or random oscillation tests in still water

Forced surge sinusoidal oscillation tests were carried out at the range of 3.75 to 15 cm in amplitude, and the oscillation period of 17sec. The range corresponds to Keulegan-Carpenter numbers(K_c number) of 1.6 to 6.2. This test was done to study the dependence of the drag force to K_c numbers.

Irregular forced oscillation tests were made to compare with the results of the sinusoidal forced oscillation. Irregular signals for the forced oscillation tests were the surge response data recorded in the following test (d).

(c) Test for measuring steady drift force

Four kinds of tests in regular waves were carried out. Encounter angles of the tests are 0, 30, 60, and 90 degrees. The frequency range of the regular waves was from 3.0 to 9.8 rad/sec.

(d) Test for measuring a quadratic transfer function of surge motion

In order to experimentally obtain the quadratic transfer function of a moored floating structure, the estimation of the cross bispectrum between waves and responses is required as mentioned in the Chapter 2.2. Therefore, in order to generate irregular waves over long duration, the filtered signals were used, which we obtained by means of passing the white noise signals generated from a noise generator into band pass filters. The rolloff(cuttoff characteristics) of the band pass filters was 24db/oct.. Four kinds of irregular waves were generated. The central frequencies f of the band pass filter were 0.4, 0.5, 0.6 and 0.7 Hz. In the case of f equal to 0.7 Hz, the duration time of irregular waves was 90 minutes, and for the other cases it was 45 minutes. The encounter angle of these tests is only head sea.

3.4.2 Numerical calculation

(1) Method

Computation of the first order hydrodynamic forces was made by a program based on the three dimensional potential theory. In the computation the mean wetted surface of the body is approximated by 480 facets. The cpu time consumed to calculate the first order forces was about one hour on the FACOM M180 II AD computer. The steady and slowly varying drift forces were calculated by integrating pressure distributions over the wetted surface. The component due to second order potentials was not taken into account. The cpu time for calculation of drift forces was 10 minutes for the same computer.

(2) Check of numerical accuracy

In order to check the numerical accuracy of drift forces, computed results were compared with the Pinkster's. All of calculations were executed in double precisions. Comparisons between ours and Pinkster's are shown in Fig.3.3. In this figure black circles show the present results and broken and solid lines show Pinkster's results. The legends (1), 2), 3), 4)) denote components of steady drift force in Eqs.(2.16) through (2.19) and "total" means a sum of these components. There are a important points to note in this figure. The present calculations for the component 1) in the horizontal mean drift force are less than Pinkster's results. The other three terms and results of the vertical mean drift force agree very well. The component 1) is the largest and is opposite in sign to the components 2),3) and 4), whose sum is comparable in magnitude with the component 1). Thus, small percentage errors in term I give rise to larger percentage errors in the total drift force. The differences in the component 1) are also certainly due to the difference of the way modelling the waterline.

3.4.3 Hydrodynamic force characteristics of surge motion

(a) Free oscillation test in still water

An example of experimental results is shown in Fig.4. By using this data, a virtual mass and equivalent damping coefficient were obtained as follows:

Let x_n be sequential peak values(amplitudes) of damping curve. And It is assumed that the decaying motion can be represented by:

$$x = X_0 \exp[-\frac{N_{11}^e}{2(M_1 + m_{11})}] \sin(\frac{2\pi t}{T_0} + \Psi) \tag{3.36}$$

where T_0 is the natural period, $(M_1 + m_{11})$ the virtual mass, and N_{11}^e the equivalent linearized damping coefficient. Then if we plot $\mid x_{n+2} - x_{n+1} \mid$ as a function $\mid x_{n+1} - x_n \mid$ and the damping is constant, from Eq.(3.36) we get:

$$\mid x_{n+2} - x_{n+1} \mid = \exp[-\frac{N_{11}^e}{4(M_1 + m_{11})}] \mid x_{n+1} - x_n \mid \tag{3.37}$$

Thus by the least square method, the minimum error estimate of the inclination Θ can be obtained. The natural period T_0 is obtained from the mean of zero-upcrossing periods and zero-downcrossing periods. Then the virtual mass and equivalent damping coefficient are given by:

$$M_1 + m_{11} = \frac{T_0^2 C_{11}}{4\pi^2} \tag{3.38}$$

$$N_{11}^e = -\frac{T_0 C_{11} \log(\Theta)}{\pi^2} \tag{3.39}$$

where C_{11} is a restoring force coefficient.

The results obtained in this way are shown in Table 3.2. In order to apply this method, a large number of peak values is required and the motion equation must be linear. If the number of peak values is small, the accuracy of hydrodynamic force coefficients will become poor. So we must study whether the hydrodynamic coefficients obtained from Eqs.(3.38) and (3.39) have a good accuracy.

(b) Forced irregular oscillation test in still water

The forced irregular oscillation tests were carried out in still water by using the surge motion signals (including the slow drift motion) obtained from the motion measurement experiments in waves. This test was done to study the accuracy of the hydrodynamic force coefficients obtained from the free oscillation test. The hydrodynamic force coefficients by this test are given as follows:

Let S_{xF} be a cross-spectrum between the forced surge displacement x and the hydrodynamic reaction force F and S_x be a auto-spectrum of x. Then the hydrodynamic force coefficients can be obtained from the following equation.

$$C_{11} - (M_1 + m_{11}) = \Re\{\frac{S_{xF}(\omega)}{S_x(\omega)}\} \tag{3.40}$$

$$N_{11}^{e} = \Im\left\{\frac{\frac{S_{xF}(\omega)}{S_x(\omega)}}{\omega}\right\} \tag{3.41}$$

This method can be applied only to the case of linear motion equation. If the hydrodynamic forces in the motion equation are nonlinear, note that those coefficients obtained by this method express nothing but equivalent linearized coefficients. Comparison between the surge hydrodynamic coefficients obtained from the free oscillation test and ones from the irregular forced oscillation test is shown in Fig.3.6. The horizontal axis indicates the non-dimensional frequency $\hat{\omega} = \omega\sqrt{\frac{D}{g}}$, where D is the diameter of one column and ω is the surge motion frequency. In this figure white circles show the hydrodynamic coefficients obtained from the irregular forced oscillation test while black circle show those from the free oscillation test. The broken line indicates the numerical results calculated by the three dimensional source distribution method. The damping force coefficient is nondimensionalized by $\rho\nabla\sqrt{\frac{g}{D}}$.

The inertia coefficients obtained from the forced irregular oscillation test are distributed around the numerical values calculated by the three dimensional source distribution method while those from the free oscillation test agree well with the numerical values. The equivalent damping coefficients from the irregular forced oscillation test take negative value in some frequency range and distribute in the wide region from -0.1 to 0.2. Both results from the forced irregular oscillation test and the free oscillation test are in rough agreement. From this figure it is found that the inertia force in low frequencies can roughly be predicted from the three dimensional potential theory and the damping force can be obtained from the free oscillation test in still water. But in general, it is well known that the hydrodynamic forces depend on the magnitude of motion displacement. Thus in order to investigate the motion displacement dependency of hydrodynamic forces, the sinusoidal forced oscillation test was carried out. The motion amplitudes in this test were changed from 3.75 to 15cm, and the motion period was a constant period (17.5 sec., i.e. ω=0.0429). Results are shown in Fig.3.7. The horizontal axis is the Keulegan-Carpenter number (K_c number), which is defined by $2\pi X_0/D$ (where X_0 is the motion amplitude and D is the column diameter). The solid line indicates the results obtained from the free oscillation test, and the broken line shows the results calculated by using the three dimensional source distribution method. From this figure it is seen that the hydrodynamic forces acting on this structure do not depend much on the K_c number against our expectation. However one of the authors and Takaiwa[7] have conducted the forced and free damping tests for a tanker, a box-shape barge, and a semisubmersible, and they obtained the K_c number dependency of drag coefficients for theses structures. According to their results, the drag coefficients appear to be inverse proportional to K_c number in the range of small K_c number. This means that the equivalent damping coefficients do not depend on K_c number in this range of K_c number, but the further researches will be

required to examine this problem.

Within this experiment, inertia force coefficient $(1 + m_{11}/M_1)$ in low frequencies can roughly be estimated at 2.0, and the equivalent damping coefficient (N^e_{11}) is about 4.6 $kg \cdot sec/m$ (3.56 $ton \cdot sec/m$ in the prototype structure).

3.4.4 Frequency response functions of surge motion

The spectra of irregular waves generated in the experiments are shown in Fig.3.8. And the statistical values are indicated in Table 3.3. The Blackman-Tukey method was used in the spectral analysis. The number of lags was 256 and the Hamming window was used. The number of data taken for the analysis was about 35500 in the case of wave condition 4 and it was about 23000 in the other cases. The sampling interval was 120msec for the analysis and it was 60msec when the data were measured.

In order to get the quadratic transfer functions we need the cross bispectrum estimates as mentioned in Appendix B. The utilization of the Fast Fourier Transform have significant advantage to compute the full components of the cross bispectum. For present purpose however the full computation is not required, only results on or near the line $\omega_1 = \omega_2$ in bi-frequency plane are needed because our discussion concentrates upon slowly varying forces. Thus, we used the method developed by Dalzell[8] to estimate the cross bispectrum. The window function used in the computation of cross bispectrum was the Hamming type extended to two dimensions. The coefficients of the window function, i.e. e_1 and e_2 were 0.54 and 0.46 respectively.

For the spectral analysis based on the Blackman-Tukey method the maximum lag number must be less than 1/10 of sampling data. And Dalzell[8] showed that in order to get a stable cross bispectrum, the maximum lag number must be less than 1/200 or 1/250 of sampling data. Futhermore, as shown by Appendix B, if the lag number of the spectrum analysis is m, one of cross bispectrum analysis becomes m/2. In this case we decided that m was 256.

The auto spectra of surge motion are shown in Fig.3.9. The surge response in the case of wave condition 4 is the largest in the four wave conditions and low frequency motions are most dominant in the surge responses. The first order frequency response function, which is obtained from the cross spectra between the surge motion and waves, is shown in Fig.3.10. In the figure, the white circles indicate the experimental results. The solid line shows the theoretical value due to the usual linear motion prediction method which takes into account the viscous damping force obtained from the experiments(see Chapter 3.4.3). The experimental results and the linear theoretical curve are in good agreement.

3.4.5 Characteristics of steady drift force

The steady wave drift forces in wave direction are shown in Figs.3.11 through 3.14. In these figures, χ means a encounter angle to waves and circles indicate

the experimental results, where black circles are for the experimental results with the wave height higher than 7 cm and white circles are for ones with the wave height lower than that. The solid line shows the theoretical curve based on the potential theory and the dotted line shows the modified theoretical curve obtained by taking into account of the viscous drift force (this will be mentioned later) in addition to the potential theory. Fine lines indicate the results obtained from the experiment in irregular waves as follows:

As indicated in the previous section or Appendix B, if the cross bispectrum estimates between waves and second order forces can be directly obtained from the experiment in irregular waves, the frequency response characteristics of drift forces can be estimated with good accuracy. But it is difficult to measure the wave forces including the second order forces when the body is oscillating. Thus we adopted the indirect method instead of the direct measuring method of wave forces. First, we estimated the quadratic transfer function G_2 from the cross bispectrum between the surge motion and waves. Second, we determined the frequency characteristics of the steady drift force in irregular waves by the product between the diagonal components of G_2 and the spring constant. In these figures, the abscissa expresses the non-dimensional wave frequency $\hat{\omega}$, the vertical axis means the mean (steady) drift force coefficients in wave direction, those are normalized by $\frac{1}{2}\rho g\zeta_0^2 L$ (where L is the total length of the floating body and ζ_0 is the incident wave amplitude). And H/D is the ratio between the wave height and the diameter of column. When $H/D < 0.5$, that is, the wave height is less than half of the column diameter, the experimental results agree well with the theoretical line based on the potential theory. But, when H/D becomes larger than 0.5, both results are different considerably. As the cause of the difference, the following physical factors may be considered:

(a) Viscous drift force(surface force):

This occurs from the product of a wave force term, which is in proportion to a squared fluid velocity in the Morison equation, and a wave surface elevation. Chakravarti[9] and Standing[10] has reported that this force exists.

(b) Steady force due to other viscous drag force:

A vertical viscous drag force changes by angle of pitch motion. And its force produces the horizontal viscous force. Huse[11] expressed the horizontal steady viscous force as:

$$F_{vis} = - < C_{dZ}\, v_z \mid v_z \mid \xi_{51} > \tag{3.42}$$

where $< \cdot >$ denotes time mean value, v_z is a relative vertical velocity between a vertical wave particle velocity and a heaving velocity and ξ_{51} is the pitch motion and C_{dZ} is the vertical drag coefficient.

(c) Steady force due to mass transfer velocity of waves:

Stokes[12] has shown that the horizontal mean velocity in the direction of wave propagation occurs in the vicinity of wave surface and this phenomenon is caused by the nonlinearity of free surface condition. This velocity is in proportion to the squared wave height. If a steady drag force can be produced by the mass transfer velocity, it may be proportional to the fourth power of wave height.

(d) Drift force due to the second order potentials:

Standing and the others[10] has shown that the second order potential makes no contribution to the horizontal steady force or the steady turning moment. The absence of a steady drift force due to the second order wave can also be explained in physical terms. A steady force would imply the presence of a mean pressure gradient, which would in turn imply a steady acceleration throuout the fluid. This is not possible in the horizontal steady state situation.

In the four factors, we need not consider (d) because the drift force due to the second order potential does not produce a steady force.

Figure 3.15 a) shows the variation of steady drift force coefficient vs. the wave height at the wave frequency ω equal to 4.387 rad/sec(1.16 rad/sec in actual structure, and 0.5254 in the non-dimensional frequency). And Fig. 3.15 b) shows it for each wave frequencies. It is clear from these figures that the steady drift force coefficient linearly increases with an increase of the wave height when H/D is greater than 0.5. This means that the steady drift force is proportional to the third power of wave height when $H/D > 0.5$. Thus the factor (c) is not considered. If the factor (b) is significant, the steady drift force component (4) represented by Eq.(2.19) must also be significant. Because since the first order wave force in the vertical direction includes the force component proportional to the vertical velocity v_y, the component (4), in natural, becomes large when the factor (b) is dominant compared with other factors. Thus, we studied the contribution ratio of each steady drift force components ((1) to (4)) to the total steady drift force by numerical calculations. Figure 3.16 shows the results.

As found from the figure, for this structure, the force components (1) and (2) are dominant compared with other components, that is, the contribution of the force components (3) and (4) to the total force is very small compared with the force components (1) and (2). Accordingly, also the factor (b) is not dominant. Finally the phenomenon, which the steady drift force is proportional to the third power of wave height in some frequency range, is caused by the viscous drift force or surface (drift) force.

Since it is very difficult to strictly evaluate this force, we shall study the force on a simple vertical circular cylinder within the linear wave theory. This investigation is referred to Appendix C. This viscous drift force has the following characteristics.

(1) The viscous drift force is in proportion to the third power of wave height and it is expressed by the product of the horizontal drag force in the Morison equation and the instantaneous wave surface elevation. And if the drag force can equivalently be linearized, the viscous drift force can also be represented by the second term in the Volterra functional power series.

(2) The slowly varying viscous drift force increases with increasing the mean wave frequency of two different wave components.

(3) The viscous drift force does not depend on the draft but the ratio between the wave height and the diameter of the cylinder.

The second result shows that the slowly varying drift force including the viscous drift force can be expressed by the second term of the Volterra functional series. But in order to strictly deal with the viscous drift force, it is necessary to take into account the interaction between viscous and potential flows, furthermore we must consider the problems of diffraction and memory effects in the Morison equation.

For simplicity, we applied the Standing's method to estimate the viscous drift force acting on the structure considered.

Standing[9] has shown the relation between the steady viscous drift force and the potential drift force on a fixed vertical circular cylinder, resting on the sea-bed and piercing the free surface as follows:

$$R = \left\{ \frac{\frac{H}{D}}{2\pi^3 \frac{D}{\lambda}^2 C_d} \right\} \tag{3.43}$$

where D is a diameter of the cylinder, H the wave height, λ the wave length and C_d the drag coefficient.

Figure 3.17 shows the contribution rate of viscous and potential components to the steady drift force. The dotted line indicates a wave breaking limit. White circles are the experimental results and the solid line shows the curve of R equal to 1 , i.e., the viscous steady drift force is equal to the potential steady drift force, when $C_d = 1$. It is clear that the viscous steady drift force is larger than the potential one when $H/D > 0.5$. Thus if the ratio of the viscous drift force to the potential one is high, we must take into account the viscous drift force as follows:

$$\tilde{F}_d = (1 + R)F_d \tag{3.44}$$

where F_d is the potential steady drift force and $\tilde{F}_d$ is the steady drift force corrected by viscous effect, i.e., the steady drift force including both the viscous and potential drift forces.

In the case of experiments in irregular waves, H is replaced by half of the significant wave height and C_d is 0.5. The drag coefficient was obtained from a result of the towing test. $\tilde{F}_d$ is shown by the thick dotted line in Fig.3.17. From this figure it is found that the estimate of the steady drift force corrected by viscous effect agrees with the experimental results.

3.4.6 Characteristics of slowly varying drift force

Numerical contours of real and imaginary parts of slowly varying drift force f_{ij} are shown as a function of two variables ω_i and ω_j in Fig.3.18. The variables $\hat{\omega}_i$ and $\hat{f}_{ij}$ are normalized by:

$$\hat{\omega}_i = \omega_i \sqrt{\frac{D}{g}} \tag{3.45}$$

$$\hat{f}_{ij} = \frac{f_{ij}}{\frac{1}{2}\rho g \mid a_i \mid\mid a_j \mid L} \tag{3.46}$$

where a_i and a_j are amplitudes of two different waves respectively.

It is found from this figure that the real part of $\hat{f}_{ij}$ has the peak in the vicinity of $(\hat{\omega}_i, \hat{\omega}_j) = (0.806, 0.806)$, but it is flat except in the the vicinity, and that the imaginary part is also flat along the line $\hat{\omega}_i = \hat{\omega}_j$. This result may infer that the Newman approximation can be applied to this model.

Comparison between the numerical and experimental results with respect to the slowly varying drift force is shown in Fig.3.19. The left side indicates the amplitude of quadratic transfer function of slowly varying drift force and the right side does the phase of it. The thin dotted lines are the experimental results in irregular waves(those results are obtained from the cross bispectrum analysis), the solid line is the numerical results based on the potential theory, the dash-dotted line obtained from applying the Newman approximation to the numerical results, and the broken line the results obtained from the applying the Newman approximation to the numerical values corrected by the viscous effect; i.e. the values estimated by Eq.(3.44). And $\Delta\omega$ indicates the difference of two different wave frequencies and the horizontal axis is the mean frequency of them.

Although the slowly varying drift force may directly be obtained from the experiment, we indirectly obtained the force in the following way.

Using the quadratic transfer function of surge motion, G_2 (which is obtained from cross bispectral analysis of the experimental data) and the transfer function of surge motion to the external force, H_L (which is obtained from the free oscillation test in still water), the quadratic transfer function of the slowly varying drift force G_2^f can indirectly be obtained by the following relation:

$$G_2^f(\omega_1, -\omega_2) = \frac{G_2(\omega_1, -\omega_2)}{H_L(\omega_1 - \omega_2)} \tag{3.47}$$

where

$$H_L(\omega) = \frac{1}{C_{11} - (M + m_{11})\omega^2 + iN_{11}^e\omega} \tag{3.48}$$

and we assume that the hydrodynamic force coefficients of Eq.(3.48) do not change in waves.

From this figure the numerical value based on the potential theory is much lower than the experimental results, but the former has the same tendency as the latter. Comparisons of the solid and dash-dotted lines reveal that the Newman approximation can be applied in this case. And the broken line, i.e. the numerical results corrected by taking into account the viscous effect, agrees with the experimental results. This means that in order to estimate the slow drift motion of the floating structure supported by many legs with small diameter, we should take into account not only the potential drift force but also the viscous one.

3.4.7 Variation of hydrodynamic force coefficients of slow drift motion in waves

In the section 2.1, we state that the damping coefficient of slow drift motion in waves is different from one in still water. In this section we shall investigate if such phenomenon occurs in the following way.

First, let G_2, G_2^f and H_L be the quadratic transfer function of surge motion, the quadratic transfer function of slowly varying drift force and the transfer function of surge motion to external force, respectively. Let them hold the relationship of Eq.(3.47). And we shall introduce the transfer function of slow drift motion to instantaneous wave power, $\Xi(\omega)$, given by :

$$\begin{aligned}\Xi(\omega) &= \frac{S_{x\zeta^2}}{S_{\zeta^2}(\omega)} \\ &= \frac{\int_{\omega'} S_\zeta(\omega-\omega')S_\zeta(\omega')G_2^*(\omega-\omega',\omega')d\omega'}{\int_{\omega'} S_\zeta(\omega-\omega')S_\zeta(\omega')d\omega'}\end{aligned} \tag{3.49}$$

where $S_{x\zeta^2}$ is the cross spectrum between the surge motion x and instantaneous wave power ζ^2, and S_{ζ^2} the auto spectrum of ζ^2. Then from Eqs.(3.23) and (3.47), the following relation is satisfied:

$$\Xi^*(\omega) = H_L(\omega)W_2(\omega) \tag{3.50}$$

Thus, if the Newman approximation can be applied, the non-dimensional transfer function of surge motion to external force, $\overline{H}_L$ can be obtained by:

$$\overline{H}_L(\omega) = \frac{\Xi^*(\omega)}{\Xi(0)} \tag{3.51}$$

Comparison between $\overline{H}_L$ obtained from Eq.(3.51) and $\tilde{H}_L(= C_{11}\cdot H_L)$ obtained from Eq.(3.48) is shown in Fig.3.20. In the figure the thin lines are the results of $\overline{H}_L$ and the solid line is the result of $\tilde{H}_L$, where the value $\Xi(0)(= H_L(0)\cdot W_2(0))$

in Eq.(3.51) is estimated from (3.26) as follows:

$$\Xi(0) = \frac{\overline{F}^{(2)}}{C_{11}\sigma_\zeta^2} \tag{3.52}$$

From this figure, $\overline{H}_L$ is in good agreement with $\tilde{H}_L$ in case of wave condition 1, but in other cases, the peak frequency of $\overline{H}_L$ moves towards the low frequency side and the peak value becomes small when the peak frequency of wave spectrum becomes high, as compared with $\tilde{H}_L$. Namely, this means that when the peak frequency of wave spectrum becomes high, the damping coefficient of slow drift motion in waves becomes bigger than one in still water. In order to examine an increase rate in the damping coefficient, we got the hydrodynamic coefficients by means of the least square method from Eq.(3.52), under the assumption that $\overline{H}_L$ is equivalent to Eq.(3.48). These results are shown in Table 3.5. Obviously, the phenomenon that the damping force in waves becomes larger than one in still water occurs. The amount is $1.6 \sim 1.7$ times the damping force in still water. Furthermore the virtual mass in waves decreases 10 % of one in still water.

3.4.8 Time domain simulation

(1) Surge motion equation in time domain and its solution

If the added mass and the damping forces of slow drift motion in still water do not change in waves and the coupling terms are neglected, a surge motion equation of the floating body moored by linear springs may be represented in time domain as follows:

$$(M_1 + m_{11}(\infty))\ddot{X}_1 + \int_{-\infty}^{t} K_{11}(t-\tau)\dot{X}_1 d\tau + a_{11}(\dot{X}_1, \dot{\zeta}; t) + C_{11}X_1$$

$$= F^{(1)}(t) + F^{(2)}(t) \tag{3.53}$$

where

M_1 ; mass
$m_{11}(\infty)$; added mass at $\omega = \infty$
a_{11} ; viscous damping force
C_{11} ; restoring force coefficient
K_{11} ; memory effect function
$F^{(1)}$; first order force
$F^{(2)}$; second order force

Moving all terms in Eq.(3.53) except for inertia terms to the right hand side, Eq.(3.53) becomes equivalent to the Newton equation as:

$$M_1\ddot{X}_1 \quad = -m_{11}(\infty)\ddot{X}_1 - \int_{-\infty}^{t} K_{11}(t-\tau)\dot{X}_1 d\tau - a_{11}(\dot{X}_1, \dot{\zeta}; t) - C_{11}X_1$$

$$+F^{(1)}(t)+F^{(2)}(t) \tag{3.54}$$

Then we can numerically solve the above equation in time domain if the viscous damping force is known. In order to solve Eq.(3.54) in time domain, we used the Newmark-β method[14]. According to the Newmark-β method, when a surge motion at a time t_n is expressed by X_1^n, X_1^{n+1} at $t_{n+1}=t_n+\Delta t$ can be represented as follows:

$$X_1^{n+1}=X_1^n+\Delta t\dot{X}_1^n+\frac{\Delta t^2}{2}\ddot{X}_1^n+\beta\Delta t^2(\ddot{X}_n^{n+1}-\ddot{X}_1^n) \tag{3.55}$$

$$\dot{X}_1^{n+1}=\dot{X}_1^n+\frac{\Delta}{2}(\ddot{X}_1^{n+1}+\ddot{X}_1^n) \tag{3.56}$$

After iterations, the motion equation, that is, Eq.(3.54) can be solved in time domain, where we use $1/4$ as a value of β. When this value is used, it is mathematically proven that the solution is absolutely stable.

The judgement of convergence was conducted under the following condition:

$$\left|\frac{\ddot{X}_{1,m}^{n+1}-\ddot{X}_{1,m}^n}{\ddot{X}_{1,m}^{n+1}}\right|\leq\frac{1}{100} \tag{3.57}$$

where the subscript m denotes the iteration number.

(2) Hydrodynamic force in time domain

From the Fourier transform to the first two terms in the left hand side of Eq.(3.53), the following relations are given;

$$m_{11}(\omega)=m_{11}(\infty)-\frac{1}{\omega}\int_0^\infty K_{11}(t)\sin\omega t dt \tag{3.58}$$

$$N_{11}^{(1)}(\omega)=\int_0^\infty K_{11}(t)\cos\omega t dt \tag{3.59}$$

where

$m_{11}(\omega)$; added mass in frequency domain
$N_{11}^{(1)}(\omega)$; radiation wave damping in frequency domain

Then if the added mass and the radiation wave damping force over infinite range are given, the hydrodynamic forces in time domain, i.e. $m_{11}(\infty)$ and $K_{11}(t)$, can be obtained from the relations (3.58) and (3.59). But this procedure is not easy, because it is impossible to get the frequency-domain hydrodynamic force numerically over infinite range. Thus we extrapolate $N_{11}^{(1)}(\omega)$, which is obtained in some frequency range, by using the spline function, get the frequency

point ω_0 that the extrapolated value becomes zero, and calculate the following integral over $\omega_0 \geq \omega \geq 0$.

$$K_{11}(t) = \frac{2}{\pi}\int_0^{\omega_0} N_{11}^{(1)}(\omega)\cos\omega t d\omega \tag{3.60}$$

We will check the accuracy of the above numerical approximation later.

(3) Viscous hydrodynamic force

In order to get the viscous hydrodynamic damping forces, one divides wetted surfaces of a floating body into several blocks, and obtaines the viscous damping force from integrating the viscous drag acting on the centre of projection area of all blocks: That is

$$a_{11} = N_{11}^{(2)}\dot{X}_1 \mid \dot{X}_1 \mid \tag{3.61}$$

$$N_{11}^{(2)} = \frac{1}{2}\rho\iint_S n_1 C_d dS \tag{3.62}$$

In this paper, for simplicity, the viscous drag force was determined by the following equivalent linearized form:

$$a_{11} = N_{11}^{e}\dot{X}_1 \tag{3.63}$$

where the experimental value shown in the section 3.4.3 was used as the value of N_{11}^{e} in this case.

(4) Wave force

(a) First order force

According to the linear system theory in the field of communication theory, the first order wave excitation acting on a floating body can be represented as;

$$F^{(1)}(t) = \int g_1^f(t)\zeta(t-\tau)d\tau \tag{3.64}$$

where g_1^f is a impulse response function of first order wave excitation, and its Fourier transform , i.e. frequency response function, becomes as:

$$g_1^f(\tau) = \frac{1}{2\pi}\int G_1^f(\omega)\exp(i\omega t)d\omega \tag{3.65}$$

If the wave spectrum shape $U(\omega)$ is known, Rice has shown that the first order wave excitation can be represented by the following stochastic integral form:

$$F^{(1)}(t) = \int \mid G_1^f(\omega) \mid \cos(\omega t + \mu(\omega) - arg(G_1^f(\omega)))\sqrt{2U(\omega)d\omega} \tag{3.66}$$

Note that the Rice's representation does not depend on the initial value, i.e. it is a stochastic integral representation, and it is not a physical causal system.

(b) Steady and slowly varying drift forces

Using the system function w_2 defined in Eq.(3.18), the slowly varying drift force including the steady drift force can be represented as:

$$F^{(2)}(t) = \int w_2(\tau)\zeta^2(t-\tau)d\tau \tag{3.67}$$

where

$$w_2(\tau) = \frac{1}{2\pi}\int W_2(\omega)\exp(i\omega\tau)d\omega \tag{3.68}$$

and

$$W_2(\omega) = \frac{1}{\sigma_\zeta^2}\int G_2^f(\omega-\omega',\omega')S_\zeta(\omega')d\omega' \tag{3.69}$$

If $G_2^f(\omega_i,\omega_j)$ is smooth enough for ω_i and ω_j and $\frac{\partial G_2^f}{\partial \omega_i}$ and $\frac{\partial G_2^f}{\partial \omega_j}$ are small, we can generate the slowly varying drift force by passing $\frac{\overline{F^{(2)}}}{\sigma_\zeta^2}\cdot\zeta^2(t)$ into a low pass filter, as shown in the section 3.2.

(5) Comparison between simulation results and experimental ones

Before doing the simulation we investigated that the assumption (3.60) can be applied. Takagi and Saito[15] has shown theoretically an asymptotic behaviour of the memory effect functions for a half submerged sphere. Comparisons between their results and the calculated results due to Eq.(3.60) are shown in Fig.3.21. It is found from this figure that both results are in agreement although a slight deformation is observed to the calculated memory effect function. It is considered from practical point of view that the present calculation method is accurate enough to get memory effect functions since in general radiation damping forces exponentially decrease with increasing wave frequency. However we should note that the added mass $m_{11}(\infty)$ is slightly modified by the truncation effect.(see e.g. Fig.3.22). In this paper calculations were carried out untill the frequency range such that a stable added mass, $m_{11}(\infty)$ is given.

Comparisons between simulation results due to Eq.(3.53) and experimental results of slow drift surge motion for each wave conditions are shown in Figs.3.23 and 3.24, and the surge motion spectra of each results are indicated in Fig.3.25. The slowly varying drift forces are simulated by using both Eqs.(3.18) and (3.27). As an amplitude of $\vartheta(\omega)$, which expresses the frequency characteristics of a low pass filter in Eq.(3.27), a squared cosine type such that $\vartheta(\omega)=1$ for $\omega=0$ and $\vartheta(\omega)=0$ for ω equal to the peak frequency of wave spectrum is used. A time interval for simulation is 60msec. From this figure it is found that both results are in good agreement in the case that the first order motion is dominant, but that the simulation results become larger than the experimental results when the slow drift motion is dominant. It is considered that this is caused by a wave drift damping force.

REFFERENCES IN CAPTER 3

[1] Volterra, V.: Theory of Functional and Integral and Integro Differential Equations, Blackie and sons Ltd, London, (1930).

[2] Hasselmann, K.:Non linear ship motions in irregular waves, J. Ship Res., Vol.10, 1966.

[3] Rice, S. O.:Mathematical analysis of random noise, Bell System Technical Journal, 1944.

[4] Wiener, N.: Nonlinear Problems in Random Theory, M.I.T. Press and John Wiley & Sons, 1958.

[5] Triantafylou, M. S.: A consistent hydrodynamic theory for moor ed and positioned vessels, J. Ship Res., Vol.26, 1982.

[6] Tick, L.J.: The Estimation of Transfer Functions of Quadratic Systems, Technometrics, vol.3, No.4, 1961.

[7] Kinoshita, T. and Takaiwa, K.: Slow Motion Forced Oscillation Test of Floating Body in Waves (2nd Report), J. Nav. Arch. of Japan, vol.164, 1988.

[8] Dalzell, J. F.: Cross-bispectral analysis: Application to Ship Resistance in Waves, J. Ship Res., Vol.18, No.1, 1974.

[9] Chakrabarti, S. K.:Steady drift force on vertical cylinder-vis cous vs. potential, Appl. Ocean Res., Vol.6, No.2, 1984.

[10] Standing, R.G., Dacunha, N.M.C. and Matten, R.B.: Mean Wave Drift Forces: Theory and Experiment, NMI R124, 1981.

[11] Huse, E.:Wave induced mean force on platforms in direction opposite to wave propagation, Noewegian Maritime Res., Vol.5, 1977.

[12] Stokes, G.G.: On the theory of Oscillatory Waves, In Proceedings Cambridge Philosophical Society 8,1847.

[13] Kato, S. and Ando, S.:Statistical Analysis of Low Frequency Responses of a Moored Floating Offshore Structure (1st report), Papers of Ship Research Institute, Vol.23, No.5, 1986.

[14] Togawa, H.:Vibration analysis by using finite element method, Science Co. Ltd., 1976.

[15] Takagi, M. and Saito, K.: On the Description of Non- Harmonic Wave Problems in the Frequency Domain(1st,2nd,3rd,4th,5th,6th, and 7th reports), J. Kansai Soc. N.A., vol.'s. 182, 184, 187,188, 191,192, Japan.

Chapter 4

Stochastic analysis of second order responses

This section develops a theory of two probabilistic subjects associated with obtaining the second order response of a moored floating structure in the horizontal plane. The first method utilized to obtain the total second order response p.d.f. assumes neither a weakly nonlinear response nor a pure quadratic response. This theory is based on the "*approximate theory*" of continuous distribution in mathematical statistics where the p.d.f. of the total second order response can be represented by the Laguerre expansion which express the first term by a Gamma p.d.f. This is similar to the Vinje's method which is comparable to the Gram-Charlier expansion which expresses the first term by a Gaussian p.d.f., although the Gram-Charlier expansion does not uniformly converge and negative probabilities may occur. The use of the Laguerre expansion/Gamma p.d.f. method to obtain the total second order response p.d.f. can be applied to solve the above problems, furthermore it can also treat the case of equal double eigenvalues that the Naess' method cannot. The second method utilized obtains the highest mean amplitude of the total second order response of a moored floating structure. By introducing an assumption that a response and its time derivative processes are mutually independent, it is shown that the p.d.f. of the positive maxima or the negative minima can be expressed by the derivative of the p.d.f. of the instantaneous response.

As a basic study, the applicability of the present method is first discussed by comparisons between the Naess' exact p.d.f. solution for pure second order responses of moored floating semi-circular and rectangular 2- D structures. Next, the statistical interferences of the linear and quadratic responses on the p.d.f. and the 1/n th highest mean amplitude are investigated by changing the damping and restoration coefficients of the response system. Finally we investigate the practicability of the present method through comparisons between the

measured results and the estimates obtained from the present method.

4.1 Probabilistic Approach to The Total Second Order Response of a Moored Floating Structure

4.1.1 Instantaneous p.d.f.

(1) Exact Theory

The total second order response of a moored floating structure that is being subjected to a Gaussian random excitation at some fixed time may be expressed as:

$$X(t) = X^{(1)} + X^{(2)} \tag{4.1}$$

where the linear term is given by:

$$X^{(1)} = \int_{\tau} g_1(\tau)\zeta(t-\tau)d\tau \tag{4.2}$$

and the nonlinear second order term as:

$$X^{(2)} = \int_{\tau_1}\int_{\tau_2} g_2(\tau_1,\tau_2)\zeta(t-\tau_1)\zeta(t-\tau_2)d\tau_1 d\tau_2 \tag{4.3}$$

In equations (4.2) and (4.3), $\zeta(t)$ denotes the surface elevation which is a stationary Gaussian random variable with a zero mean. The kernel g_1 is a linear impulse response function. The kernel g_2 is analogous to the linear impulse response function and is called the quadratic impulse response function (see 3.1). And we assume that they are continuous and absolutely integrable, then they possess a Fourier transform as shown previously(Eq.(3.7)).

In order to represent the quadratic process $X^{(2)}$ by a sum of random variables, yielding the same probability distribution, the Kac & Siegert theory(K-S method) is used. This leads to the following representation:

$$X(t) = \sum_{j}^{\infty} c_j W_j(t) + \sum_{j}^{\infty} \lambda_j W_j^2(t) \tag{4.4}$$

where W_j is a set of independent Gaussian random variables of zero mean value and unit variance. The λ_j are eigenvalues which satisfy:

$$\int_{-\infty}^{\infty} K(\omega_1,\omega_2)\Psi_j(\omega_2)d\omega_2 = \lambda_j\Psi_j(\omega_1) \tag{4.5}$$

The parameters c_j, which represent the linear response, can be determined by:

$$c_j = \int_{-\infty}^{\infty} G_1(\omega)\sqrt{S_\zeta(\omega)}\Psi_j^*(\omega) \tag{4.6}$$

where $*$ indicates a complex conjugate and S_ζ is a two-sided wave spectrum. In equation (4.5) is a set of orthogonal eigenfunctions which satisfies:

$$\int_{-\infty}^{\infty} \Psi_j(\omega)\Psi_k^*(\omega)d\omega = \begin{cases} 1 & , j = k \\ 0 & , j \neq k \end{cases} \tag{4.7}$$

and kernel function $K(\omega_1, \omega_2)$ is a Hermite kernel defined by:

$$K(\omega_1, \omega_2) = \sqrt{S_\zeta(\omega_1)S_\zeta(\omega_2)}G_2(\omega_1, \omega_2) \tag{4.8}$$

When the eigenvalues λ_j and the parameters c_j are known, the p.d.f. is given by:

$$p_X(x) = \frac{1}{2\pi}\int_{-\infty}^{\infty} \exp(-ixs)\phi_X(s)ds \tag{4.9}$$

where the characteristic function is

$$\phi_X(s) = \prod_{j=1}^{\infty} \frac{1}{\sqrt{1-2i\lambda_j s}} \exp\left[-\frac{c_j^2 s^2}{\sqrt{2(1-2i\lambda_j s)}}\right] \tag{4.10}$$

The mean, the variance and the higher order cumulants are given by:

$$\begin{aligned} k_1 &= \overline{X} = E[X(t)] = \sum \lambda_j \\ k_2 &= \sigma_X^2 = \sum c_j^2 + 2\sum \lambda_j^2 = \sigma_1^2 + \sigma_2^2 \\ k_m &= \sum 2^{m-1}(m-1)!\lambda_j^m + \sum m!\lambda_j^{m-2}c_j^2 \quad \text{for } m \geq 3 \end{aligned} \tag{4.11}$$

Kac and Siegert[1] and Neal[2] concluded that the p.d.f. expressed in Eq.(4.9) cannot be determined in a closed form and therefore must be computed numerically. Although this is true in most cases, it can be written in a closed form in some special cases which will be discussed next.

(2) NAESS' APPROACH

Naess[3),4),5)] introduced a slow drift approximation such that $G_2(\omega_1, \omega_2) = 0$ when $\omega_1 \cdot \omega_2 > 0$. This indicates that the high frequency component which corresponds to sum of ω_1 and ω_2 is negligible. This is a physically acceptable fact, and it is a convenient approximation for our purpose. Naess determined

that the Eq.(4.5) eigenvalue problem generated a set of double eigenvalues as follows:

$$K(\omega_1, \omega_2) = 0 \quad \text{for } \omega_1 \cdot \omega_2 < 0$$

$$\int_0^\infty K(\omega_1, \omega_2)\tilde{\Psi}_j(\omega_2)d\omega_2 = \tilde{\lambda}_j\tilde{\Psi}_j(\omega_1) \quad \text{for } \omega_1 \geq 0 \tag{4.12}$$

$$\lambda_{2j-1} = \lambda_{2j} = \tilde{\lambda}_j$$

where

$$\Psi_{2j-1}(\omega) = \begin{cases} \frac{1}{\sqrt{2}}\tilde{\Psi}_j(\omega) & , \omega \geq 0 \\ \frac{1}{\sqrt{2}}\tilde{\Psi}_j^*(\omega) & , \omega < 0 \end{cases}$$

$$\Psi_{2j}(\omega) = \begin{cases} -\frac{i}{\sqrt{2}}\tilde{\Psi}_j(\omega) & , \omega > 0 \\ 0 & , \omega = 0 \\ \frac{i}{\sqrt{2}}\tilde{\Psi}_j^*(\omega) & , \omega < 0 \end{cases} \tag{4.13}$$

and also that the linear response is negligibly small when compared to the second order response, i.e., $c_j \equiv 0$. The p.d.f. of the pure second order response can be shown in the closed form as follows:

$$p_X(x) = \begin{cases} \sum \frac{l_j}{2\tilde{\lambda}_j} \exp(-\frac{x}{2\tilde{\lambda}_j}) & , x \geq 0 \\ \sum \frac{l_j}{2|\tilde{\lambda}_j|} \exp(\frac{x}{2|\tilde{\lambda}_j|}) & , x < 0 \end{cases} \tag{4.14}$$

where

$$l_j = \prod_{\substack{k=1 \\ k \neq j}}^{N} \frac{1}{(1 - \frac{\tilde{\lambda}_k}{\tilde{\lambda}_j})} \tag{4.15}$$

and the set of eigenvalues g are divided into two groups, $\lambda_j, j = 1, \cdots, M$, for $\lambda_j > 0$ and $\lambda_j, j = M+1, \cdots, N$, for $\lambda_j < 0$. The above results are then valid unless equal double eigenvalues exist.

(3) APPROXIMATE THEORY

(i) Gram-Charlier expansion method

The authors[6] showed that if the nonlinear response considered here is weakly nonlinear the instantaneous p.d.f. can be represented by the Gram- Charlier expansion. The expansion is the Hermite expansion, the first approximation of which is the Gaussian p.d.f.. We shall indicate their method in brief.

If the eigenvalues λ_j are very small compared with c_j, X may approach Gaussian. So we replace $X - E[X]$ by Z and introduce the error function $p_\epsilon(z)$ defined by

$$p_\epsilon(z) = p_X(z) - N(0, \sigma_X^2) \tag{4.16}$$

where $N(0, \sigma_X^2)$ is the zero mean Gauss p.d.f. with variance equal to σ_X^2. If p_ϵ can be represented by a family of orthogonal functions with weighting function $\{w(z)h_n(z)\}$, it can be expanded in the following form:

$$p_\epsilon(z) = \sum_{n=1}^{\infty} \alpha_n h_n(z) w(z) \tag{4.17}$$

where

$$\alpha_n = \int_{-\infty}^{\infty} h_n(z) p_\epsilon(z) dz \tag{4.18}$$

If $w(z)$ is the Gaussian p.d.f., it is well-known that $h_n(z)$ are given by the Hermite polynomials. From the properties of the Hermite polynomials the p.d.f. can be approximated by the Gram-Charlier expansion:

$$p_X(x) \simeq \frac{1}{2\pi\sigma_X}[1 + \sum_{n=3}^{\infty} \frac{\bar{b}_n}{n!\sigma_X^n} H_n\{\frac{x - \overline{X}}{\sigma_X}\} \exp(-\frac{x - \overline{X}}{2\sigma_X^2})] \tag{4.19}$$

where H_n are the Hermite polynomials and $\bar{b}_n$ represent the higher moments defined by

$$b_n = E[(x - \overline{X})^n] \quad \text{for } n \geq 3 \tag{4.20}$$

And the moments functions can be obtained from frequency domain integrals of transfer functions and wave spectrum as shown in Appendix F.

This method has a significant advantage in the point of obtaining the approximate solution from numerical integral procedures. However, we should note that the Gram-Charlier expansion does not always converge uniformly and that the negative probabilities occur if the expansion is truncated at finite order. The occurrence of negative probabilities is physically inconsistent.

Edgeworth[7] investigated the convergence of the Gram-Charlier series and he has shown that if only a few terms are computed, the best grouping of terms in Eq.(4.19) is not that associated with taking terms in their natural order(i.e. $0, 3, 4, 5, \cdots$). And he proposed regrouped series. The grouping is

0
0,3 .... 1st approximation
0,3,4,6 .... 2nd
0,3,4,6,5,7,9 .. 3rd

This list implies that if the 0 and 3 terms are used as the first approximation, the addition of terms 4 and 6 gives the next order approximation, and so forth. This regrouped series is called "*Edgeworth series*". The Gram-Charlier series up to third order is equal to the Edgeworth series.

(ii) Asymptotic solution method

Naess[4] found an exact series form solution for the instantaneous p.d.f. of total second order response. His argument is as follows:

From equation (4.10) and the slow drift approximation, the c.f., $\phi_X(s)$ is given by

$$\phi_X(s) = \prod_{j=1}^{N} \phi_j(s) \tag{4.21}$$

$$\phi_j(s) = \frac{1}{1 - 2i\tilde{\lambda}_j s} \exp[-\frac{(c_{2j-1}^2 + c_{2j}^2)}{2(1 - 2i\tilde{\lambda}_j s)}] \tag{4.22}$$

It is seen that $\phi_X(s)$ has isolated essential singularities at $s = -\frac{i}{2\tilde{\lambda}_j}$. Rewriting $\phi_j(s)$ as

$$\phi_j(s) = \frac{i}{2\tilde{\lambda}_j(s - s_j)} \exp[-\frac{ib_j s^2}{s - s_j}] \tag{4.23}$$

where $b_j = (c_{2j-1}^2 + c_{2j}^2)4\tilde{\lambda}_j$ and $s_j = -\frac{i}{2\tilde{\lambda}_j}$, it can be shown that

$$\begin{aligned} \phi_X(s)\exp(-ixs) \quad &= \frac{i\tilde{\phi}_j(s)}{2\tilde{\lambda}_j(s - s_j)} \exp\{-i(s_j x + 2b_j s_j)\} \\ &\times \exp\{-i[(b_j + x)(s - s_j) + \frac{b_j^2 s^2}{s - s_j}]\} \end{aligned} \tag{4.24}$$

where the function $\tilde{\phi}_j = \frac{\phi_X(s)}{\phi_j(s)}$. Hence $\tilde{\phi}_j(s)$ is analytic in a neighborhood of s_j, which implies that

$$\tilde{\phi}_j(s) = \sum_{n=0}^{\infty} a_n^{(j)}(s - s_j)^n \quad \text{for } |s| < e_j \ (e_j \text{ are any constants}) \tag{4.25}$$

The p.d.f. can be obtained from integrating (4.24) from $-\infty$ to ∞ with respect to s. Invoking the residue theorem, consequently we get:

$$p_X(x) = \begin{cases} \sum \frac{l_j}{2\tilde{\lambda}_j} \exp(-\frac{x}{2\tilde{\lambda}_j} - \frac{b_j}{\tilde{\lambda}_j}) Q_j(x) & x \geq 0 \\ \sum \frac{l_j}{2|\tilde{\lambda}_j|} \exp(\frac{x}{2|\tilde{\lambda}_j|} - \frac{b_j}{\tilde{\lambda}_j}) Q_j(x) & x < 0 \end{cases} \tag{4.26}$$

where the function $Q_j(x)$ are defined by

$$Q_j(x) = \sum_{m=0}^{\infty} (\frac{i}{2|\tilde{\lambda}_j|})^m a_m^{(j)} \ (\frac{b_j}{b_j + x})^{m/2} I_m(\frac{\sqrt{b_j(b_j + x)}}{|\tilde{\lambda}_j|}) \tag{4.27}$$

and $I_m(x)$ denotes the modified Bessel function of integer order m. The expansion coefficients $a_m^{(j)}$ can be derived from the Taylor expansion of the function

$$\tilde{\phi}_j(s) = \prod_{\substack{k=1 \\ k \neq J}}^{\infty} \phi_k(s)$$

around $s = s_j$. When $b_j = 0, j = 1, \cdots, N$, i.e. when the first order response is neglected, it is easily seen that since $I_0(0) = 1$ and

$$a_0^{(j)} = \prod_{\substack{k=1 \\ k \neq J}}^{\infty} \phi_k(s_j)$$

,equation (4.26) reduces to equation (4.14).

Since it is very difficult to numerically evaluate equation (4.26), Naess obtained the aymptotic solution for $x \to \infty$ from (4.26) when $\tilde{\lambda}_1$ is dominant compared with the other eigenvalues, i.e. when the following approximation is adopted.

$$\tilde{\phi}_1(s) \simeq \tilde{\phi}_1(s_1) = a_0^{(1)} = \prod_{k=2}^{N} \phi_k(s_1) \tag{4.28}$$

From Eq.(4.22) it is found that

$$a_0^{(1)} = \prod_{j=2}^{N} \frac{1}{(1 - \frac{\tilde{\lambda}_j}{\tilde{\lambda}_1})} \exp[\frac{\tilde{\lambda}_j b_j}{\tilde{\lambda}_1(\tilde{\lambda}_1 - \tilde{\lambda}_j)}] \tag{4.29}$$

Using the following asymptotic relation:

$$I_0(x) \sim \frac{1}{\sqrt{2\pi x}} \exp(x) \quad \text{as } x \to \infty \tag{4.30}$$

it can now be shown that

$$p_X(x) \sim \frac{a_0^{(1)}}{2\sqrt{2\pi\tilde{\lambda}_1}} (\frac{\sqrt{b_1(b_1 + x)}}{\tilde{\lambda}_1})^{-1/2} \exp[-\frac{(\sqrt{b_1 + x} + \sqrt{b_1})^2}{2\tilde{\lambda}_1}] \quad \text{as } x \to \infty \tag{4.31}$$

This implies that p_X behaves like $O(\exp(-x))$ for $x \to \infty$ when $\tilde{\lambda}_1 \gg \tilde{\lambda}_j$.

Vinje[8] also found the same expression as (4.31). But his result is in error as noted by Naess.

(iii) New approximate theory

An alternative approach to Naess' exact solution will now be developed. If the number of the eigenvalues are finite, then from Eq.(4.4) the total response $X(t)$ may be decomposed into the following form:

$$X(t) = Z_1 + Z_2 \tag{4.32}$$

where

$$Z_1 = \sum_{j=1}^{M}(c_j W_j + \lambda_j W_j^2) \tag{4.33}$$

$$Z_2 = \sum_{j=M+1}^{N}(c_j W_j + \lambda_j W_j^2) \tag{4.34}$$

It can be mathematically proven that Z_1 and Z_2 are mutually independent in a statistical sense(e.g. Papoulis[10]). If the time is fixed and $c_j \equiv 0$, Z_1 becomes a random variable which is always positive while Z_2 is always negative. In this case it can be proven from the approximate theory of continuous random distribution in mathematical statistics that the p.d.f. of Z_1 and $-Z_2$ can be expanded to a series of the generalized Laguerre polynomials[11]. The first term of the series is the two parameter Gamma p.d.f.. For example, if $Y = \lambda_1 W_1^2 + \cdots + \lambda_n W_n^2$ and $\lambda_j > 0 (i = 1, \cdots, n)$, then the p.d.f. of Y can be expanded by the following series with uniform convergence:

$$p_Y(x) = p_\gamma(x, 2\theta; \frac{\nu}{2})[1 + \sum_{k=1}^{\infty} B_k L_k^{(\frac{\nu}{2}-1)}(\frac{x}{2\theta})] \tag{4.35}$$

where p_γ is the Gamma p.d.f. with two parameters θ and ν, $L_k^{(\frac{\nu}{2})}$ is the generalized Laguerre polynomials, and B_k represents the coefficients determined from the orthogonal property of the Laguerre polynomials. Since the parameters θ and ν are unknown, they can be determined by eliminating B_1 and B_2. Then p_γ becomes a second order approximation for p_Y, and the first and second order moments of p_Y agree with those of p_γ. The same approximation can be also applied in the case of $c_j \neq 0$ by transforming Z_1 in Eq.(4.33) into the following form:

$$Y_1 = Z_1 + \sum \frac{c_j}{4\lambda_j} = \sum \lambda_j V_j^2$$

$$V_j = W_j + \frac{c_j}{2\lambda_j} \tag{4.36}$$

Eq.(4.36) is the same quadratic form of Gaussian random variables as the case for $c_j = 0$, except that $E[V_j(t)] = \frac{c_j}{2\lambda_j} \neq 0$. Since the p.d.f. of $V_j^2(t)$ becomes a non-central χ^2 p.d.f. and V_j are mutually independent, the p.d.f. of Y can be represented by a series form of the non-central χ^2 p.d.f. Using the fact that a non-central χ^2 p.d.f. can be expanded by the generalized Laguerre polynomials, the p.d.f. of Y can also be represented by a series form using a Gamma p.d.f. and a generalized Laguerre polynomials like Eq.(4.35). There is, however, statistical interference between the linear and the quadratic responses at the higher order moments greater than third order(e.g. Eq.(4.11)), thus it is insufficient to adequately describe this statistical interference approximation by using only

the leading two terms. Therefore we must extend the two term approximation to at least a three term approximation, i.e. approximate the response by means of a Gamma p.d.f. is defined with three parameters($\theta, \nu, and \delta$) in the following form:

$$p_\gamma(x, \delta, 2\theta; \frac{\nu}{2}) = \frac{1}{(2\theta)^{\nu/2}\Gamma(\nu/2)}(x-\delta)^{\nu/2-1}\exp(-\frac{x-\delta}{2\theta})\mho(x-\delta) \qquad (4.37)$$

where $\mho(x-\delta)$ is the step function defined as:

$$\mho(x-\delta) = \begin{cases} 1 & x \geq \delta \\ 0 & x < \delta \end{cases} \qquad (4.38)$$

θ is the generating number of Gamma p.d.f., and ν the degrees of freedom.

The corresponding c.f. becomes:

$$\phi_\gamma(u, \delta, 2\theta; \nu/2) = \frac{1}{(1-2i\theta u)^{\nu/2}}\exp(i\delta u) \qquad (4.39)$$

Taking the difference between the cumulant-generating function of Z_1 and that of a random variable which yields a three parameter (θ, ν, δ) Gamma p.d.f. we obtain,

$$\begin{aligned} \Delta \quad &\equiv \log\phi_{Z_1} - \log\phi_\gamma \\ &= -\frac{1}{2}\sum_{j=1}^{M}\log(1-2i\lambda_j u) + \frac{\nu_1}{2}\log(1-2i\theta_1 u) - \sum_{j=1}^{M}\frac{c_j^2 u^2}{2(1-2i\lambda_j u)} \\ &\quad -i\delta_1 u \end{aligned} \qquad (4.40)$$

Substituting $iu = \frac{\xi_1}{1+2\theta_1\xi_1}$ into equation (4.40) we get:

$$\begin{aligned} \Delta \quad &\equiv -\frac{1}{2}\sum_{j=1}^{M}\log[1-2(\lambda_j-\theta_1)\xi_1] + \frac{M-\nu_1}{2}\log(1+2\theta_1\xi_1) \\ &\quad + \sum_{j=1}^{M}\frac{c_j^2}{2}[\frac{\xi_1^2}{\{1-2(\lambda_j-\theta_1)\xi_1\}(1+2\theta_1\xi_1)}] - \frac{\delta_1\xi_1}{(1+2\theta_1\xi_1)} \end{aligned} \qquad (4.41)$$

If θ_1 is taken such as $2\theta_1 > max\lambda_j (j = 1, \cdots, M)$, $|2(\lambda_j - \theta_1)\xi_1)| \leq |2\theta_1\xi_1| \leq 1$ for all ξ_1. Thus Δ can be expanded into a uniform convergence power series. Consequently the expansion form of Δ is given by:

$$\Delta \quad = (\sum\lambda_j - \nu_1\theta_1 - \delta_1)\xi_1 + (\sum\lambda_j^2 - 2\sum\lambda_j\theta_1 + \nu_1\theta_1^2 + \sum\frac{c_j^2}{2} + 2\theta_1\delta_1)\xi_1^2$$

$$+[\frac{3}{4}(\sum\lambda_j^3-3\sum\lambda_j^2\theta_1+3\sum\lambda_j\theta_1^2-\nu_1\theta_1^3)-4\theta_1^2\delta_1+\sum\lambda_j c_j^2$$

$$-2\sum c_j^2\theta_1]\xi_1^3+O(\{2\theta_1\xi_1\}^4) \tag{4.42}$$

The first, second and third terms of the right hand side of equation (4.42) may be eliminated if the unknown variables θ_1, ν_1 and δ_1 are determined as follows:

$$\theta_1=\frac{4\sum\lambda_j^3+3\sum\lambda_j c_j^2}{4\sum\lambda_j^2+2\sum c_j^2}$$

$$\delta_1=\sum\lambda_j-\frac{(2\sum\lambda_j^2+\sum c_j^2)^2}{4\sum\lambda_j^3+3\sum\lambda_j c_j^2} \tag{4.43}$$

$$\nu_1=\frac{2(2\sum\lambda_j^2+\sum c_j^2)^3}{(4\sum\lambda_j^3+3\sum\lambda_j c_j^2)^2}$$

If the slow drift approximation obtained by Naess is applied, the parameters in Eq.(4.43) should be replaced by $\tilde{\delta}_1=2\delta_1$, $\tilde{\nu}_1=2\nu_1$, and $\tilde{\theta}_1=\theta_1$. Thus the p.d.f. of Z_1 can be approximately evaluated in the following form:

$$p_{Z_1}(x)\simeq p_\gamma(x,\tilde{\delta}_1,2\tilde{\theta}_1;\tilde{\nu}_1/2) \tag{4.44}$$

This becomes the third order approximation of p_{Z_1} because the first, second, and third order moments completely agree with the actual ones. Equation (4.44) can be exactly expanded by the generalized Laguerre polynomials as follows:

From Eq.(4.42) the c.f. of Z_1 is given by the expansion form as:

$$\phi_{Z_1}=\phi_\gamma(u,\tilde{\delta}_1,2\tilde{\theta}_1;\tilde{\nu}_1/2)\exp[\sum_{n=4}^{\infty}A_n\xi_1^n]$$

$$=\phi_\gamma\sum_{k=0}^{\infty}B_k\xi_1^k \tag{4.45}$$

where $B_0=1$, $B_1=B_2=B_3=0$.

Using the following relation

$$\frac{\partial^k}{\partial\tilde{\theta}_1^k}\phi_\gamma=\tilde{\nu}_1(\tilde{\nu}_1+2)\cdots(\tilde{\nu}_1+2k-2)\xi_1^k\phi_\gamma \tag{4.46}$$

results in

$$\phi_{Z_1}=\sum_{k=0}^{\infty}\frac{B_k}{\tilde{\nu}_1(\tilde{\nu}_1+2)\cdots(\tilde{\nu}_1+2k-2)}\frac{\partial^k}{\partial\tilde{\theta}_1^k}\phi_\gamma \tag{4.47}$$

The partial derivative of ϕ_γ with respect to $\tilde{\theta}_1$ can also be represented in another form by:

$$\frac{\partial^k}{\partial\tilde{\theta}_1^k}\phi_\gamma=\frac{(-1)^k e^{i\tilde{\delta}_1 u}}{\tilde{\theta}_1^k\Gamma(\tilde{\nu}_1/2)}\int_0^\infty e^{2iu\tilde{\theta}_1 x}\frac{\partial^k}{\partial x^k}(e^{-x}x^{\tilde{\nu}_1/2+k-1})dx \tag{4.48}$$

Using the generalized Laguerre polynomials,

$$L_r^{(\alpha)}(x) = \frac{e^x x^{-\alpha}}{r!}\frac{d^r}{dx^r}(e^{-x}x^{r+\alpha}) \tag{4.49}$$

where $\alpha > -1$, $r = 0, 1, 2, \cdots$, Eq.(4.48) can be rewritten as follows:

$$\frac{\partial^k}{\partial\tilde{\theta}_1^k}\phi_\gamma = \frac{(-1)^k}{\tilde{\theta}_1^k\Gamma(\tilde{\nu}_1/2)}\int_{\tilde{\delta}_1}^{\infty} k!\exp(-\frac{s-\tilde{\delta}_1}{2\tilde{\theta}_1})(\frac{s-\tilde{\delta}_1}{2\tilde{\theta}_1})^{\tilde{\nu}_1/2-1}L_k^{(\tilde{\nu}_1/2-1)}(\frac{s-\tilde{\delta}_1}{2\tilde{\theta}_1})e^{ius}\frac{ds}{d\tilde{\theta}_1} \tag{4.50}$$

Finally we obtain the complete form of the p.d.f. of Z_1 in the following series form

$$\begin{aligned} p_{Z_1} \quad &= p_\gamma(x, \tilde{\delta}_1, 2\tilde{\theta}_1; \tilde{\nu}_1/2)[1 + \sum_{k=4}^{\infty} B_k \frac{(-1)^k k!\Gamma(\tilde{\nu}_1/2)}{\tilde{\theta}_1^k\Gamma(\tilde{\nu}_1/2+k)} \\ &\times L_k^{(\tilde{\nu}_1/2-1)}(\frac{x-\tilde{\delta}_1}{2\tilde{\theta}_1})] \end{aligned} \tag{4.51}$$

where

$$B_k = \frac{\tilde{\theta}_1^k}{(-1)^k}E[L_k^{(\tilde{\nu}_1/2-1)}(\frac{x-\tilde{\delta}_1}{\tilde{\theta}_1})] \tag{4.52}$$

This final expansion form is not used except in the cases where the moments higher than third order are of importance.

The p.d.f. of $-Z_2$, as well as that of Z_1, can be also approximated by a three parameter Gamma p.d.f.($\tilde{\theta}_2$, $\tilde{\nu}_2$, and $\tilde{\delta}_2$) as follows:

$$p_{Z_2}(x) \simeq p_\gamma(x, \tilde{\delta}_2, 2\tilde{\theta}_2; \tilde{\nu}_2/2) \tag{4.53}$$

The results of Eqs.(4.44) and (4.53) indicate that the total second order response process $X(t)$ can be approximated by the difference of the two independent random variables which yield a Gamma distribution with three parameters. From the convolution integrals of the Gamma p.d.f.'s the p.d.f. of the total second order response can be obtained by:

$$p_X(x) = \begin{cases} f(\tilde{\theta}_1, \tilde{\theta}_2; \tilde{\delta}_1, \tilde{\delta}_2)\int_0^\infty (z+x-\tilde{\delta}_1+\tilde{\delta}_2)^{\tilde{\nu}_1/2-1}z^{\tilde{\nu}_2/2-1}e^{-az}dz & \\ \times \exp(-\frac{x-\tilde{\delta}_1+\tilde{\delta}_2}{2\theta_1}) & x \geq \tilde{\delta}_1 - \tilde{\delta}_2 \\ f(\tilde{\theta}_1, \tilde{\theta}_2; \tilde{\delta}_1, \tilde{\delta}_2)\int_0^\infty (z-x+\tilde{\delta}_1-\tilde{\delta}_2)^{\tilde{\nu}_2/2-1}z^{\tilde{\nu}_1/2-1}e^{-az}dz & \\ \times \exp(\frac{x-\tilde{\delta}_1+\tilde{\delta}_2}{2\theta_2}) & x < \tilde{\delta}_1 - \tilde{\delta}_2 \end{cases} \tag{4.54}$$

where

$$f(\tilde{\theta}_1, \tilde{\theta}_2; \tilde{\delta}_1, \tilde{\delta}_2) = \frac{1}{(2\tilde{\theta}_1)^{\tilde{\nu}_1/2}(2\tilde{\theta}_2)^{\tilde{\nu}_2/2}\Gamma(\tilde{\nu}_1/2)\Gamma(\tilde{\nu}_2/2)},$$

$$a = \frac{1}{2\tilde{\theta}_1} + \frac{1}{2\tilde{\nu}_2} \tag{4.55}$$

and the multiple-valued integrants take a principal value.

(iv) Convergence to Gaussian p.d.f

When the eigenvalues λ_j are very small compared with c_j, i.e. when λ_j are neglected, the total second order response process, $X(t)$ certainly approaches Gaussian. In this section we shall show this fact from the present theory.

From Eq.(4.43) it is found that

$$\begin{aligned} \tilde{\theta}_1 &= \frac{\sigma_X}{\sqrt{2\tilde{\nu}_1}} \\ \tilde{\delta}_1 &= \overline{X} - \sqrt{\frac{\tilde{\nu}_1}{2}}\sigma_X \end{aligned} \tag{4.56}$$

Namely the parameters of the Gamma p.d.f. are not mutually independent, two parameters in the three can be represented by the rest if σ_X and $\overline{X}$ are fixed. Taking $\tilde{\nu}_1$, which represents the degree of freedom of the Gamma p.d.f., as an independent parameter, replacing the variable x by z like

$$z = \frac{x - \overline{X}}{\sigma_X}$$

and setting $n = \tilde{\nu}_1/2$, the Gamma p.d.f. can be rewritten from Eq.(4.37) as:

$$p_\gamma(z) = \begin{cases} \frac{\sqrt{n}}{\Gamma(n)}(\sqrt{n}z + n)^{n-1}\exp(-\sqrt{n}z - n) & \text{for } z > -\sqrt{n} \\ 0 & \text{for } z \le -\sqrt{n} \end{cases} \tag{4.57}$$

When $\lambda_j \ll 1$, i.e. $n \gg 1$, we shall consider the asymptotic behavior of Eq.(4.57) as $n \to \infty$.

Noting that the first term of asymptotic expansion of Gamma function $\Gamma(z)$ is given by

$$\Gamma(z+1) \simeq \sqrt{2\pi}z^{z+1/2}e^{-z} \qquad \text{as } z \to \infty$$

and the Taylor expansion of $\log(1+u)$ for $|u| < 1$ is represented as:

$$\log(1+u) = u - \frac{1}{2u^2} + o(u^2)$$

then we have:

$$\begin{aligned} \log p_\gamma \quad &= -\log\sqrt{2\pi} + \{-\frac{1}{4n^2} + \frac{1}{3n^2} + \cdots\} - \frac{z^2}{2} + \frac{z^3}{3\sqrt{n}} \\ &-(\frac{z}{\sqrt{n}} + \frac{z^2}{2n} + \cdots) + o(1) \end{aligned} \tag{4.58}$$

If $n \to \infty$, from equation (4.58) it is found that

$$\log p_\gamma \sim -\log\sqrt{2\pi} - \frac{z^2}{2} + O(\frac{z}{\sqrt{n}})$$

that is

$$p_\gamma \sim \frac{1}{\sqrt{2\pi}} \exp(-\frac{z^2}{2}) \qquad \text{as } n \to \infty \tag{4.59}$$

This implies that p_γ can be approximated by the Gaussian p.d.f. when n is sufficiently large. But we should note that the the range which the Gamma p.d.f can be regarded as the Gaussian p.d.f. is limitted to the variable range of $z < \sqrt{n}$.

4.1.2 Maxima p.d.f.

Statistical prediction of the maxima of a random process is usually performed using the Rayleigh distribution under the condition that a random process is a stationary, narrow banded, Gaussian process with zero mean. But in the case of a second order response for a moored floating structure, this condition may no longer be satisfied. In order to exactly obtain the maxima p.d.f. of a nonlinear response, the expected number of maxima greater than a specified level is required as shown by Lin[12].

First, according to Lin, we shall show the exact theory.

Figure 4.1 is an explanatory sketch of a random process $X(t)$ for which the maxima(or minima) could be anywhere in the range of $(-\infty, \infty)$ and several maxima(or minima) could occur during one cycle as defined by mean crossings. Here, maxima are defined as peaks which satisfy the condition $\dot{X}(t) = 0$ and $\ddot{X}(t) < 0$. Whereas minima are defined as troughs satisfying the condition $\dot{X} = 0$ and $\ddot{X} > 0$. As shown in Fig.4.1 maxima and minima can take both negative and positive values. The magnitude of the maxima with positive values $\{X(t) > 0, \dot{X} = 0, \ddot{X} < 0\}$ or the minima with negative values $\{X(t) < 0, \dot{X} = 0, \ddot{X} > 0\}$ would be critical if they exceed a certain value, and hence the statistical extreme values of these maxima and the minima provide valuable information for the engineering design purpose.

For the problem of a mooring system the positive maxima are the most important, if the direction drifted by waves is positive. Since the statistical properties of negative minima can be estimated from those of positive maxima by means of the transform of random variables, the positive maxima are considered in the following analysis.

It can be assumed that $X(t)$ is stationary and zero mean without loss of generality. Then the expected number of maxima above a specified level $X(t) = \xi$, denoted as $E[M(\xi)]$, is obtained by:

$$E[M(\xi)] = \int_\xi^\infty \int_{-\infty}^0 |\dot{x}| p_{X\dot{X}\ddot{X}}(x, 0, \ddot{x}) d\ddot{x} \tag{4.60}$$

The total expected number of maxima with positive values, denoted as $E[M(-\infty)]$, becomes

$$E[M(-\infty)] = \int_{-\infty}^{\infty} dx \int_{-\infty}^{0} |\ddot{x}| p_{X\dot{X}\ddot{X}}(x, 0, \ddot{x}) d\ddot{x} \tag{4.61}$$

where $p_{X\dot{X}\ddot{X}}$ is the joint p.d.f.

Huston & Skopinski[13] has assumed that the ratio of their two expected numbers is approximately equivalent to the probability in which the maximum values exceed a level y, i.e. $E[M(y)/M(-\infty)] \simeq E[M(y)]/E[M(-\infty)]$. Under this assumption the probability in which the maximum positive values exceed a level y becomes

$$P_p = 1 - E[M(y)/M(-\infty)] \simeq 1 - E[M(y)]/E[M(-\infty)] \tag{4.62}$$

Then maxima p.d.f. is given by:

$$p_p(y) = -\frac{1}{E[M(-\infty)]} \int_{-\infty}^{0} \ddot{x} p_{X\dot{X}\ddot{X}}(y, 0, \ddot{x}) d\ddot{x} \tag{4.63}$$

In the case that $X(t)$ is the Gaussian process, p_p has already been obtained by Cartwright & Longuet-Higgins[14]. It can be prescribed by two parameters, i.e. spectrum band width parameter and variance. As well known, when the band width parameter is close to 1, i.e. wide banded process, p_p approaches the Gaussian p.d.f., and when the parameter close to 0, p_p approaches the Rayleigh p.d.f.

But statistical characteristics and maxima p.d.f. of nonlinear responses has not been found out yet. So we must introduce some approximations to obtain p_p for the nonlinear response.

For this purpose the following assumptions are introduced.

(1) The response is narrow banded, i.e. the negative maxima and positive minima are negligible.

(2) The response is stationary.

(3) The expected number of crossings at a specified level with a positive gradient is equal to that of maxima over it, i.e. one-to-one correspondence between zero-upcrossings and maxima.

Assumption (1) imposes considerable limitations to our objective. However the condition is usually satisfied, except for fatigue analysis, because if the specified level is sufficiently high, the negative maxima or positive minima that exist over this level are infrequent. In general, using these assumptions, the maxima (or minima) probability is overestimated as compared with exact one because the expected number of maxima over a specified level is always greater than those crossing that level. Since statistical properties of the minima can be

obtained from those of the maxima, by means of a variable transform, only the maxima will be considered in the following analysis.

Using the above assumptions, then

$$M(y) \simeq N^+(y) \tag{4.64}$$

where N^+ is a random number crossing a specified level y at positive gradient and its expectation per unit time is given by:

$$E[N^+(y)] = \frac{1}{2}\int_{-\infty}^{\infty} |\dot{x}| p_{X\dot{X}}(y, \dot{x}) d\dot{x} \tag{4.65}$$

Thus a p.d.f. for an event where the maxima are greater than a level $y + \overline{X}$ is given by:

$$p_p(y) = -\frac{d}{dy}\{\frac{\int_0^{\infty} p_{X\dot{X}}(y + \overline{X}, \dot{x})\dot{x}d\dot{x}}{\int_0^{\infty} p_{X\dot{X}}(\overline{X}, \dot{x})\dot{x}d\dot{x}}\} \tag{4.66}$$

where $p_{X\dot{X}}$ is a joint probability density function of the response X and its time derivative $\dot{X}$.

In this way, under narrow band assumption the problem obtaining the maxima p.d.f. of nonlinear response can be transformed to the problem obtaining the joint p.d.f. $p_{X\dot{X}}$.

(i) Series approximate solution

Obviously if instantaneous p.d.f.'s can be expanded into useful series representations, one would expect that similar useful generalized expansions would also exist for higher dimension p.d.f.'s.

A particularly useful expansion for our purpose was introduced by the autors[6]. The following development closely follows their original works.

Let $p(x_1, x_2)$ be a joint p.d.f. for the variables x_1 and x_2. The corresponding instantaneous p.d.f.'s are then

$$\begin{aligned} p_1(x_1) &= \int p(x_1, x_2) dx_2 \\ p_2(x_2) &= \int p(x_1, x_2) dx_1 \end{aligned} \tag{4.67}$$

Using the instantaneous p.d.f.'s as weighting functions, we can construct two sets of orthonormal polynomials $\{\Lambda_{1n}(x_1)\}$ and $\{\Lambda_{2n}(x_2)\}$ from the integral relation

$$\begin{aligned} \int p_1(x_1)\Lambda_{1m}(x_1)\Lambda_{1n}(x_1)dx_1 &= \delta_{mn} \\ \int p_2(x_2)\Lambda_{2m}(x_2)\lambda_{2n}(x_2)dx_2 &= \delta_{mn} \end{aligned} \tag{4.68}$$

If we assume that it is permissible to expand $p(x_1, x_2)$ in terms of those two sets of orthonormal functions, then

$$p(x_1, x_2) = p_1(x_1)p_2(x_2)\sum_{m,n} a_{mn}\Lambda_{1m}(x_1)\Lambda_{2n}(x_2) \tag{4.69}$$

By employing Eq.(4.68) in Eq.(4.69), we can evaluate the expansion coefficients,

$$a_{mn} = \int\int p(x_1, x_2)\Lambda_{1m}(x_1)\Lambda_{2n}(x_2)dx_1dx_2 \tag{4.70}$$

If the matrix (a_{mn}) is diagonal, i.e. $a_{mn} = a_n\delta_{mn}$,

$$p(x_1, x_2) = p_1(x_1)p_2(x_2)\sum_{n} a_n\Lambda_{1n}(x_1)\Lambda_{2n}(x_2) \tag{4.71}$$

This is equivalent to the Mercer expansion[15] of the kernel function in the integral equation (see Appendix E).

The validity of Eq.(4.71) can be illustrated as follows:

Let $p(x_1, x_2)$ be the joint Gaussian p.d.f. as

$$p(x_1, x_2) = \frac{1}{2\pi\sigma^2\sqrt{1-\varrho^2}}\exp\{-\frac{(x_1^2 + x_2^2 - 2\varrho x_1x_2)}{2\sigma^2(1-\varrho^2)}\} \tag{4.72}$$

with corresponding p.d.f.

$$p(x) = \frac{1}{\sqrt{2\pi}\sigma}\exp(-\frac{x^2}{2\sigma^2}) \tag{4.73}$$

Using the Mehler's expansion[16] given by

$$\frac{1}{\sqrt{1-u^2}}\exp[-\frac{\{u^2(x_1^2 + x_2^2) - 2ux_1x_2\}}{2(1-u^2)}]$$

$$= \sum_{n=0}^{\infty}\frac{u^n}{n!}H_n(x_1)H_n(x_2) \tag{4.74}$$

where $H_n(x)$ is the Hermite polynomials of order n, and inserting Eq.(4.74) into (4.72),we get

$$p(x_1, x_2) = \frac{1}{2\pi\sigma^2}\exp\{-\frac{x_1^2 + x_2^2}{2\sigma^2}\}\sum_{n=0}^{\infty}\frac{\varrho^n}{n!}H_n(\frac{x_1}{\sigma})H_n(\frac{x_2}{\sigma}) \tag{4.75}$$

Since the matrix a_{mn} in Eq.(4.70) is not always diagonal in general cases, the joint p.d.f. $p_{X\dot{X}}$, the first approximation of which is the joint Gaussian p.d.f.,

may be expressed as:

$$p_{X\dot{X}}(x,\dot{x}) = \frac{1}{2\pi\sigma_X\sigma_{\dot{X}}}\exp\{-\frac{(x-\overline{X})^2}{2\sigma_X^2}-\frac{\dot{X}^2}{2\sigma_{\dot{X}}^2}\} \times\sum_{m,n} b_{mn}H_m(\frac{x-\overline{X}}{\sigma_X})H_n(\frac{\dot{x}}{\sigma_{\dot{X}}}) \tag{4.76}$$

where $\overline{X}$ is the mean of X and b_{mn} is a function of the higher moments of X and $\dot{X}$.

Vinje[17] has found the same equation as (4.76) by using the Taylor expansion of cumulants. Hineno[18] and Dalzell[19] extended the above method to the method obtaining three dimensional joint p.d.f.'s, i.e. $p_{X\dot{X}\ddot{X}}$.

(ii) Independence approximation

Although X and $\dot{X}$ are not generally mutually independent, let their independence be assumed. Then a p.d.f. of maxima that are greater than $y+\overline{X}$ is given by:

$$p_p(y) = -\frac{d}{dy}\{\frac{p_X(y+\overline{X})}{p_X(\overline{X})}\} \quad , y \geq 0 \tag{4.77}$$

This means that the maxima p.d.f. can be represented in terms of the derivative of the p.d.f. of the instantaneous response.

4.1.3 1/n th highest mean amplitude and extreme value

From the maxima p.d.f., 1/n th highest mean value can be represented as:

$$\overline{X}_{\frac{1}{n}} = \int_{\overline{X}_{\frac{1}{n}}}^{\infty} x p_p(x)dx \tag{4.78}$$

$$1/n = 1 - P_p(\overline{X}_{\frac{1}{n}}) \tag{4.79}$$

where P_p is the peak probability distribution function.

An extreme value will be derived by applying the order statistics. The extreme value is defined here as the largest maxima that occur in N observations.

Let $(\eta_1, \eta_2, \cdots, \eta_N)$ be an ordered sample of size N, where η_i have the same p.d.f. given by Eq.(4.66). If η_i is recorded as $\eta_1, \eta_2, \cdots, \eta_N$, η_i can be regarded as the output of an independent random variable z_i. Thus the random variable z_N, which is the largest η_N in the ordered sample, has the following p.d.f.:

$$f(z_N;N) = N p_p(z_N)[1-P_p(z_N)]^{N-1} \tag{4.80}$$

Then the estimation of an extreme response is obtained as:

$$E[z_N] = \int_0^{\infty} Z \cdot f(Z;N)dZ \tag{4.81}$$

Approximation based on Poisson distribution law

Naess[5] has introduced an alternative approximation based on Poisson distribution law to obtain the extreme statistics. His approximation is as follows:

The statistics of high level excursions and extreme values of the total second order response are largely determined by the mean upcrossing frequency $\nu_Z^+ = E[N^+(z)]$ for large z. If extreme values are associated with very high levels and upcrossings of such levels are rare events, then the probability such that the extreme values, i.e. $\hat{Z}(T) = max\{X(t) : T \geq t \geq 0\}$, is less than any level z is given by:

$$P_{rob}\{\hat{Z}(T) \leq z\} = \exp(-\nu_Z^+ T) \quad \text{as } z \to \infty \tag{4.82}$$

where T is an observation time. This leads to the assumption that these upcrossings are statistically independent, which in term implies the Poisson probability law. Except in the case of narrow banded process, this would be a reasonable approximation. Now considering the expected value as a statistical measure of the extreme value, its expectation is given as:

$$E[\hat{Z}(T)] = \int_0^\infty z dP_{\hat{Z}}(z) \tag{4.83}$$

where $P_{\hat{Z}}(z) = P_{rob}\{\hat{Z}(T) \leq z\}$.

Since the number of observations N can be replaced by $N = \nu_0^+ T$, we get:

$$\begin{aligned} \log[(1 - P_p(z))^N] &= N \log(1 - \frac{\nu_Z^+ T}{N}) \\ &= -\nu_Z^+ T + O(\frac{\nu_Z^+ T}{N}) \end{aligned} \tag{4.84}$$

This implies that $(1 - P_p)^N$ approaches $\exp(-\nu_Z^+ T)$ as $N \to \infty$. That is, Eq.(4.81) tends to Eq.(4.83) when $N \to \infty$. Thus it is expected that both Eq.(4.81) and Eq.(4.83) lead to a same extreme value estimate for a large N.

4.2 Numerical Examples

From this point forward it will be assumed that the rapidly varying part of the pure second order response is negligible. In this case, the Naess' method does then yield a complete analytical solution for the pure second order response, but it can not be applied to the problem of obtaining the total second order response p.d.f. unless the linear response is negligibly small. Unfortunately an exact closed form or numerical solution for this case has not yet been found. The direct approach to the problem by approximating the p.d.f. using a power series would probably theoretically work, but the effort involved is considered too great. The logical and most conservative approach is to attempt to utilize only a few terms of series expansion. Experience dictates that an important

step in series solution techniques lies in the choice of an expansion function which closely represents the desired nonlinearity characteristics with a minimum number of terms. The present method, "*new approximate theory* " is a series expansion approach that approximates the total second order response p.d.f. by three terms of the generalized Laguerre expansion. This method also gives an approximate solution for the pure second order response. So exactly speaking, the method is a third order approximation because the first, second, and third order statistical moments completely agree with the exact ones. Additionally a convolution integral has to be conducted in the present method which is not the case for the exact Naess' solution. Thus it should not be inferred that the present method is more efficient than the exact Naess' solution. The present method will however be effective in evaluating the effect of the statistical interference between first and second order responses for the extreme response.

(1) Investigation to the pure second order forces and responses

In this section, the present method will be compared to the exact Naess' solution for pure second order forces and sway motion responses in order to show that the present method is an accurate enough approximation. The moored floating structures that will be used for comparisons are two dimensional, lie in the horizontal plane, and have linear restoring forces. The half submerged circular structure has a diameter of 20m, and the half submerged rectangular structure has beam to draft ratio of 2. The principal dimensions are given in Table 4.1. In order to compare the present method for pure second order forces with the Naess' method, the quadratic transfer function $G_2^f(\omega_1, -\omega_2)$ of slow drift forces is required. Thus the same numerical estimates used by Naess were utilized (Faltinsen and Løken[20]).

Tables 4.2 and 4.3 indicate the numerical estimates of the quadratic transfer functions that were obtained by Faltinsen and Løken. To specify the sea state an International Ship Structure Congress (ISSC) spectrum with a significant wave height $H_s = 2m$ and an average period $T_1 = 5.5sec$ is used and is given by:

$$\hat{S}_\zeta(\omega) = \frac{173H_s^2}{T_1^4\omega^5}\exp(-\frac{691}{T_1^4\omega^4}) \tag{4.85}$$

Using this data as a basis, the eigenvalue problem was numerically solved by Naess[5].

Figure 4.2 (a) compares the p.d.f. obtained from the present method and the exact one for the half circular structure, and Fig.4.2 (b) indicates the same comparison for the rectangular cylinder. The results of the present method closely agree with the exact ones except in the peaked area. The difference in the vicinity of the peak may be attributed to the difference between the exact higher order moments greater than the third order, and the ones obtained from the present method.

A comparison of both methods for the pure second order motions will be presented next.

First consider the linear dynamic system as:

$$\ddot{X}_2 + 2\kappa\omega_0\dot{X}_2 + \omega_0^2 X_2 = \frac{F^{(2)}(t)}{M} \tag{4.86}$$

where $F^{(2)}(t)$ is the slowly varying drifting force, $X_2(t)$ the corresponding slow drift sway response, κ a relative damping coefficient , ω_0 the undamped natural frequency, and M the total mass including an added mass per unit length of the cylinders. Parameter values for κ, ω_0, and M are given in Table 4.1. The linear transfer function $H_L(\omega)$, which corresponds to equation (4.68), is given by:

$$H_L(\omega) = \frac{1}{(\omega_0^2 - \omega^2) + 2i\kappa\omega_0\omega} \tag{4.87}$$

Thus, the quadratic transfer function of the slow drift sway response can be represented by:

$$G_2(\omega_1, -\omega_2) = \frac{H_L(\omega_1 - \omega_2)G_2^f(\omega_1, -\omega_2)}{M} \tag{4.88}$$

The same input wave spectrum given in Eq.(4.85) was used for calculating the eigenvalues for the sway response. Naess calculated only eight eigenvalues. This is equivalent to assuming that a random seastate has only eight frequency components. This number is insufficient if a practical seastate situation is considered. Furthermore Naess' results appear to be too inaccurate to estimate eigenvalues for a lightly damped oscillator since the amplitude of H_L changes suddenly at $|\omega_1 - \omega_2| \simeq \omega_0$. As a result, the authors[21] extended the quadratic transfer functions given in Tables 4.2 and 4.3 to higher dimensional matrices by interpolation, then solved the eigenvalue problems, and investigated the relationship between the variances between the pure second order responses and the dimension of the quadratic transfer matrices. From this it was determined that the variances of pure second order response change largely with a decrease of the dimension, and that at least a dimension greater than 200 is required for getting stable variances. Thus based on the above determination 200 dimensions of the quadratic transfer matrices were used.

Figures 4.3 (a), (b), (c) show respectively the p.d.f.'s of pure second order sway motion responses, their tail behavior, and their 1/n th highest mean values for case 1 of Table 4.1. Figures 4.4 (a), (b), (c) show the same parameters for case 2, and Figs. 4.5 (a), (b), (c) case 3. These figures indicate that the p.d.f. calculated by the present method is in good agreement with Naess' exact p.d.f. in contrast to the differences in the pure second order force responses of Fig.4.2 which were discussed previously. There is however a noticeable difference in the tail of the p.d.f. shown in Figs. 4.3 (b), 4.4 (b), and 4.5 (b). The effect of this difference is small because the difference in the 1/n th highest mean

amplitude by the present method shown in Figs. 4.3 (c), 4.4 (c), and 4.5 (c) is only slightly lower than the exact one, i.e. a difference of less than 3%. This difference becomes small as the damping coefficient decreases, i.e. the difference between the Naess' and the present methods in Fig.4.3 (c) is smaller than 1%. Therefore it is considered from practical point of view that the present method is a good approximation with a high degree of accuracy.

The difference between the p.d.f. of pure second order responses and the Gaussian p.d.f. with equal mean and variance will briefly be discussed next. Before doing this it should be noted that the Rayleigh method in figures 4.3 (c), 4.4 (c), and 4.5 (c) is an approximation to predict the 1/n th highest mean amplitude under the assumptions that responses are Gaussian and narrow banded, i.e. the maxima p.d.f. is a Rayleigh p.d.f. When the damping coefficient κ is significantly reduced to a value of 3×10^{-5}, it can be seen by comparing Fig.4.3 (a) to Figs.4.4 (a) and 4.5 (a) that the mean value, which is the mean drift displacement, is small. Similarly the asymmetry of the p.d.f. about the mean value is small, indicating that the pure second order response p.d.f. approaches the Gaussian p.d.f. However the difference becomes much more significant in the tail response as well as the 1/n th highest mean amplitude. This is as expected because the tail of the pure second order response p.d.f. behaves like $O(\exp(-x))$(e.g. Eq.(4.14)), while that of a Gaussian p.d.f. behaves like $O(\exp(-x^2))$. When κ is increased there is an increase in the mean value and the asymmetry of the p.d.f. around the mean value. Thus as the damping coefficient is increased there is a greater deviation between the p.d.f. of the pure second order response and the Gaussian p.d.f. This results in Gaussian approximation that will significantly underestimate high level excursions and extreme responses. The use of moored circular or rectangular structures shows no differences and thus do not influence this conclusion.

(2) Statistical interference between first and second order responses

In general the first and second order responses are not mutually independent so it is important to study the statistical interference of both responses. Thus we shall consider the following system:

$$\ddot{X} + 2\kappa\omega_0\dot{X} + \omega_0^2 X = \frac{(F^{(1)}(t) + F^{(2)}(t))}{M} \tag{4.89}$$

where $F^{(1)}$ is a linear wave exciting force, $M = 3.21 \times 10^5$ kg/m, ω_0 =0.1 rad/sec, and the damping coefficient κ being equal to 0.1,0.006, and 0.0001.

Calculations were conducted only for the half circular cylinder. The wave exciting forces were calculated based on two dimensional potential theory(see Table 4.4). The ratio of the standard deviation of the second order exciting force response to the first order response (σ_2/σ_1) is 3.31×10^{-4}, and the ratios for the sway motion response are 1.36, 2.9, and 4.96 for κ=0.1, κ=0.006 and κ=0.0001, respectively. The numerical results are shown in Figs.4.6 through

4.8, and are compared to the Gaussian p.d.f. and the p.d.f. for pure second order responses. Based on these figures, it was determined that the p.d.f. of the total second order response was widely distributed, while that of the pure second order response was narrowly distributed, with the Gaussian p.d.f. being located between these two distributions. The width of the p.d.f. of the total second order response is strongly dependent on the damping coefficient. When the damping coefficient is decreased, the width of the p.d.f. of the total second order response becomes narrow and approaches that of the pure second order response. The difference between the p.d.f.'s. of the pure and total second order responses in the tail region may be caused by the following reasons:

> Since maximum double amplitudes of a pure first order response can possibly occur at the pure second order response peaks, the probability density of the total second order response increases as compared to the pure second order tail response.

Furthermore it should be noted that the p.d.f. of total second order response differs from the Gaussian p.d.f. in the tail region even though both p.d.f.'s are, on the whole, in good agreement as the damping force decreases to zero. With respect to the 1/n th highest mean amplitude, the results shown in the total second order response are the largest of the three responses and significantly deviate from the well-known expected value that is estimated using the assumption that the peak p.d.f. is a Rayleigh p.d.f. when the damping coefficient is increased . Thus, if the pure second order approximation is used to predict the highest mean values of the total second order responses or if the assumption that the peak p.d.f. is a Rayleigh p.d.f. are applied, this will cause a large underestimation of high level excursions and extreme values. This fact was experimentally confirmed by the authors[9].

The statistical interference between the first and second order responses can be significantly large as shown by the use of these examples, and so it must be taken into account for the motion prediction of moored vessels in random seas.

(3) Relationship between the damping and restoring force coefficients and 1/10 th highest mean amplitude

In this section the variation of the 1/10 th highest mean amplitudes is investigated following changes in damping and restoring force coefficients. Fig.4.9 (a) shows the relationship between the damping coefficient and the 1/10 th highest mean amplitude. In this figure all the lines approach the well -known expected value for the Rayleigh p.d.f. as the damping coefficient is decreased, but the results of the total second order response deviate considerably from the estimated one with an increase in the damping coefficient.

The relation between the restoring force coefficient and the 1/10 th highest mean amplitude is shown in Fig.4.9 (b). In this figure the X axis indicates the

undamped natural frequency because the restoring force coefficient is proportional to the square of the natural frequency if the total mass is held constant. When the restoring force is increased the 1/10 th highest mean amplitude of the pure second order response approaches the well-known expected value for the Rayleigh p.d.f., while the 1/10 th highest mean amplitude of the total second order response deviates from its expected value for Rayleigh p.d.f. by becoming larger.

4.3 Comparisons between estimates and experimental results

In order to investigate the applicability of the present method to the measured slow drift motion, we shall compare the results estimated by the present method with the statistics obtained from the model test(see 3.4.1).

(1) Instantaneous p.d.f.

First of all, we must solve the eigenvalue problem (4.5) for obtaining the instantaneous p.d.f. Utilizing the quadratic transfer function with viscous effect shown in 3.4.5, the integral equation leads to the linear algebraic equations with 512 dimensions since the lag number of the wave spectrum was 256. However if we adopt the slow drift approximation indicated by Naess, the integral equation generates a set of double eigenvalues. Thus the algebraic equations can be reduced to a set of 256 frequencies in the positive frequency range. In the 256 frequencies we use only the 32 frequency components which are within a frequency range where the wave spectral densities are more than 10 % to the peak.

Table 4.5 shows the examples of eigenvalues obtained by solving the 32 dimensional algebraic equations.

Comparisons between the statistical values estimated from the relation (4.11) and the sample ones obtained from the time average of the measured data are shown in Table 4.6, where $\tilde{\theta}_i$ and $\tilde{\nu}_i$ are parameters of Gamma p.d.f. and "*wave condition No.*" indicated in the tables corresponds to the number shown in Table 3.3. From both tables it is seen that the estimated statistical values agree with the sample ones even though the number of eigenvalues used for calculation is a few.

The instantaneous p.d.f.'s of slowly varying second order surge response are indicated in Figs.4.10 and 4.11. In these figures the solid line shows the line due to the present method, the dash-dotted line expresses the Gaussian distribution function and the broken line the result of the third order Gram-Charlier expansion. The probability distribution is asymmetry with respect to the mean value even if the restoring force is linear, and it has the tendency that the tail spreads towards the direction drifted by waves. And the difference between the

probability distribution due to the present method and the Gaussian distribution is certainly significant at the tail and the agreement of the present method and the third order Gram-Charlier series method with the observed histograms is still good.

(2) Maxima p.d.f.

For mooring design purpose, positive maxima is the most important of all maxima. Figure 4.12 compares the observed positive maxima and the estimated maxima p.d.f.'s. The dash-dotted line is the Rayleigh p.d.f., the solid line is the curve due to the present method, and the broken line is the result due to the third order Gram-Charlier series method, where an assumption of the independence between the response process and its time derivative process was used for comparison. From this figure, it is found that the observed positive maxima histograms exponentially spread towards the tail and that the estimated p.d.f.'s due to the present method are in rough agreement with the observed ones.

(3) Extreme response

Comparisons between the extreme responses due to the present method and the maximum excursions in N_p observations in the total measured data are shown in Figs.4.13 and 4.14. In these figures the dash-dotted line indicates the estimation results by Longuet-Higgins' method[14], which uses the assumption that the maxima p.d.f. yields the Rayleigh p.d.f., and the black circles represent the largest values in each observations of maxima in the long measured data, the broken line is the result due to the third order Gram-Charlier series method, and the solid line is the estimate due to the present method. The extreme values are normalized by the standard deviation of the response. From these figures it is found that the results from the Longuet-Higgins' method significantly underestimate the extreme values whereas those from the present method show fairly good agreement with the largest excursions in the measured data, which are samples of the extreme values.

REFFERENCES IN CAPTER 4

[1] Kac, M. and Siegert, A.J.F.: On the Theory of Noise in Radio Receivers with Square Law Detecter, Journ. of Appl. Physics, vol.18, 1947.

[2] Neal, E: Second Order Hydrodynamic Forces due to Stochastic Excitation, Proc. of 10th ONR Symposium, 1974.

[3] Naess, A.: Statistical Analysis of Second-Order Response of Marine Structures, Journ. of Ship Res., vol.29, 1985.

[4] Naess, A.: The Statistical Distribution of Second-Order Slowly- Varying Forces and Motions, Appl. Ocean Res., vol.8, 1986.

[5] Naess, A.: On the Statistical Analysis of Slow-Drift Forces and Motions of Floating Offshore Structure, 5th OMAE Symposium, vol.1, 1986.

[6] Kato, S. and Ando, S.: On the Statistical Prediction of Horizontal Motions of Moored Floating Structures in Random Waves, Journ. Soc. Nav. Arch. Japan, No.158, 1985. (in Japanese)

[7] Shibata, Y.: Normal Distribution - Characteristics and Applications -, University of Tokyo Press, 1981.

[8] Vinje, T.: On the Statistical Distribution of Second Order Forces and Motion, I.S.P., vol.30, 1983.

[9] Kato, S. and Ando, S.: Statistical Analysis of Low Frequency Responses of a Moored Floating Offshore Structure (1st Report), Papers of Ship Research Institute, vol.23, No.5, 1986.

[10] Papoulis, A.: Probability, Random Variables, and Stochastic Processes, McGraw-Hill, Inc., New York, 1965.

[11] Moriguchi, S. et al.: Mathematical Formulas III, Iwanami, Pub., Tokyo, 1959.

[12] Lin, Y.K.: Probabilistic Theory of Structural Dynamics, Mcgraw-Hill, New York, 1967.

[13] Huston, W.B. and Skopinski, T.H.: Probability and Frequency Characteristics of Some Flight Buffet Loads, NACA TN3733, 1956.

[14]. Cartwright, D.E. and Longuet-Higgins, M.S.: The Statistical Distribution of the Maxima of a Random Function, Proc. of the Royal Society, vol.237, 1956.

[15] Courant, R. and Hilbert, D.: Methoden der Mathematischen Physik, New York, Interscience, Pub., 1931.

[16] Watson, G.N.: Generating Functions for Polynomials II, Journal of the London Mathematical Society, vol.8, 1933.

[17] Vinje, T.: On the Calculation of Maxima of Nonlinear Wave Forces and Wave Induced Motion, I.S.P., vol.23, No.268, 1976.

[18] Hineno, M.: A Calculation of the Statistical Distribution of the Maxima of Nonlinear Responses in Irregular Waves (2nd Report), J. Soc. Nav. Arch. Japan, vol.159, 1986.

[19] Dalzell, J.F.: Approximations to the Probability Density of Maxima and Minima of the Response of a Nonlinear System, U.S. Naval Academy Report, No.EW-22-84, 1984.

[20] Faltinsen, O.M. and Løken, A.E.: Slow Drift Oscillations of a Ship in Irregular Waves, Appl. Ocean Res., vol.1, 1979.

[21] Kinoshita, T., Kato, S., and Takase, S: Non-normality of Probability Density Function of Total Second Order Responses of Moored Vessels in Random Seas, J. Soc. Nav. Arch. Japan, No.164, 1988.

Chapter 5

Conclusions

This paper describes the researches about the slowly varying second order response simulations of moored floating structures in random seas and its stochastic analysis.

First, we reviewed the study on the slowly varying drift forces causing the slowly varying response and discussed four problems excluded in the investigations obtained up to now. As the most important problems in them, the following problems are treated in this paper.

a) Hydrodynamic forces of slow drift motion in still water are modified in waves.

b) The Newman-Pinkster's approximation for the slowly varying drift force does not satisfy the condition of physical causality.

Second, it is shown that the total second order force including slow drift forces can be represented by a two term Volterra functional series. Physical meanings of the kernel functions in the functional series are investigated from a viewpoint of frequency response functions (or transfer functions) and a method estimating the kernel ones from experimental data is also studied, which is the method using the bispectrum (a kind of higher order spectra). Furthermore a new functional model such that the second term of the Volterra functional series can be represented by the equivalent linear process of instantaneous wave power is developed. The new function model is based on the Wiener filter theory.

Several kinds of experiments have been carried out. Relation between the kernel function and the frequency response function of the slow drift force is investigated through comparisons between the experimetal results and numerical calculations. And the applicability of the newly developed functional model is studied by comparing between the experimental data and numerical simulations. And the unsolved problems a)(i.e. how much the hydrodynamic forces in still water are modified in waves) and b) are investigated by using the new functional model.

Finally, on the basis of the obtained results a theory of probability density functions(p.d.f.'s) is developed for an instantaneous total second order response and its maxima, in order to predict 1/n th highest mean amplitudes and extreme responses. New formulas for the total second order p.d.f.'s which include not only quadratic but also linear responses are derived. These new p.d.f.'s can be represented by the generalized Laguerre polynomials of which the first term is a Gamma p.d.f. consisting of three parameters. Assuming that the response and its time derivative processes are mutually independent, the 1/n th highest mean amplitude can be evaluated numerically from the derivative of the instantaneous response p.d.f.. This method is first applied to the sway motion of moored floating semi-circular and rectangular two dimensional cylinders, and the applicability of the method is studied by comparisons with Naess' exact solution. The variation of the 1/n th highest mean amplitude of the total second order response is then investigated following increases in damping and restoring forces. And comparisons between the experimental results and the calculated ones obtained from the present theory are carried out. The applicability of the present theory is confirmed.

The summary of the results obtained in this paper are as follows:

(1) The total second order responses(forces and motions) can be represented by a two term Volterra functional series and the quadratic transfer function in the second term of the functional series physically correspond to a frequency characteristic of the mean and slowly varying drift responses. On the basis of the mathematical fact that by using the Wiener filter theory, the second term of the Volterra functional series can be expressed by an equivalent linear process of instantaneous wave power in stochastic sense, a new functional model is developed. This model can be used not only to simulate mean and slowly varying drift responses of moored floating structures but also to solve the problems a) and b) mentioned previously.

(2) The quadratic transfer function in the Volterra functional series (or present functional model) can not only be estimated from the bispectral analysis of experimental data, but also be calculated from pressure integrals over the instantaneous wetted surface of a floating body within the potential theory. As to the quadratic transfer function, comparison between the result obtained through the cross bispectral analysis of experimental data and the numerical ones is conducted. As the result, it is found that the numerical result based on the potential theory is remarkably lower than the experimental ones and the difference of both results can be accounted for by viscous drift force, which occurs by the finiteness of incident wave amplitude and is proportional to the third power of wave amplitude. If the viscous drift force is taken into account to the quadratic transfer function obtained from numerical calculations even though it is approximately

evaluated, the corrected numerical result is in good agreement with the experimental one. And the linear frequency response function can roughly be estimated from the ususal linear motion prediction method considering the viscous damping force. But when the slow drift motion response is dominant compared with the linear motion response, the damping force at the slow drift motion increases by 1.6 times as large as one in still water whereas the added mass force at the slow drift motion becomes smaller than that in still water. It may be considered that for semi-submersibles this phenomenon is attributed to not only the nonlinear coupled viscous damping but also the wave drift damping and others.

(3) Comparisons between the simulated results due to the present functional model and the experimental ones have been conducted in time domain, and it has confirmed that both results are in good agreement, however it remains unsolved how much and why the added mass and the damping forces in still water are modified in waves.

(4) An approximate solution is presented for calculating the p.d.f.'s (instantaneous p.d.f. and maxima p.d.f.) of total second order responses including first order as well as second order motions. It is confirmed through comparisons with Naess' exact solution that the present method is an accurate approximation for pure second order forces and responses.

(5) Using the present method, an investigation to determine the statistical interference between the first and second order responses was conducted for a system with a linear damping and a linear restoring forces. The p.d.f. of the total second order response differs from that of the pure second order response. In fact it becomes a widely-banded distribution with an increase in the damping coefficient. Additionally it significantly deviates from the Gaussian p.d.f..

(6) The 1/10 th highest mean amplitude of the total second order response is greater than that obtained using the pure second order approximation or by using the conventional method which is estimated under the assumption that the peak p.d.f. is a Rayleigh p.d.f.. Thus the statistical interference between the first order and second order responses must be taken into account for prediction of extreme responses and high level excursions. The statistical interference changes with variations in the damping and restoring forces.

(7) As to the extreme response, comparison between the result obtained from the present method and one from the model test during long duration has been carried out. It is confirmed that the usual prediction method based on the Longuet-Higgins' method significantly underestimates the measured results while the present method estimates them very well. And

it is shown that the extreme response of the total second order response is greater than that based on the assumption of the pure second order response.

Moreover, some subjects excluded in this paper, for example, mooring forces, comparisons between estimated results and at-sea experimental results etc., are going to be completed in future.

Acknowledgment

This work has been supported in part by the special coordination fund for T.T.R.D.(Transport Technology Research & Development) of the Ministry of Transport of the Japanese Government, as a part of the research on evaluation of mooring system of floating offshore structures. And the stochastic research of the work has been conducted as the cooperative study between SRI(Ship Research Institute) and I.I.S.(Institute of Industrial Science of University of Tokyo).

The author is grateful to acknowledge Prof. H. Maeda of I.I.S., University of Tokyo for some discussions and criticism and would like to do Mr. Takase, who is a graduate student of University of Tokyo, for some calculations. And the author would like to acknowledge Mr. S. Ando, who is the Head of Ocean Engineering Division of SRI, for his sincere encouragement and support and also appreciates the assistances in the experiments of K. Hoshino, who is one of research staffs in Ocean Engineering Division of SRI. The computations were carried out on the Acos 910/8 and Fujitsu FACOM M-180 II AD computers at the central computer centre of SRI.

APPENDICES

Contents

Appendix A

Theory of wave drift forces based on the potential theory

The wave drift force based on the potential theory is the low frequency component of the second order force caused by nonlinear interaction between first order phenomena at multiple frequency. In order to exactly evaluate the force it is necessary to formulae the second order problem in a sophisticated manner.

In this section we introduce the regular perturbation technique formulated by Ogilvie[1].

A.1 Coordinate system

we define two sets of axes:

$Oxyz = Ox_1x_2x_3$: inertial(space fixed) axes;
$O'x'y'z' = O'x'_1x'_2x'_3$: body fixed axes.

The $Oxyz$ axes have their origin in the plane of the undisturbed free surface with z axis pointing upwards. The two sets of axes coincide when the body is at rest.(see Fig.A.1)

A.2 Boundary value problem

We consider hydrodynamic forces acting on the floating body oscillating in waves under the coordinate system shown in Fig.A.1. The theory is based on the assumption that the fluid surrounding the body is inviscid, irrotational, homogeneous, and incompressible. The fluid motions may then be described by a

velocity potential from which the velocity field can be derived by taking the gradient:

$$\vec{V} = \nabla\Phi \tag{A.1}$$

where $\Phi(\vec{x}, t)$ is a velocity potential and it satisfies the Laplace equation:

$$\text{[L]: } \Delta\Phi = 0 \tag{A.2}$$

If the potential Φ is known, the pressure in a point in the fluid may be determined using the Bernoulli equation:

$$\frac{p(x,y,z,t)}{\rho} = -\Phi_t - \frac{(\nabla\Phi)^2}{2} - gz \tag{A.3}$$

where ρ is the fluid density, g is the gravitational acceleration. If the elevation of the free surface is given by $\zeta(x, y, t)$, the following two conditions must be satisfied:

$$\frac{D(z-\zeta)}{Dt} = \Phi_z - \zeta_t - \Phi_x\zeta_x - \Phi_y\zeta_y = 0 \quad \text{on } z = \zeta \tag{A.4}$$

$$\frac{p_0}{\rho} = -\Phi_t - (\nabla\Phi)^2 - gz \quad \text{on } z = \zeta \tag{A.5}$$

The first shows the kinematic condition of free surface and the second does that the pressure is constant on the free surface. These free surface conditions are exact under the assumption that viscosity and surface tension are negligible.

Eliminating ζ from the conditions, the free surface conditions can be rewritten as:

$$\begin{aligned}\text{[F]: } & \Phi_{tt} + g\Phi_z + 2(\Phi_x\Phi_{xt} + \Phi_y\Phi_{yt} + \Phi_z\Phi_{zt}) + \Phi_x^2\Phi_{xx} + \Phi_y^2\Phi_{yy} + \Phi_z^2\Phi_{zz} \\ & +2(\Phi_x\Phi_y\Phi_{xy} + \Phi_y\Phi_z\Phi_{yz} + \Phi_z\Phi_x\Phi_{zx}) = 0 \qquad \text{on } z = \zeta\end{aligned} \tag{A.6}$$

Let the body surface, S, be given by an equation of the form:

$$S(x, y, z, t) = 0$$

and let $\vec{n}$ be a unit vector normal to the body surface, pointing outward from the fluid, thus into the body. A body condition given by:

$$\text{[H]: } \frac{\partial\Phi}{\partial n} = \vec{n} \bullet \nabla\Phi = v_n \tag{A.7}$$

where v_n is the normal component of velocity of the body itself.

If a bottom surface is given by $z = h(x, y)$, the bottom condition becomes:

$$\text{[B]: } \frac{\partial\Phi}{\partial n} = 0 \quad \text{on } z = h(x, y) \tag{A.8}$$

In addition, an outgoing wave radiation condition must be satisfied.

In general, it is difficult to directly solve the above boundary value problem in time domain because the free and body surfaces moves with time, and the boundary value problem must have already been solved to determine the movements of free and body surfaces. These problems can usually be solved by making a linearization by means of a perturbation technique. In order to carry out a perturbation analysis, we assume that there exists a small parameter that provides a basis for ordering all quantities that arise. We can think of this parameter as the maximum wave slope, for example, although its precise definition does not really matter. We assume further that quantities such as and can be expressed as power series in:

$$\Phi(x,y,z,t) \sim \sum \epsilon^j \varphi_j(x,y,z,t) + O(\epsilon^{N+1}) \tag{A.9}$$

$$\zeta(x,y,t) \sim \sum \epsilon^j \zeta_j(x,y,t) + O(\epsilon^{N+1}) \tag{A.10}$$

Substituting these expansions into the free surface conditions, and assuming that all quantities that are supposed to be evaluated on $z = \zeta$ can be evaluated alternatively by expansions with respect to $z = 0$, then we get the following pairs of free surface boundary conditions for the first and second order problems:

$$O(\epsilon): \qquad \varphi_{1tt} + g\varphi_{1z} = 0 \quad \text{on } z = 0 \tag{A.11}$$

$$\zeta_1 = -\frac{\varphi_{1t}}{g}\,|_{z=0} \tag{A.12}$$

$$O(\epsilon^2): \qquad \varphi_{2tt} + g\varphi_{2z} = -\frac{\partial}{\partial t}(\varphi_{1x}^2 + \varphi_{1y}^2 + \varphi_{1z}^2) + \frac{\varphi_{1t}}{g}\frac{\partial}{\partial z}(\varphi_{1tt} + g\varphi_{1x}) \text{ on } z = 0 \tag{A.13}$$

$$\zeta_2 = [-\frac{\varphi_{2t}}{g} - \frac{1}{2}g(\varphi_{1x}^2 + \varphi_{1y}^2 + \varphi_{1z}^2) + \frac{\varphi_{1t}\varphi_{1tz}}{g^2}]\,|_{z=0} \tag{A.14}$$

In addition, we need a bottom condition and a radiation condition for each problem.

A.3 Body surface condition

Before considering the body surface condition, we shall define the transformation of coordinates.

Let the position of O′ with respect to O be denoted by the vector $\vec{\xi} = (\xi_1, \xi_2, \xi_3)$ and let the position vector to a point in space be denoted by

$$\vec{X} = (x,y,z) = (x_1, x_2, x_3) \tag{A.15}$$

$$\vec{X}' = (x',y',z') = (x_1', x_2', x_3') \tag{A.16}$$

respectively, in the two coordinate systems. The position vectors are related by a linear transformation

$$\vec{X}' = \mathbf{D}(\vec{X} - \vec{\xi}) \tag{A.17}$$

$$\vec{X} = \mathbf{D}^{-1}\vec{X}' + \vec{\xi} \tag{A.18}$$

where $\mathbf{D}$ is a matrix presenting the rotation of body and $\mathbf{D}^{-1}$ is its transpose. For such matrices, we note that the product $\mathbf{D} \bullet \mathbf{D}^{-1}$ is the unit matrix.

In order to consider the rotations, we may use the concept of Euler angles (or an equivalent) to specify the instantaneous orientation of the body, and the resulting expression for $\mathbf{D}$ depends on the order in which the three rotations are taken. The order is, of course, arbitrary, since any displacement of a rigid body can be described as the sum of a translation and a single rotation about some axis. But that axis constantly changing in time, and so we must use a systematic method of describing the kinematics of the body. Our choice is to take roll, pitch, and yaw, in that order. These are not the Euler angles described in a textbook, but they are more useful for our present problem.

First, neglect the translations and consider only rotations (thus O and O' coincide). Define a new coordinate system $O\tilde{x}\tilde{y}\tilde{z}$ that is identical to the $Oxyz$ system except for a positive rotation ξ_4 about the x axis. Thus $\tilde{x} = x$. The transformation from $\vec{\tilde{X}}$ to $\vec{X}$ is simple:

$$\begin{aligned}\vec{\tilde{X}} &= \mathbf{A}\vec{X} \\ &= \begin{pmatrix} 1 & 0 & 0 \\ 0 & \cos\xi_4 & \sin\xi_4 \\ 0 & -\sin\xi_4 & \cos\xi_4 \end{pmatrix} \vec{X}\end{aligned} \tag{A.19}$$

Then we make a second rotation, this time through an angle ξ_5 about the $\tilde{y}$ axis. Let the new axes be denoted by $O\hat{x}\hat{y}\hat{z}$.

$$\begin{aligned}\vec{\hat{X}} &= \mathbf{B}\vec{\tilde{X}} \\ &= \begin{pmatrix} \cos\xi_5 & 0 & -\sin\xi_5 \\ 0 & 1 & 0 \\ \sin\xi_5 & 0 & \cos\xi_5 \end{pmatrix} \vec{\tilde{X}}\end{aligned} \tag{A.20}$$

Finally, the third rotation, through the angle ξ_6 about the $\hat{z}$ axis, brings the axes into coincidence with the $Ox'y'z'$ axes:

$$\begin{aligned}\vec{\hat{X}}' &= \mathbf{C}\vec{\hat{X}} \\ &= \begin{pmatrix} \cos\xi_6 & \sin\xi_6 & 0 \\ -\sin\xi_6 & \cos\xi_6 & 0 \\ 0 & 0 & 1 \end{pmatrix} \vec{\hat{X}}\end{aligned} \tag{A.21}$$

The complete transformation is obtained by applying these in order, according

to the usual rules of matrix multiplication:

$$\mathbf{D} = \begin{pmatrix} c_5c_6 & c_4s_6 + s_4s_5c_6 & s_4s_6 - c_4s_5c_6 \\ -c_5s_6 & c_4c_6 + s_4c_5s_6 & s_4c_6 + c_4s_4s_6 \\ s_5 & -s_4c_5 & c_4c_5 \end{pmatrix} \tag{A.22}$$

where $s_n = \sin\xi_n, c_n = \cos\xi_n, n = 4,5,6$ and $\mathbf{D}^{-1}$ is equal to the transpose matrix of $\mathbf{D}$.

If $\vec{\xi} = (\xi_1, \xi_2, \xi_3)$ and $\vec{\alpha} = (\xi_4, \xi_5, \xi_6)$ can be expanded in the following form;

$$\vec{\xi} = \epsilon\vec{\xi}^{(1)} + \epsilon^2\vec{\xi}^{(2)} + O(\epsilon^3) \tag{A.23}$$

$$\vec{\alpha} = \epsilon\vec{\alpha}^{(1)} + \epsilon^2\vec{\alpha}^{(2)} + O(\epsilon^3) \tag{A.24}$$

then this becomes:

$$\begin{aligned} \mathbf{D} &= \mathbf{D}^{(0)} + \epsilon\mathbf{D}^{(1)} + \epsilon^2\mathbf{D}^{(2)} + O(\epsilon^3) \\ &= \begin{pmatrix} 1 & 0 & 0 \\ 0 & 1 & 0 \\ 0 & 0 & 1 \end{pmatrix} + \begin{pmatrix} 0 & \xi_6 & -\xi_5 \\ -\xi_6 & 0 & \xi_4 \\ \xi_5 & -\xi_4 & 0 \end{pmatrix} \\ &\quad -\frac{1}{2}\begin{pmatrix} \xi_5^2+\xi_6^2 & -2\xi_4\xi_5 & -2\xi_4\xi_6 \\ 0 & \xi_4^2+\xi_6^2 & -2\xi_5\xi_6 \\ 0 & 0 & \xi_4^2+\xi_5^2 \end{pmatrix} + O(\epsilon^3) \end{aligned} \tag{A.25}$$

Thus, from Eq.(A.18) $\vec{X}$ can be expressed as:

$$\vec{X} = \vec{X}' + \epsilon[\vec{\xi}^{(1)} + \vec{\alpha}^{(1)} \times \vec{X}'] + \epsilon^2[\vec{\xi}^{(2)} + \vec{\alpha}^{(2)} \times \vec{X}'] + \epsilon^2\mathbf{H}\vec{X}' + O(\epsilon^3) \tag{A.26}$$

where

$$\epsilon^2\mathbf{H} = \epsilon^2[\mathbf{D}^{(2)}]^{-1} \tag{A.27}$$

If X' is a fixed point vector, the velocity is

$$\vec{u} = \dot{\vec{X}} = \epsilon[\dot{\vec{\xi}}^{(1)} + \dot{\vec{\alpha}}^{(1)} \times \vec{X}'] + \epsilon^2[\dot{\vec{\xi}}^{(2)} + \dot{\vec{\alpha}}^{(2)} \times \vec{X}'] + \epsilon^2\dot{\mathbf{H}}\vec{X}' + O(\epsilon^3) \tag{A.28}$$

where the dot $\bullet$ denotes time derivative.

Let $\vec{n}$ be a unit vector normal to the body, directed into the body. In the $O'x'y'z'$ axes, the same vector is denoted by $\vec{n}'$. Since $\vec{n}$ does not depend on the translation vector $\vec{\xi}$, from (A.19) to (A.24) it is represented by

$$\vec{n} = \vec{n}' + \epsilon[\vec{\alpha}^{(1)} \times \vec{n}'] + \epsilon^2[\vec{\alpha}^{(2)} \times \vec{n}'] + \epsilon^2\mathbf{H}\vec{n}' + O(\epsilon^3) \tag{A.29}$$

while a rotational normal vector is obtained from vector products of (A.26) and (A.29) as:

$$\vec{X}\times\vec{n} = \vec{X}'\times\vec{n}' + \vec{\xi}\times\vec{n}' + \vec{\alpha}\times(\vec{X}'\times\vec{n}') + \vec{\xi}\times(\vec{\alpha}\times\vec{n}') + \epsilon^2\mathbf{H}(\vec{X}'\times\vec{n}') + O(\epsilon^3) \tag{A.30}$$

since the following vector relation holds:

$$\vec{A} \times (\vec{B} \times \vec{C}) + \vec{B} \times (\vec{C} \times \vec{A}) + \vec{C} \times (\vec{A} \times \vec{B}) = \vec{0}$$

Next we shall consider a kinematic condition on the body itself. We assume that the body surface can be described in $O'x'y'z'$ axes (the body fixed coordinate system) by an equation of the form

$$S'(x', y', z') = 0 \tag{A.31}$$

or in $Oxyz$ axes (space fixed coordinate system)

$$S(x, y, z, t) = 0 \tag{A.32}$$

The hydrodynamic problem forces us to use the $Oxyz$ coordinates, in which the unit normal on $S = 0$ is a function of time. So we reinterpret (A.31):

> $S'(x, y, z) = 0$ specified the body surface in its equilibrium position, and we use the transformation of coordinates to express $\vec{n}$ in terms of $\vec{n}'$, the unit normal vector to the body surface in its mean position.

As noted earlier,(A.29) provides this relationship. In order to avoid any possible ambiguity, we shall use the following notations:

S : exact wetted surface, described with respect to $Oxyz$ axes ($S(x, y, z, t) = 0$);

S' : exact wetted surface, described with respect to $O'x'y'z'$ axes ($S'(x', y', z') = 0$);

S_m : wetted surface of the body in its equilibrium condition ($S'(x, y, z) = 0$).

The boundary condition is

$$\vec{n} \nabla \Phi = \vec{n} \bullet \vec{u} \quad \text{on} S \tag{A.33}$$

where $\vec{u}$ is the velocity of the surface S. Equation (A.28) gives $\vec{u}$ in terms of the vector $\vec{X}'$ of a body point in the body fixed coordinate system, but we reinterpret $\vec{X}'$ as the position vector in the $Oxyz$ axes of that body point when the body is at rest. So, if we replace $\vec{X}'$ by $\vec{X}$ in (A.28) and consider $\vec{X}$ as a point on the surface S_m, then (A.28) gives the actual velocity of that point on the body, but referred to the location of the point on S_m. Similarly, we use (A.29) to give the actual normal vector, but referred to the corresponding point on S_m.

In (A.33) $\nabla\Phi$ has to be evaluated. We assume that the velocity potential and its derivatives can be evaluated on the exact surface through Taylor expansions with respect to points on the mean surface:

$$\nabla\Phi = \epsilon \nabla\varphi_1 + \epsilon^2 \nabla\varphi_2 + O(\epsilon^3) \tag{A.34}$$

and

$$\nabla\varphi_i = \nabla\varphi_i^m + [(\vec{X} - \vec{X}')\nabla]\nabla\varphi_i^m + \cdots \text{ on } S_m \qquad \text{(A.35)}$$

where $(\vec{X} - \vec{X}')$ is given by (A.26).

Substituting (A.35) into (A.34), and using Eqs.(A.23) and (A.24), Eq.(A.34) can be expanded by the quantities of the body surface S_m as:

$$\nabla\Phi = \epsilon\nabla\varphi_1^m + \epsilon^2\{\nabla\varphi_2^m + [(\vec{\xi}^{(1)} + \vec{\alpha}^{(1)} \times \vec{X}')\nabla]\nabla\varphi_1^m\} + O(\epsilon^3) \qquad \text{(A.36)}$$

Now, when all of the terms are organized according to powers of ϵ, we have the pairs of conditions:

$$O(\epsilon) \quad : \vec{n}'\nabla\varphi_1^m = \vec{n}'[\dot{\vec{\xi}}^{(1)} + \vec{\alpha}^{(1)} \times \vec{X}'] \quad \text{on } S_m \qquad \text{(A.37)}$$

$$O(\epsilon^2) \quad : \vec{n}'\nabla\varphi_2^m = \vec{n}'[\dot{\vec{\xi}}^{(2)} + \vec{\alpha}^{(2)} \times \vec{X}'] + \dot{\mathbf{H}}\vec{X}' - [(\vec{\xi}^{(1)} + \vec{\alpha}^{(1)} \times \vec{X}')\nabla]\nabla\varphi_1^m$$
$$+(\vec{\alpha}^{(1)} \times \vec{n}')[(\dot{\vec{\xi}}^{(1)} + \vec{\alpha}^{(1)} \times \vec{X}') - \nabla\varphi_1^m] \qquad \text{(A.38)}$$

where all quantities on the right hand sides are to be evaluated on S_m.

Condition (A.37) is familiar from ship motion theory. In (A.38), the left hand side and the first term on the right hand side are identical to (A.37) except that the index 1 is replaced by 2. With respect to the other terms on the right hand side, it is observed that the second term accounts for nonlinear effects included in the velocity $\vec{u}$, the third term corrects for the fact that $\vec{n}'\nabla\varphi_1^m$ in (A.37) is figured on the mean position of the body instead of on its instantaneous position, and that the last term accounts for the difference in direction between $\vec{n}$ and $\vec{n}'$.

A.4 Force and moment

The three components of force and three components of moment on the body can also be expressed initially as follows:

$$F_i(t) = \iint_S n_i p dS \qquad (i = 1,..,6) \qquad \text{(A.39)}$$

where S is the exact wetted surface of the body, and $p = p(x, y, z, t)$ is the fluid pressure on the body surface. The six quantities n_i, defined in (A.29) and (A.30), must be evaluated instantaneously as functions of time.

In order to proceed further analytically, we transform the integral over S into an integral over S_m, the wetted surface of the body in its equilibrium position in calm water. This requires two kinds of adjustments.

The first is that since S is displaced and rotated with respect to S_m, we must express p and n_i in terms of their values on S_m . For the latter, we use (A.29) and (A.30), the primes now denoting quantities evaluated on S_m. For

p, we assume that values on S can be obtained in terms of a Taylor expansion with respect to S_m,

$$p\,|_S = p\,|_{S_m} + (\vec{X} - \vec{X}')\nabla p)\,|_{S_m} + \cdots \tag{A.40}$$

Since p contains a hydrostatic pressure term, $-\rho g z$, the first term on the right hand side is $O(1)$ and the second term is $O(\epsilon)$. But the hydrostatic pressure has no effect after the second term of the expansion, and so the first unwritten term is actually $O(\epsilon^3)$.

The other is that the integration over S is to be carried right up to the water surface, $z = \zeta$, but the integration over S_m goes up only to $z = 0$ which is equivalent to $z = \xi_3 + y\xi_4 - x\xi_5$ on S (as shown in Fig.A-2). Let ΔS be the part of S between $z = \xi_3 + y\xi_4 - x\xi_5$ and $z = \zeta$. Then, to second order,

$$\begin{aligned}\iint_{\Delta S} n_i p dS \quad &= -\rho \int_{C_m} dl \int_0^{\epsilon[\zeta - \xi_{31} - y\xi_{41} + x\xi_{51}] + \cdots} dz \\ &\times (n_i' + \cdots)\{gz + \epsilon[\varphi_{1t}^m + g(\xi_{31} + y\xi_{41} - x\xi_{51})] + \cdots\}\end{aligned} \tag{A.41}$$

where C_m is the intersection of S_m and the plane $z = 0$, and in the double indices, i.e. ξ_{ij}, the first, i, denotes the orientation of the axis, and the second, j, shows the term in the perturbation expansions. On the right hand side, we can now drop the prime on n_i', since the indicated domain of integration makes it clear that n_i is being evaluated on the mean position of the body. Two further simplifications can be made consistently:

$$\begin{aligned} n_i(x, y, z) &= n_i(x, y, 0) + O(\epsilon) \\ \varphi_{1t}^m(x, y, z, t) &= \varphi_{1t}^m(x, y, 0, t) + O(\epsilon) = -g\zeta_1(x, y, t)\end{aligned}$$

So Eq.(A.41) can be evaluated as:

$$\iint_{\Delta S} n_i p dS = -\frac{\rho g}{2}\epsilon^2 \oint_{C_m} dl n_i [\zeta_1 - \xi_{31} - y\xi_{41} + x\xi_{51}]^2 \tag{A.42}$$

Now let us consider the force. We have divided S into two parts, i.e. the main integral over S_m and the integral given by (A.41). Organizing the results by order of magnitude, we obtain

$$\begin{aligned}\vec{F} \quad &= -\rho g V \vec{k} \\ &-\epsilon\rho\{\iint_{S_m} \vec{n}\varphi_{1t}^m dS + gA_{WP}(\xi_{31} + y_f\xi_{41} - x_f\xi_{51})\vec{k}\} \\ &-\epsilon^2\rho \iint_{S_m} \{\vec{n}[\varphi_{2t}^m + \frac{|\nabla\varphi_1^m|^2}{2} + (\vec{\xi}^{(1)} + \vec{\alpha}^{(1)} \times \vec{X})\nabla\varphi_{1t}^m] + [\vec{\alpha}^{(1)} \times \vec{n}]\varphi_{1t}^m\} dS\end{aligned}$$

$$-\frac{g}{2}\epsilon^2 \oint_{C_m} dl\vec{n}[\zeta_1^2 - 2\zeta_1(\xi_{31} + y\xi_{41} - x\xi_{51})]$$

$$+g\epsilon^2 A_{WP}\{(\xi_{32} + y_f\xi_{42} - x_f\xi_{51}) + \xi_{61}(x_f\xi_{41} + y_f\xi_{51})\}\vec{k} + O(\epsilon^3) \quad \text{(A.43)}$$

where

$\vec{k}$ = unit vector in z direction

$\vec{n}, \vec{X}$ = normal and point vectors in the body-fixed coordinate system

V = volume of displaced water at equilibrium

$$V = \iint_{S_m} zdxdy = \iint_{S_m} xdydz = \iint_{S_m} ydxdz$$

A_{WP} = area of water plane at equilibrium

x_f = position of longitudinal centre of flotation

y_f = position of transverse centre of flotation

$$x_f A_{WP} = \iint_{S_m} xdxdy = \frac{1}{2}\oint x^2 dy$$
$$y_f A_{WP} = \iint_{S_m} ydxdy = \frac{1}{2}\oint y^2 dx$$

Next we divide the first and second order potentials into three parts in the following forms:

$$\begin{aligned} \varphi_1^m &= \varphi_1^I + \varphi_1^d + \varphi_1^r \\ \varphi_2^m &= \varphi_2^I + \varphi_2^d + \varphi_2^r \end{aligned} \quad \text{(A.44)}$$

where the indices I, d, and r denotes the incident wave potential, diffraction potential, and radiation potential respectively. Furthermore, we decompose Eq.(A.43) as:

$$\vec{F} = -\vec{F}_{HS}^{(0)} - \epsilon(\vec{F}_W^{(1)} + \vec{F}_{HD}^{(1)} + \vec{F}_{HS}^{(1)}) - \epsilon^2(\vec{F}_W^{(2)} + \vec{F}_{HD}^{(2)} + \vec{F}_{HS}^{(2)}) + O(\epsilon^3) \quad \text{(A.45)}$$

where the indices, W, HD, and HS denote the wave force, the hydrostatic force, and the hydrodynamic force respectively. Then, organizing the results by order of magnitude, we get:

$$O(1): \quad \vec{F}_{HS}^{(0)} = \rho g V \vec{k} \quad \text{(A.46)}$$

$$O(\epsilon): \quad \vec{F}_W^{(1)} = \rho \iint_{S_m} \vec{n}(\varphi_{1t}^I + \varphi_{1t}^d)dS \quad \text{(A.47)}$$

$$\vec{F}_{HD}^{(1)} = \rho \iint_{S_m} \vec{n}\varphi_{1t}^{r} dS \tag{A.48}$$

$$\vec{F}_{HS}^{(1)} = \rho g A_{WP}(\xi_{31} + y_f\xi_{41} - x_f\xi_{51})\vec{k} \tag{A.49}$$

$$\begin{aligned} O(\epsilon^2): \quad \vec{F}_W^{(2)} &= -\frac{\rho g}{2}\oint_{C_m} dl\vec{n}[\zeta_1 - (\xi_{31} + y\xi_{41} - x\xi_{51})]^2 \\ &+\rho\iint_{S_m}\{\vec{n}[\varphi_{2t}^I + \varphi_{2t}^d + \frac{|\nabla\varphi_1^m|^2}{2} + (\vec{\xi}^{(1)} + \vec{\alpha}^{(1)} \times \vec{X})\nabla\varphi_{1t}^m]\}dS \\ &+\vec{\alpha}^{(1)} \times \vec{F}^{(1)} + \rho g A_{WP}\xi_{61}(x_f\xi_{41} + y_f\xi_{51})\vec{k} \end{aligned} \tag{A.50}$$

$$F_{HD}^{(2)} = \rho \iint_{S_m} \vec{n}\varphi_{2t}^{r} dS \tag{A.51}$$

$$\vec{F}_{HS}^{(2)} = \rho g A_{WP}(\xi_{32} + y_f\xi_{42} - x_f\xi_{52})\vec{k} \tag{A.52}$$

where in order to lead (A.50) the following relation is used.

$$\begin{aligned} &\iint_{S_m}(\vec{\alpha}^{(1)} \times \vec{n})\varphi_{1t} dS - \frac{g}{2}\oint_{C_m} dl\vec{n}[\zeta_1^2 - 2\zeta_1(\xi_{31} + y\xi_{41} - x\xi_{51})] \\ &= \vec{\alpha}^{(1)} \times \vec{F}^{(1)} - \frac{g}{2}\oint_{C_m} dl\vec{n}[\zeta_1 - (\xi_{31} + y\xi_{41} - x\xi_{51})]^2 \end{aligned} \tag{A.53}$$

where

$$\vec{F}^{(1)} = \vec{F}_W^{(1)} + \vec{F}_{HD}^{(1)} + \vec{F}_{HS}^{(1)} \tag{A.54}$$

From (A.50) it is found that the second order force, i.e. $F_W^{(2)}$, consists of the following five terms:

(1) The first term is the component caused by fluid pressure between mean and instantaneous wave surfaces

$$\vec{F}_1^{(2)} = -\frac{\rho g}{2}\oint_{C_m} dl\vec{n}[\zeta_1 - (\xi_{31} + y\xi_{41} - x\xi_{51})]^2 \tag{A.55}$$

(2) The second term comes from the quadratic pressure term in the Bernoulli equation.

$$\vec{F}_2^{(2)} = \frac{\rho}{2}\iint_{S_m} \vec{n}|\nabla\varphi_1^m|^2 dS \tag{A.56}$$

(3) The third arises from the variation of the acting point of fluid pressure.

$$\vec{F}_3^{(2)} = \rho \int\int_{S_m} \vec{n}\{(\vec{\xi}^{(1)} + \vec{\alpha}^{(1)} \times \vec{X})\nabla\varphi_{1t}^m\}dS \tag{A.57}$$

(4) The fourth comes from the variation of direction of first order wave force with respect to rotation of a body.

$$\vec{F}_4^{(2)} = \vec{\alpha}^{(1)} \times \vec{F}^{(1)} \tag{A.58}$$

(5) The last term is the component due to second order potentials

$$\vec{F}_5^{(2)} = \rho \int\int_{S_m} \vec{n}(\varphi_{2t}^I + \varphi_{2t}^d)dS \tag{A.59}$$

Appendix B

Estimation of Cross Bispectrum

FFT, BT and MEM method have been used as the estimation of auto and cross spectra. But the general estimation of bispectra has not been developed so far. In this section, we shall introduce the Dalzell's method[2] as one example of the estimations of cross bispectrum.

Since the sample(one record obtained by experiments) is necessarily finite, it is possible only to estimate cross bispectral averages rather than actual densities:

$$\breve{C}(\Omega_1, \Omega_2) = \iint H(\Omega_3, \Omega_4) C(\Omega_1 + \Omega_3, \Omega_2 + \Omega_4) d\Omega_3 d\Omega_4 \qquad \text{(B.1)}$$

where the average $H(\Omega_3, \Omega_4)$ is weighted by the kernel function, which is called "*cross bispectral window*". The window by analogy with scalar spectrum analysis must take a peak at a bi-frequency $(0.0, 0.0)$, fall off rapidly elsewhere, and remain near zero away from the peak. As for a usual scalar spectrum analysis, a too-broad window makes the estimates bad and a too- narrow window with respect to sample length increases the variance of the estimate. It is clear that since the window is for averaging over frequency, its integral should be unity;

$$\iint H(\Omega_3, \Omega_4) d\Omega_3 d\Omega_4 = 1 \qquad \text{(B.2)}$$

Because the data is sequentially sampled at time interval Δt, bi-frequencies outside the principal range:

$$-\frac{\pi}{\Delta t} < \Omega_1 < \frac{\pi}{\Delta t}$$
$$-\frac{\pi}{\Delta t} < \Omega_2 < \frac{\pi}{\Delta t}$$

are aliased with those inside. It is assumed that the data is sampled at a sufficiently short time interval so that the cross bispectrum is negligible outside

the principal range. According to Dalzell's work[2], the time interval should be about half the interval for a scalar spectrum analysis. Because the data is sampled sequentially, a lag window of the form:

$$h(\tau_1, \tau_2) = \sum_j \sum_k a_j b_k \delta(\tau_1 - j\Delta t)\delta(\tau_2 - k\Delta t) \tag{B.3}$$

is chosen, where the a_j and b_k are real, and $\delta(t)$ is the Dirac's delta function. Then the cross bispectrum estimate is given by:

$$\check{C}(\Omega_1, \Omega_2) = \sum_{j=-m}^{m} \sum_{k=-n}^{n} \tilde{R}_{\eta\eta X}(-j\Delta t, -k\Delta t) a_j b_k \exp\{i\Delta t(j\Omega_1 + k\Omega_2)\} \tag{B.4}$$

This estimator involves the third order correlation function. Setting time, that is, $t = n\Delta t$, the correlation function can be expressed by the form readily available with the sequentially sampled data as:

$$\tilde{R}_{\eta\eta X}(-j\Delta t, -k\Delta t) = E[\tilde{\eta}(n\Delta t + j\Delta t)\tilde{\eta}(n\Delta t - j\Delta t)\{X(n\Delta t + k\Delta t) - \overline{X}\}] \tag{B.5}$$

The expected value is conventionally estimated by a summation over the available sample divided by the sample length and this interpretation is followed so that

$$\begin{aligned} \check{R}(j,k) &= \frac{1}{N'} \sum_n \eta'(n+j)\eta'(n-j)X'(n+k) \\ &\equiv \tilde{R}_{\eta\eta X}(-j\Delta t, -k\Delta t) \end{aligned} \tag{B.6}$$

where:

N' = number of products summed

$\eta'(n)$ = wave elevation time series corrected to zero sample mean

$X'(n)$ = nonlinear response time series corrected to zero sample mean

Next, the main problem is to construct the cross bispectral window $H(\Omega_3, \Omega_4)$. Considering m and n as maximum lags, Eq.(B.4) becomes:

$$\check{C}(\Omega_1, \Omega_2) = \sum_{j=-m}^{m} \sum_{k=-n}^{n} \check{R}(j,k) a_j b_k \exp\{i\pi(j\frac{l_1}{m} + k\frac{l_2}{n}\} \tag{B.7}$$

where $\Omega_1 = \frac{\pi l_1}{m\Delta t}, \Omega_2 = \frac{\pi l_2}{n\Delta t}$.

In choosing the cross bispectral window, it was assumed that the natural choice would be a two-dimensional analogy with the spectral windows to be

used in the estimation of the wave spectrum. The continuous lag window corresponding to the scalar spectrum window is of the form:

$$A(\tau) = q[e_1 + e_2 \cos(\frac{\pi\tau}{m\Delta t})] \tag{B.8}$$

where e_1 and e_2 are coefficients of window function.

Since optimum window function for cross bispectrum estimate has not been known yet, we determined the coefficients as $e_1 = 0.54$ and $e_2 = 0.46$. These coefficients are equal to ones of the Hamming type window function. In Eq.(B.3) the lag window is a product, one factor for each lag variable. The factors may be different. This would result in spectral windows differently shaped in the sum and difference frequencies, as well as having different bandwidths. There appeared no justification for a difference in normalized shape of the window. It was assumed that a discrete version of the scalar spectrum lag window would be appropriate for each of the factors, so that in Eq.(B.3) let:

$$\begin{aligned} a_j(\tau) &= q_j[e_1 + e_2 \cos(\tfrac{\pi j}{m})] \\ b_k(\tau) &= q_k[e_1 + e_2 \cos(\tfrac{\pi k}{n})] \end{aligned} \tag{B.9}$$

where q_j and q_k are constants independent j and k and they are determined by normalization condition, that is, Eq.(B.2). Since the cross bispectral window $H(\Omega_3, \Omega_4)$ and the lag window are a transform pair and thus:

$$\begin{aligned} H(\Omega_3, \Omega_4) &= \frac{q_j q_k}{(2\pi)^3}[\sum_{j=-m}^{m} (e_1 + e_2 \cos(\frac{\pi j}{m})) \cos(\Delta t j \Omega_3)] \\ &\times [\sum_{k=-n}^{n} (e_1 + e_2 \cos(\frac{\pi k}{n})) \cos(\Delta t k \Omega_4)] \end{aligned} \tag{B.10}$$

This result shows that the cross bispectral window is real and symmetric in j and k, and is continuous in Ω_1 and Ω_2. The window also has a period of $\Omega = \frac{2\pi}{\Delta t}$.

Unknown constants q_j and q_k can be determined from normalization condition, Eq.(B.2) as:

$$q_j q_k = \{\frac{\Delta t}{(e_1 + e_2)}\}^2 \tag{B.11}$$

Then the estimate of the cross bispectral averages becomes:

$$\begin{aligned} \breve{C}(\Omega_1, \Omega_2) &= \{\frac{\Delta t}{2\pi(e_1 + e_2)}\}^2 \sum_{j=-m}^{m} \sum_{k=-n}^{n} (e_1 + e_2 \cos(\frac{\pi j}{m}))(e_1 + e_2 \cos(\frac{\pi k}{n})) \\ &\times \exp\{i\pi(\frac{l_1 j}{m} + \frac{l_2 k}{n})\} \frac{1}{N'} \sum_{n} \eta'(n + j)\eta'(n - j)X'(n + k) \end{aligned} \tag{B.12}$$

Multiplying $\Delta\Omega_1 \bullet \Delta\Omega_2$ in the above equation and summing over all values of l_1 and l_2, the integration of the cross bispectrum approaches the following form:

$$\Delta\Omega_1 \Delta\Omega_2 \sum_{l_1,l_2} \breve{C}(\Omega_1, \Omega_2) = 4\pi^2 \breve{R}(0,0)[1 + \frac{1}{2m} + \frac{1}{2n} + \frac{1}{4nm} + O(\frac{1}{(nm)^2})] \tag{B.13}$$

Thus the estimate of the cross bispectrum has a error. But the error is small compared with the true value and is negligible for practical values of m and n.

Appendix C

Viscous drift force acting on a vertical circular cylinder with small diameter

The forces on a small vertical cylinder due to waves is represented by the Morison equation. For a unit length of the submerged portion of the cylinder, the force is given by:

$$f_x = \frac{C_m \rho \pi D^2}{4} \dot{u} + \frac{\rho D C_d}{2} u|u| \tag{C.1}$$

where u is a horizontal component of wave particle velocities, D is a diameter of the cylinder, and C_m and C_d are inertia and drag coefficients.

If current is not included and the linear wave theory can be applied, a surface elevation $\zeta(t)$ and the horizontal component of wave particle velocities are represented in the following form:

$$\zeta(t) = \frac{H_w}{2} \cos \omega t \tag{C.2}$$

$$u(t) = \frac{H_w \omega}{2} \exp(\kappa z) \cos \omega t \tag{C.3}$$

where H_w is a wave height, κ is a wave number, and ω is a circular wave frequency.

Substituting the equations (C.2) and (C.3) into (C.1), the horizontal force acting on the vertical cylinder can be expressed as:

$$F_x = \int_{-h}^{\zeta} f_x dz$$

$$= [-\frac{Cm\pi\rho D^2 Hw\kappa g}{8}\sin\omega t + \frac{C_d\rho D H_w^2\omega^2}{8}\cos\omega t|\cos\omega t|]$$
$$\times\{\frac{\exp(\kappa\zeta)-\exp(-\kappa h)}{\kappa}\} \tag{C.4}$$

Thus if it is assumed that $\kappa\zeta \ll 1$, F_x can be divided into the following two parts($F_x^{(1)}$ and $F_x^{(2)}$):

$$F_x^{(1)} = [-\frac{C_m\pi\rho D^2 H_w\kappa g}{8}\sin\omega t + \frac{C_d\rho D H_w^2\omega^2}{8}\cos\omega t|\cos\omega t|]$$
$$\times\{\frac{1-\exp(-\kappa h)}{\kappa}\} \tag{C.5}$$

$$F_x^{(2)} = [-\frac{C_m\pi\rho D^2 H_w\kappa g}{8}\sin\omega t + \frac{C_d\rho D H_w^2\omega^2}{8}\cos\omega t|\cos\omega t|]\zeta \tag{C.6}$$

where $\frac{F_x^{(1)}}{D^2}$ is the force per section area integrated over $-h$ to 0.0 with respect to z. It expresses a first order force when $\kappa\zeta = O(\epsilon)$. And $F_x^{(2)}$ indicates a higher order force and it does not depend on the draft. In F_x, the most important term for the drift force is $F_x^{(2)}$, which can also be represented by the alternative form like:

$$F_x^{(2)} = f_x\,|_{z=0}\times\zeta \tag{C.7}$$

Namely this is the product of the wave elevation ζ and the horizontal force per unit length at the still water surface, that is, it is the wave force integrated over the range from the still water surface to the instantaneous wave surface when the horizontal wave particle velocity is distributed as shown by Fig.(C-1). Thus the force expressed by Eq.(C.7) is called a "**free surface force**".

Since the linear wave theory is applicable only for infinitesimal wave amplitudes and it is valid up to the still water level, extension of expression for the water particle kinematics up to the free surface of a finite amplitude wave is questionable. Therefore in order to exactly discuss, it is necessary to use the finite wave amplitude theory. But since our interest is to study fundamental characteristics of a viscous drift force, we dare to use the linear wave theory.

By using the Hilbert transform, an out-of-phase component of the surface elevation ζ can be expressed by:

$$\eta(t) = -\frac{1}{\pi}\int_{-\infty}^{\infty}\frac{\zeta(\tau)}{(t-\tau)}d\tau \tag{C.8}$$

Then the horizontal velocity component u_0 on $z=0$ is given by the derivative of η as follows:

$$u_0 = \dot{\eta}(t) = \frac{1}{\pi}\int_{-\infty}^{\infty}\frac{\zeta(\tau)}{(t-\tau)^2}d\tau \tag{C.9}$$

And similarly the horizontal acceleration becomes:

$$\dot{u}_0 = \ddot{\eta}(t) = -\frac{2}{\pi}\int_{-\infty}^{\infty}\frac{\zeta(\tau)}{(t-\tau)^3}d\tau \tag{C.10}$$

From the characteristics of the Hilbert transform, it is easily found that u_0 is in phase with ζ, and $\dot{u}_0$ out of phase with it.

It is well known that C_d and C_m in the Morison equation are the functions of the Keulegan-Carpenter number and the Reynolds number. In addition, we may assume that these hydrodynamic force coefficients can also be represented by a function of wave frequency.

$$f_x(t) = \int_\tau g_1(\tau)\dot{u}_0(t-\tau)d\tau + \int_\tau g_2(\tau)u_0(t-\tau)|u_0(t-\tau)|d\tau \tag{C.11}$$

Similarly applying this system representation for Eq.(C.7), $F_x^{(2)}$ has:

$$\begin{aligned} F_x^{(2)}(t) &= \int_\tau g_1(\tau)\dot{u}_0(t-\tau)\zeta(t-\tau)d\tau \\ &+ \int_\tau g_2(\tau)u_0(t-\tau)|u_0(t-\tau)|\zeta(t-\tau)d\tau \end{aligned} \tag{C.12}$$

Now, by using the equivalent linearization technique, $u_0|u_0|$ can be approximated in the following forms:

i) in the case that ζ is a regular wave process,

$$u_0|u_0| = \alpha u_0 = \frac{4\pi H_w \omega}{3} u_0 \tag{C.13}$$

ii) in the case that ζ is a Gaussian random process,

$$u_0|u_0| = \alpha u_0 = \sqrt{\frac{8}{\pi}}\sigma_{u_0} u_0 \tag{C.14}$$

where σ_{u_0} is the standard deviation of u_0.

Since α is a function of wave frequency, it can be included in the system function h_2. Thus Eq.(C.12) can be rewritten as:

$$F_x^{(2)}(t) = \int_\tau g_1(\tau)\dot{u}_0(t-\tau)\zeta(t-\tau)d\tau + \int_\tau h_2(\tau)u_0(t-\tau)\zeta(t-\tau)d\tau \tag{C.15}$$

From the relationship between u_0 and ζ, the second term on right hand side of the above equation includes a slowly varying drift force but the first term does not. Hereafter we shall consider only the second term in Eq.(C.15). From Eq.(C.9),then, the second term can be represented in the following form:

$$F_{xs}^{(2)}(t) = \frac{1}{\pi}\int_{\tau_1}\int_{\tau_2} \frac{h_2(\tau_1)}{(\tau_2-\tau_1)^2}\zeta(t-\tau_1)\zeta(t-\tau_2)d\tau_1 d\tau_2 \tag{C.16}$$

If we define the new function g_2 by

$$g_2(\tau_1,\tau_2) = \frac{1}{2\pi}\left[\frac{h_2(\tau_1)}{(\tau_2+\tau_1)^2} + \frac{h_2(\tau_2)}{(\tau_2+\tau_1)^2}\right] \tag{C.17}$$

$F_{xs}^{(2)}$ indicates the second term in Volterra functional series, that is, g_2 is equivalent to the quadratic impulse response function. Using the Fourier transform of generalized function[3] as

$$\int_{-\infty}^{\infty} x^{-m} e^{-ixy} dx = -\frac{\pi i(-iy)^{m-1}}{(m-1)!} sgn(y), \tag{C.18}$$

the Fourier transform of Eq.(C.17) becomes:

$$G_2(\omega_1, \omega_2) = \frac{1}{4}[|\omega_2|Q(\omega_1 - \omega_2) + |\omega_1|Q(\omega_1 - \omega_2)] \tag{C.19}$$

where Q is the Fourier transform of h_2.

Finally, the quadratic transfer function of slowly varying drift force due to viscous effect can be represented by:

$$G_2(\omega_1, -\omega_2) = \frac{1}{4}[|\omega_2|Q(\omega_1 + \omega_2) + |\omega_1|Q(\omega_1 + \omega_2)] \tag{C.20}$$

If the drag coefficients C_d does not depend on the wave frequency and the waves are the combined regular waves with two frequencies, the quadratic transfer function G_2 is proportional to the square of mean frequency of two wave components. And if the wave system consists of a single-frequency wave, G_2 becomes:

$$G_2(\omega, -\omega)(\frac{H_w}{2})^2 = \frac{H_w^3}{12} C_d \rho \pi D \omega^2 \tag{C.21}$$

This result agree with the result obtained by Standing and the others[4], that is, the viscous steady drift force is proportional to the wave amplitude to the third power.

Appendix D

On the effect of exciting short period disturbances on the free and forced oscillations for the system with nonlinear damping

Free oscillation tests have been used for measuring the damping coefficient of a ship or a floating offshore structure. Especially, since moored offshore structures have a long natural period in surge motion in general and the damping force is very small at this period, the experiment is one of the best ways to get the damping force.

This appendix shows the analytical results on the influence of exciting high frequency disturbances on free and forced oscillations for the system, the damping force of which is assumed proportional to the square of velocity, and it concludes that the damping force coefficients increase by the exciting high frequency disturbances.

D.1 Free oscillation in regular high frequency exciting disturbance

The free oscillation equation including exciting disturbance $E(t)$ is described in the following equation:

$$M\ddot{X} + N\dot{X}|\dot{X}| + KX = E(t) \tag{D.1}$$

where M is the total mass coefficient, N is the damping force coefficient, K the spring constant, and the dots represent the derivatives with respect to time.

Considering Eq.(D.1) in the time when X becomes a negative value, replacing E by $\beta M\cos(n_e t)$ and dividing the both side of Eq.(D.1) by M, Eq.(D.1) becomes as follows:

$$\ddot{X} - \alpha\dot{X}^2 + n^2 X = \beta\cos(n_e t) \tag{D.2}$$

where $\alpha = \frac{N}{M}, n^2 = \frac{K}{M}$, and n and n_e are unequal.

If α is small, the solution of Eq.(D.2) and n^2 can be expanded by α. Namely, X and n^2 are expressed in the following form:

$$\begin{aligned} X &= X_0 + \alpha X_1 + \alpha^2 X_2 + \cdots \\ n^2 &= n_0^2 + \alpha n_1^2 + \alpha^2 n_2^2 + \cdots \end{aligned} \tag{D.3}$$

Substituting Eq.(D.3) into Eq.(D.2) and ordering Eq.(D.2) in term α.

$$O(1): \quad \ddot{X}_0 + n_0^2 X_0 = \beta\cos(n_e t) \tag{D.4}$$

$$O(\alpha): \quad \ddot{X}_1 + n_0^2 X_1 = \dot{X}_0^2 - n_1^2 X_0 \tag{D.5}$$

$$O(\alpha^2): \quad \ddot{X}_2 + n_0^2 X_2 = -n_1^2 X_1 - n_2^2 X_0 + 2\dot{X}_0\dot{X}_1 \tag{D.6}$$

If the initial conditions of Eq.(D.2) are $\dot{X} = 0$ and $X = a$, the initial conditions corresponding to Eq.(D.4), (D.5), and (D.6) are as follows:

$$\begin{aligned} &X_0 = a, \dot{X}_0 = 0 \\ &X_1 = 0, \dot{X}_1 = 0 \\ &X_2 = 0, \dot{X}_2 = 0 \end{aligned} \tag{D.7}$$

Accordingly, if the resonance phenomena do not occur and the ratio between the natural frequency n_0 and the frequency of exciting disturbance n_e is large enough, the period of one cycle and the decaying ratio of amplitude a_n are obtained approximately by:

$$\frac{a_{n+1}}{a_n} = 1 + \alpha\left(\frac{4a}{3} + \frac{2\bar{\beta}^2}{3ak^2}\right) \tag{D.8}$$

where $\bar{\beta} = \frac{\beta}{n_0^2}$ and $k = \frac{n_e}{n_0}$. From Eq.(D.8) it is found that the exciting disturbance exerts an influence on the decaying ratio of amplitude and the period of one cycle. Thus, in the case of measuring the damping coefficient from the result of free oscillation test, we must use the amplitude which satisfies the following relation:

$$a_n \gg \frac{\bar{\beta}}{\sqrt{2}n_1 n_e} \tag{D.9}$$

Let us confirm the above result by the numerical calculation. As a free oscillation equation, we consider the following equation:

$$\ddot{X} + \dot{X}|\dot{X}| + 9X = \beta \sin(30t) \tag{D.10}$$

The numerical results calculated for both $\beta = 0$ and $\beta = 10$ by use of Runge-Kutta-Gill method when the initial conditions are $X = 0$ and $X = 1$ are shown in Fig.D.1. From this figure it is found that the decay of amplitude in exciting disturbance is larger than that in still water. Furthermore it is confirmed that the effect of exciting disturbance occurs within

$$a_n \leq 0.08 \tag{D.11}$$

calculated by Eq.(D.9).

D.2 Forced oscillation in exciting disturbance

When the regular and irregular exciting disturbances are added into the oscillation system with nonlinear damping force, the differential equation of oscillation can be expressed in the following form:

$$M\ddot{X} + f(\dot{X}) + KX = E_1(t) + E_2(t) \tag{D.12}$$

where M, N and K are the same coefficients in the previous section, $f(\dot{X})$ is the nonlinear damping force and E_1 and E_2 are the regular and irregular exciting disturbances, respectively.

If the nonlinearity of Eq.(D.12) is not so strong, it is considered that the response of Eq.(D.12) can be represented in sum of the linear responses due to E_1 and $E2$. Namely, if z_1 and z_2 are the linear velocity responses due to $E1$ and $E2$ respectively, the nonlinear velocity response may be expressed in the following representation:

$$f(z_1 + z_2) \sim \kappa_1 z_1 + \kappa_2 z_2 \tag{D.13}$$

So, we consider the following functional

$$J = E[(Nf(z_1 + z_2) - \kappa_1 z_1 - \kappa_2 z_2)^2] \tag{D.14}$$

and determine κ_1 and κ_2 such that minimize J, that is, we shall apply the so-called equivalent linearization method. Then the Equivalent Linearized Damping (E.L.D.) coefficients κ_1 and κ_2 are given as follows:

$$\begin{aligned} \kappa_1 &= \frac{E[z_1 f(z_1 + z_2)]}{E[z_1^2]} \\ &= \frac{1}{\sigma_1^2} \int_{-\infty}^{\infty} \int_{-\infty}^{\infty} z_1 f(z_1 + z_2) p_1(z_1) p_2(z_2) dz_1 dz_2 \end{aligned} \tag{D.15}$$

$$\kappa_2 = \frac{E[z_2 f(z_1+z_2)]}{E[z_2^2]} = \frac{1}{\sigma_2^2}\int_{-\infty}^{\infty}\int_{-\infty}^{\infty} z_2 f(z_1+z_2)p_1(z_1)p_2(z_2)dz_1dz_2 \qquad \text{(D.16)}$$

where $E[\bullet]$ denotes the expectation, $p_i(i=1,2)$ are the probability density functions of $z_i(i=1,2)$ and $\sigma_i^2(i=1,2)$ are the mean square of $z_i(i=1,2)$. By use of the characteristic function ϕ_i for z_i and the Fourier transform F for $f(z_i)$, Eqs.(D.15) and (D.16) can be rewritten in the form:

$$\kappa_j = -\frac{i}{2\pi\sigma_j^2}\int_{-\infty}^{\infty} F(i\omega)\phi_k\frac{d\phi_j}{d\omega}d\omega \quad (j,k=1,2, j\neq k) \qquad \text{(D.17)}$$

where

$$\phi_j(\omega) = \int_{-\infty}^{\infty}\exp(i\omega z_j)p_j(z_j)dz \qquad \text{for } j=1,2$$

$$F(i\omega) = \int_{-\infty}^{\infty}\exp(-i\omega\dot{x})f(\dot{x})d\dot{x}$$

Let us now apply for the oscillation system with nonlinear damping force $f(\dot{X}) = \dot{X}|\dot{X}|$. If z_1 is $A\sin(\omega t)$ and z_2 is the zero-mean stationary Gaussian process, the E.L.D. coefficients κ_1 and κ_2 are given by:

$$\kappa_1 = \frac{8}{\pi A}\int_0^{\infty}\frac{J_1(A\omega)}{\omega^3}\exp(-\frac{\sigma_2^2\omega^2}{2})d\omega \qquad \text{(D.18)}$$

$$\kappa_2 = \frac{4}{\pi}\int_0^{\infty}\frac{J_0(A\omega)}{\omega^2}\exp(-\frac{\sigma_2^2\omega^2}{2})d\omega \qquad \text{(D.19)}$$

where J_0 and J_1 are the Bessel functions of the fist kind.

Considering the following relation

$$\int_0^{\infty}J_\nu(at)\exp(-b^2t^2)t^{\mu-1}dt = \frac{\Gamma(\frac{\nu}{2}-\frac{\mu}{2}+1)}{2b^\mu\Gamma(\nu+1)}\exp(-\frac{a^2}{4b^2}) \times(\frac{a}{2b})^\nu{}_1F_1(\frac{\nu}{2}-\frac{\mu}{2}+1;\nu+1;\frac{a^2}{4b^2}) \qquad \text{(D.20)}$$

Eqs.(D.18) and (D.19) can be expressed in the form:

$$\kappa_1 = \sqrt{\frac{8}{\pi}}\sigma_2\exp(-\frac{A^2}{2\sigma_2^2})_1F_1(2.5;2;\frac{A^2}{2\sigma_2^2}) \qquad \text{(D.21)}$$

$$\kappa_2 = \sqrt{\frac{8}{\pi}}\sigma_2\exp(-\frac{A^2}{2\sigma_2^2})_1F_1(1.5;1;\frac{A^2}{2\sigma_2^2}) \qquad \text{(D.22)}$$

where Γ is the Gamma function and ${}_1F_1$ is the confluent hypergeometric function[5]. From Eqs.(D.21) and (D.22) it is found that the E.L.D. coefficients change with the energy ratio between z_1 and z_2.

When $\alpha > \gamma$, the asymptotic expansion of ${}_1F_1(\alpha;\gamma;z)$ for the large value of $|z|$ is as follows:

$$ {}_1F_1(\alpha;\gamma;z) \sim \frac{\Gamma(\gamma)}{\Gamma(\alpha)} \exp(z) z^{\alpha-\gamma} \tag{D.23} $$

Accordingly, when $\frac{A^2}{2\sigma_2^2} \gg 1$,

$$ \kappa_1 \sim \frac{8A}{3\pi} \tag{D.24} $$

$$ \kappa_2 \sim \frac{4A}{\pi} \tag{D.25} $$

The result of Eq.(D.24) is identical with that of only E_1.

When $\frac{A^2}{2\sigma_2^2} \ll 1$,

$$ \kappa_1 = \kappa_2 \sim \sqrt{\frac{8}{\pi}}\sigma_2 \tag{D.26} $$

This result coincides with the result for pure Gaussian input E_2. Figures D.2 and D.3 show the calculated results of κ_1 and κ_2. From these figures it is found that the interaction effect due to two exciting disturbances on the E.L.D. coefficients is large. The energy dissipation consumed by nonlinear damping can be expressed as follows:

$$ \begin{aligned} \overline{E} &= \kappa_1 \frac{A^2}{2} + \kappa_2 \sigma_2^2 \\ &= \sqrt{\frac{8}{\pi}}\sigma_2^3 \exp(-\frac{A^2}{2\sigma_2^2}) {}_1F_1(2.5;1;\frac{A^2}{2\sigma_2^2}) \end{aligned} \tag{D.27} $$

When $\frac{A^2}{2\sigma_2^2} \gg 1$,

$$ \overline{E} \sim \frac{4}{3\pi} A^3 \tag{D.28} $$

In this case, the energy dissipation consumed by nonlinear damping is identical with that due to the sinusoidal exciting disturbance. When $\frac{A^2}{2\sigma_2^2} \ll 1$,

$$ \overline{E} \sim \sqrt{\frac{8}{\pi}}\sigma_2^3 \tag{D.29} $$

This result coincides with the energy dissipation due to random exciting disturbance. The calculated result of Eq.(D.27) is shown in Fig.D.4. From this figure it is found that the energy dissipation due to two exciting disturbances is larger than that due to pure regular exciting disturbance, further than the sum of the energy dissipations due to regular and irregular exciting disturbances respectively.

Appendix E

Instantaneous p.d.f. of total second order response based on the Kac & Siegert theory

We shall consider a second order functional series as:

$$X(t) = \int_{\tau} g_1(\tau)\zeta(t-\tau)d\tau + \int_{\tau_1}\int_{\tau 2} g_2(\tau_1,\tau_2)\zeta(t-\tau_1)\zeta(t-\tau_2)d\tau_1 d\tau_2 \tag{E.1}$$

$$\equiv X^{(1)} + X^{(2)} \tag{E.2}$$

Now considering $\zeta(t)$ as transformed "**white noise**" process, and denoting by $q(t)$ the appropriate impulse response function of the linear filter giving $\zeta(t)$ from white noise process $W(t)$, it follows that

$$\zeta(t) = \int_{-\infty}^{\infty} q(\tau)W(t-\tau)d\tau \tag{E.3}$$

where $q(\tau)$ is a weighting function and $W(t)$ is a unit white noise which satisfies:

$$E[W(t)W(t-\tau)] = \delta(\tau) \tag{E.4}$$

Substituting $\zeta(t)$ as given by Eq.(E.3) into Eq.(E.1), we get the following relations:

$$X^{(1)}(t) = \int_{0}^{\infty} k_1(\tau)W(t-\tau)d\tau \tag{E.5}$$

where

$$k_1(\tau) = \int_0^\infty g_1(s)q(\tau - s)ds \tag{E.6}$$

and

$$X^{(2)}(t) = \int_0^\infty \int_0^\infty k_2(\tau_1, \tau_2)W(t - \tau_1)W(t - \tau_2)d\tau_1 d\tau_2 \tag{E.7}$$

where

$$k_2(\tau_1, \tau_2) = \int_0^\infty \int_0^\infty g_2(u, v)q(\tau_1 - u)q(\tau_2 - v)dudv \tag{E.8}$$

Since q, g_1, and g_2 should be filter functions with physical causality, they must vanish at infinity, and for practical purpose they may be considered zero outside a bounded region. Thus we shall consider T, which is sufficiently large, as the integral upper limit of the above equations.

Now we shall consider the following integral equation :

$$\int_0^T k_2(x, y)\Lambda(y)dy = \lambda\Lambda(x) \tag{E.9}$$

Then this integral equation becomes the Fredholm type integral equation. Since $k_2(x, y)$ is symmetric kernels, it can be shown from the Fredholm type integral equation theory[6] that

1) the eigenvalues and the corresponding eigenfunctions exist,

2) the eigenfunctions are mutually orthonormal,

3) the eigenvalues are all real,

4) the Mercer's theorem can be applied to express the positive semi -definite kernel as

$$k_2(x, y) = \sum_{i=1}^{\infty} \lambda_i \Lambda_i(x)\Lambda_i(y) \tag{E.10}$$

Substituting the above relation into the Eq.(E.7), we have:

$$X^{(2)}(t) = \sum_{i=1}^{\infty} \lambda_i [\int_0^\infty \Lambda_i(\tau)W(t - \tau)d\tau]^2 \tag{E.11}$$

If the stochastic process $W_i(t), i = 1, 2, \ldots$, are defined as

$$W_i(t) = \int_0^T W(t - \tau)\Lambda_i(\tau)d\tau \tag{E.12}$$

Eq.(E.11) becomes

$$X^{(2)}(t) = \sum_{i=1}^{\infty} \lambda_i W_i^2(t) \tag{E.13}$$

Furthermore from the relation (E.3) and the orthonormality of Λ_i , it can be seen that

$$E[W_i(t)W_j(t)] = 0 \qquad \text{for } i \neq j \tag{E.14}$$

This means that $W_i(t)$ and $W_j(t)$ are uncorrelated random variables and therefore independent, since they are Gaussian, and that $E[W_i^2(t)] = 1, \{W_i\}$ is the family of the standard Gaussian random variables.

Similarly we expand the kernel k_1 in terms of the eigenfunctions $\{\Lambda_i\}$ as

$$k_1(\tau) = \sum_{i=1}^{\infty} c_i \Lambda_i(\tau) \tag{E.15}$$

where

$$c_i = \int_0^T k_1(\tau)\Lambda_i(\tau)d\tau \tag{E.16}$$

Then substituting Eq.(E.15) into Eq.(E.5) we have:

$$X^{(1)}(t) = \sum_{i=1}^{\infty} c_i W_i(t) \tag{E.17}$$

This leads to the following decomposition of the total second order response process:

$$X(t) = \sum_{i=1}^{\infty} (c_i W_i(t) + \lambda_i W_i^2(t)) \tag{E.18}$$

The instantaneous p.d.f. can be obtained from the inverse Fourier transform of its characteristic function. The characteristic function is defined by

$$\phi_X(\theta) = E[\exp(i\theta X)] = \prod_{j=1}^{\infty} E[\exp\{i\theta(c_j W_j + \lambda_j W_j^2)\}] \tag{E.19}$$

Since W_j have the p.d.f as

$$p_{W_j}(x) = \frac{1}{\sqrt{2\pi}} \exp(-\frac{x^2}{2}) \tag{E.20}$$

by using the following identity:

$$\int_{-\infty}^{\infty} \exp(itx - \frac{ax^2}{2})dx = \sqrt{\frac{2\pi}{a}} \exp(-\frac{t^2}{2a}) \qquad \text{for } a > 0 \tag{E.21}$$

the characteristic function can be rewritten as

$$\phi_X(\theta) = \prod_{j=1}^{\infty} \frac{1}{\sqrt{1 - 2i\lambda_j\theta}} \exp[-\frac{c_j^2\theta^2}{2(1 - 2i\lambda_j\theta)}] \tag{E.22}$$

By the inverse Fourier transform of the characteristic function the instantaneous p.d.f. becomes:

$$p_X(x) = \frac{1}{2\pi}\int_{-\infty}^{\infty} \phi_X(\theta)\exp(-i\theta x)d\theta \tag{E.23}$$

Next we shall consider the integral equation (E.9). It can be simplified by defining

$$\psi_i(t) = \int_0^T q(u-t)\Lambda_i(u)du, \qquad 0 \le t \le T \tag{E.24}$$

Then the integral equation (E.9) can be rewritten as

$$\int_0^T \tilde{k}_2(t,u)\psi_i(u)du = \lambda_i\psi_i(t) \tag{E.25}$$

where

$$\tilde{k}_2(t,u) = \int_0^T R_\zeta(t-\tau)g_2(\tau,u)d\tau \tag{E.26}$$

The new set of eigenfunctions $\{\psi_i\}$ will satisfy the following normalization relation

$$\int_0^T\int_0^T g_2(\tau_1,\tau_2)\psi_i(\tau_1)\psi_j(\tau_2)d\tau_1 d\tau_2 = \lambda_i\delta_{ij} \tag{E.27}$$

where δ_{ij} is the Kronecker delta and the parameters c_i are determined by

$$c_i = \int_0^T g_1(\tau)\psi_i(\tau)d\tau \tag{E.28}$$

If the time domain kernel $g_2(\tau_1,\tau_2)$ is known, the integral equation may be solved to obtain eigenvalues and eigenfunctions. However, it seems to be more common to obtain these values and functions in frequency domain than to do in time domain. For this purpose we define the Fourier transform of $\psi_i(t)$ as

$$\hat{\Psi}_i(\omega) = \frac{1}{2\pi}\int_{-\infty}^{\infty} \psi_i(t)\exp(-i\omega t)dt \tag{E.29}$$

Then we obtain the frequency domain integral equation as follows:

$$\int_{-\infty}^{\infty} S_\zeta(\omega)G_2(\omega,-\nu)\hat{\Psi}_i(\nu)d\nu = \lambda_i\hat{\Psi}_i(\omega) \tag{E.30}$$

where $S_\zeta(\omega)$ is the two-side wave spectrum.
Equation (E.30) may be rewritten as

$$\int_{-\infty}^{\infty} K(\omega,\nu)\Psi_i(\nu)d\nu = \lambda_i\Psi_i(\omega) \tag{E.31}$$

where the kernel $K(\omega, \nu)$ is defined by

$$K(\omega, \nu) = \sqrt{S_\zeta(\omega) S_\zeta(\nu)} G_2(\omega, -\nu) \tag{E.32}$$

and the eigenfunctions $\Psi_i(\omega)$ by

$$\Psi_i(\omega) = \sqrt{S_\zeta(\omega)} \hat{\Psi}_i(\omega) \tag{E.33}$$

Since G_2 is symmetric, it follows that $K(\omega, \nu) = K(\nu, \omega)$, that is, $K(\omega, \nu)$ is the Hermitian. Since the eigenfunctions Λ_i are all real, $\Psi_i(-\omega) = \Psi_i^*(\omega)$ and the normalization condition is

$$\int_{-\infty}^{\infty} \Psi_i(\omega) \Psi_j^*(\omega) d\omega = \delta_{ij} \tag{E.34}$$

Equation (E.28) for c_i becomes

$$c_i = \int_{-\infty}^{\infty} G_1(\omega) \sqrt{S_\zeta(\omega)} \Psi_i^*(\omega) d\omega \tag{E.35}$$

Appendix F

Statistical moments of total second order response

The total second order response can be represented in the following two forms:

$$X(t) = \int_{\tau} g_1(\tau)\zeta(t-\tau)d\tau + \int_{\tau_1}\int_{\tau_2} g_2(\tau_1,\tau_2)\zeta(t-\tau_1)\zeta(t-\tau_2)d\tau_1 d\tau_1 \tag{F.1}$$

or

$$= \sum_{i=1}^{\infty}(c_i + \lambda_i W_i)W_i \tag{F.2}$$

From Eq.(F.2) the expected values up to third order are given as follows:

$$E[X] = \sum \lambda_i E[W_i^2] + \sum c_i E[W_i] \tag{F.3}$$

$$E[X^2] = \sum c_i c_j E[W_i W_j] + \sum c_i \lambda_j E[W_i W_j^2] \tag{F.4}$$

$$\begin{aligned} E[X^3] &= \sum c_i c_j c_k E[W_i W_j W_k] + \sum c_i \lambda_j c_k E[W_i W_j^2 W_k] \\ &+ \sum \lambda_i c_j c_k E[W_i^2 W_j W_k] + \sum \lambda_i \lambda_j c_k E[W_i^2 W_j^2 W_k] \\ &+ \sum c_i c_j \lambda_k E[W_i W_j W_k^2] + \sum c_i \lambda_j \lambda_k E[W_i W_j^2 W_k^2] \\ &+ \sum \lambda_i c_j \lambda_k E[W_i^2 W_j W_k^2] + \sum \lambda_i \lambda_j \lambda_k E[W_i^2 W_j^2 W_k^2] \end{aligned} \tag{F.5}$$

Since $W_i (i = 1, \ldots, \infty)$ are the standard Gaussian variables with mutual independence, the following relations[7] are satisfied:

$$E[W_i] = 0 \tag{F.6}$$

$$E[W_i W_j] = \delta_{ij} \tag{F.7}$$

$$E[W_iW_jW_k] = 0 \tag{F.8}$$

$$E[W_iW_jW_kW_l] = \delta_{ij}\delta_{kl} + \delta_{ik}\delta_{jl} + \delta_{il}\delta_{jk} \tag{F.9}$$

$$E[W_iW_jW_kW_lW_m] = 0 \tag{F.10}$$

$$\begin{aligned} E[W_iW_jW_kW_lW_mW_n] &= \delta_{ij}\delta_{kl}\delta_{mn} + \delta_{ij}\delta_{km}\delta_{ln} + \delta_{ij}\delta_{kn}\delta_{lm} \\ &+\delta_{ik}\delta_{jl}\delta_{mn} + \delta_{ik}\delta_{jm}\delta_{ln} + \delta_{ik}\delta_{jn}\delta_{lm} \\ &+\delta_{il}\delta_{jk}\delta_{mn} + \delta_{il}\delta_{jm}\delta_{kn} + \delta_{il}\delta_{jn}\delta_{km} \\ &+\delta_{im}\delta_{jk}\delta_{ln} + \delta_{im}\delta_{jl}\delta_{kn} + \delta_{im}\delta_{jn}\delta_{kl} \\ &+\delta_{in}\delta_{jk}\delta_{lm} + \delta_{in}\delta_{jl}\delta_{km} + \delta_{in}\delta_{jm}\delta_{kl} \end{aligned}$$

$$\text{for } i,j,k,l,m,n = 1,\cdots,\infty \tag{F.11}$$

where δ_{ij} is the Kronecker delta.

Using the above relations, the mean value $\bar{X}$ or $E[X]$, the variance σ_X^2 or $Var[X]$, and the skewness ($\sqrt{\beta_1}$) are obtained as

$$\bar{X} = E[X] = \sum \lambda_i \tag{F.12}$$

$$\sigma_X^2 = Var[X] = E[X^2] - \bar{X}^2 = \sum c_i^2 + 2\sum \lambda_i^2 \tag{F.13}$$

$$\sqrt{\beta_1}\sigma_X^3 = E[X^3] - 3E[X^2]E[X] + 2(E[X])^3 = 8\sum \lambda_i^3 + 6\sum c_i^2\lambda_i \tag{F.14}$$

While from Eq.(F.1) the expected values are written as:

$$E[X] = \int d\tau_1 \int d\tau_2 g_2(\tau_1,\tau_2) R_\zeta(\tau_2-\tau_1) \tag{F.15}$$

$$\begin{aligned} E[X^2] &= \int d\tau_1 \int d\tau_2 g_1(\tau_1) g_1(\tau_2) R_\zeta(\tau_2-\tau_1) \\ &+ \int d\tau_1 \cdots \int d\tau_4 g_2(\tau_1,\tau_2) g_2(\tau_3,\tau_4) \\ &\times [R_\zeta(\tau_2-\tau_1)R_\zeta(\tau_4-\tau_3) + R_\zeta(\tau_2-\tau_3)R_\zeta(\tau_1-\tau_4) \\ &+R_\zeta(\tau_2-\tau_4)R_\zeta(\tau_3-\tau_1)] \end{aligned} \tag{F.16}$$

$$\begin{aligned} E[X^3] &= \int d\tau_1 \cdots \int d\tau_4 g_2(\tau_1,\tau_2) g_1(\tau_3) g_1(\tau_4) \\ &\times [6R_\zeta(\tau_3-\tau_1)R_\zeta(\tau_1-\tau_4) + 3R_\zeta(\tau_2-\tau_1)R_\zeta(\tau_4-\tau_3)] \\ &+[\int d\tau_1 \int d\tau_2 g_2(\tau_1,\tau_2) R_\zeta(\tau_2-\tau_1)]^3 \\ &+ \int d\tau_1 \cdots \int d\tau_6 g_2(\tau_1,\tau_2) g_2(\tau_3,\tau_4) g_2(\tau_5,\tau_6) \\ &\times [6R_\zeta(\tau_2-\tau_1)R_\zeta(\tau_6-\tau_3)R_\zeta(\tau_5-\tau_4) \\ &+8R_\zeta(\tau_3-\tau_1)R_\zeta(\tau_5-\tau_2)R_\zeta(\tau_6-\tau_4)] \end{aligned} \tag{F.17}$$

Transforming Eqs.(F.15), (F.16) and (F.17) to frequency domain we get:

$$\bar{X} = \int d\omega G_2(\omega, -\omega) S_\zeta(\omega) \tag{F.18}$$

$$\sigma_X^2 = \int d\omega |G_1(\omega)|^2 S_\zeta(\omega) + \int d\omega_1 \int d\omega_2 |G_2(\omega_1, \omega_2)|^2 S_\zeta(\omega_1) S_\zeta(\omega_2) \tag{F.19}$$

$$\begin{aligned}\sqrt{\beta_1}\sigma_X^3 &= 6 \int d\omega_1 \int d\omega_2 G_1(-\omega_1) G_1(\omega_2) G_2(\omega_1, \omega_2) S_\zeta(\omega_1) S_\zeta(\omega_2) \\ &+8 \int d\omega_1 \int d\omega_2 \int d\omega_3 G_2(\omega_1, \omega_2) G_2^*(\omega_2, \omega_3) G_2(\omega_3, -\omega_1) \\ &\times S_\zeta(\omega_1) S_\zeta(\omega_2) S_\zeta(\omega_3)\end{aligned} \tag{F.20}$$

where $*$ denotes the complex conjugate.

Cross and Auto spectra

Take the cross correlation function between the nonlinear response process $X(t)$ and the Gaussian wave process $\zeta(t)$ as follows:

$$\begin{aligned}E[(X(t) - \bar{X})\zeta(t-\tau)] &= \int d\tau_1 g_1(\tau_1) E[\zeta(t-\tau_1)\zeta(t-\tau)] \\ &+ \int d\tau_1 \int d\tau_2 g_2(\tau_1, \tau_2) E[\zeta(t-\tau_1) z(t-\tau_2) \zeta(t-\tau)] \\ &- \bar{X} E[\zeta(t-\tau)]\end{aligned} \tag{F.21}$$

Since the wave process is defined to be zero-mean, the last two terms are zero. Thus:

$$E[(X(t) - \bar{X})\zeta(t-\tau)] = \int d\tau_1 g_1(\tau_1) E[\zeta(t-\tau_1)\zeta(t-\tau_1)] \tag{F.22}$$

This means that the cross spectrum involves only the first term in the functional series (F.1), and thus that the linear transfer function G_1 is derivable by standard cross spectrum technique by Fourier transform. Denoting the cross spectrum as $S_{X\zeta}(\omega)$; then we get

$$S_{X\zeta}(\omega) = G_1(\omega) \cdot S_\zeta(\omega) \tag{F.23}$$

Next, taking the auto correlation function of $X(t)$:

$$\begin{aligned}&E[(X(t) - \bar{X})(X(t+\tau) - \bar{X})] \\ &= \int d\tau_1 \int d\tau_2 g_1(\tau_1) g_1(\tau_2) E[\zeta(t-\tau_1)\zeta(t+\tau-\tau_2)]\end{aligned}$$

$$+\int d\tau_1 \cdots \int d\tau_4 g_2(\tau_1,\tau_2)g_2(\tau_3,\tau_4)$$
$$\times E[\zeta(t-\tau_1)\zeta(t-\tau_2)\zeta(t+\tau-\tau_3)\zeta(t+\tau-\tau_4)]$$
$$-\bar{X}^2 \qquad \text{(F.24)}$$

and using the factorization relation[7] for higher order moments of Gaussian processes as:

$$E[X_1X_2X_3X_4] = E[X_1X_2]E[X_3X_4] + E[X_1X_3]E[X_2X_4] + E[X_1X_4]E[X_2X_3] \qquad \text{(F.25)}$$

we obtain

$$\begin{aligned} R_{XX}(\tau) &= \int d\tau_1 \int d\tau_2 g_1(\tau_1)g_1(\tau_2)R_\zeta(\tau+\tau_1-\tau_2) \\ &+ \int d\tau_1 \cdots \int d\tau_4 g_2(\tau_1,\tau_2)g_2(\tau_3,\tau_4) \\ &\times [R_\zeta(\tau+\tau_1-\tau_3)R_\zeta(\tau+\tau_2-\tau_4) \\ &+ R_\zeta(\tau+\tau_1-\tau_4)R_\zeta(\tau+\tau_2-\tau_3)] \end{aligned} \qquad \text{(F.26)}$$

The auto power spectrum is the Fourier transform of R_{XX} and is computed from the Wiener-Khintchine relations as

$$S_X(\omega) = |G_1(\omega)|^2 S_\zeta(\omega) + 2\int d\nu |G_2(\omega-\nu,\nu)|^2 S_\zeta(\omega-\nu)S_\zeta(\nu) \qquad \text{(F.27)}$$

REFFERENCES IN APPENDICES

[1] Ogilvie, T. F. : Second-order hydrodynamic effects on ocean platforms, Proc. International Workshop on Ship and Platform Motions, 1983.

[2] Dalzell, J.F.: Cross-Bi-Spectral Analysis : Application to Ship Resistance in Waves, J.S.R., vol.18, 1974.

[3] Standing, R. G., Dacunha, N. M. C., Matten, R. B.: Mean Wave Drift Forces: Theory and Experiment, NMI R124, 1981.

[4] Watson, G.N.: A Treatise on the Theory of Bessel Functions, Cambridge Univ. Press, 1966.

[5] Kac, M. and Siegert, A.J.F.: On the Theory of Noise in Radio Receiver with Square-Law Detectors, Journ. Appl. Phys., vol.18, 1946.

[6] Courant, R., and Hilbert, D.: Method of Mathematical Physics I, II, Interscience Pub., 1962.

[7] Cramér, H.: Mathematical Method of Statistics, Princeton Unv. Press, 1946.

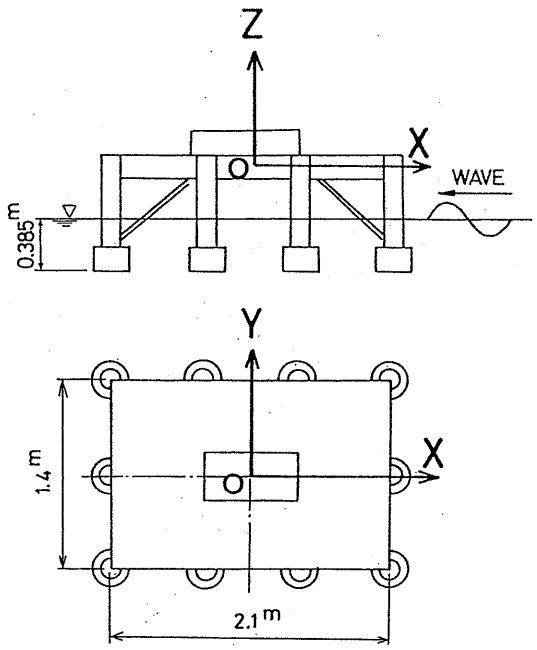

Figure 3.1 Configuration of a floating structure and the direction of incident waves

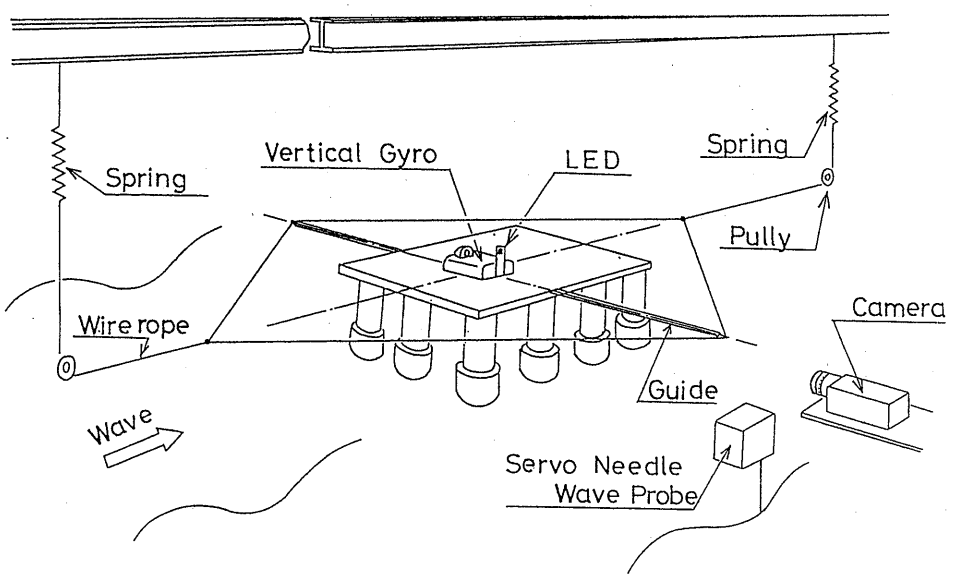

Figure 3.2 Set-up of model test

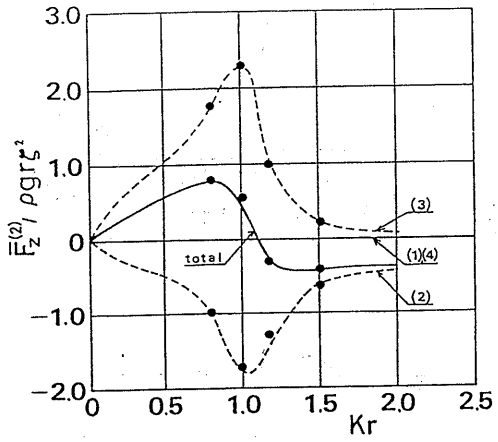

(1) Surface elevation term
(2) Quadratic pressure term
(3) Structure displacement term
(4) Rotation of force vector

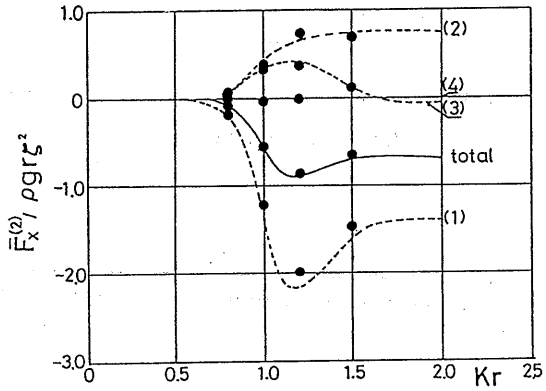

Figure 3.3 Components of the computed mean second order forces of a half sphere

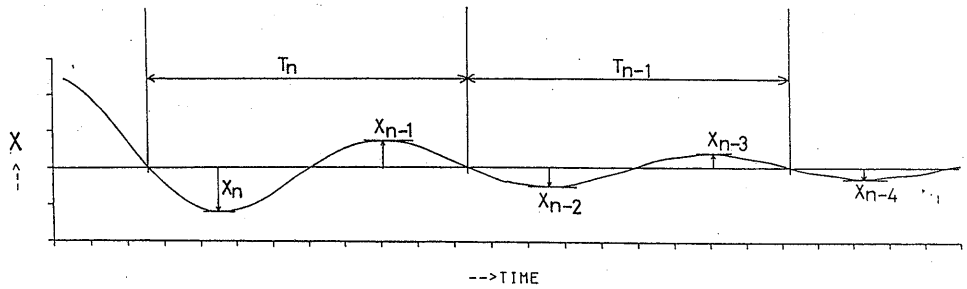

Figure 3.4 An example of the surge decaying motion

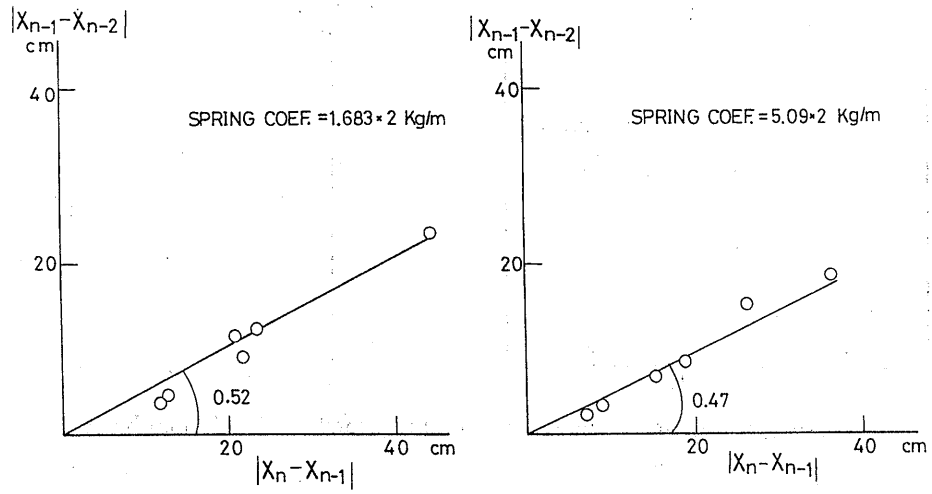

Figure 3.5 Extinction curves of surge motion

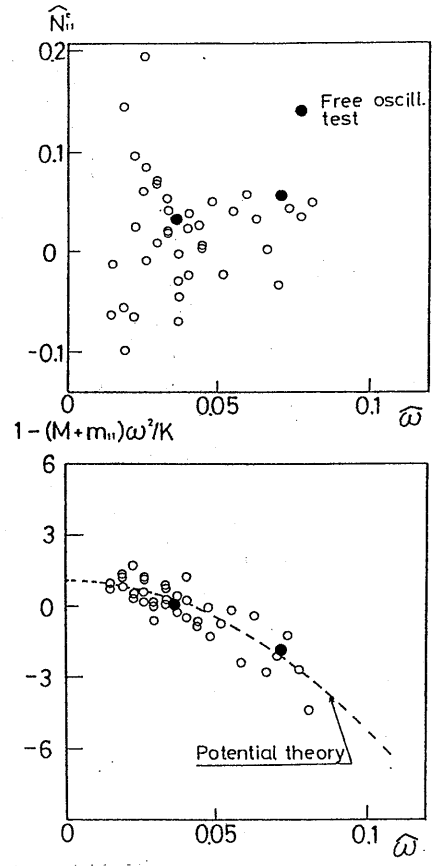

Figure 3.6 Added mass and damping coefficients (frequency base)

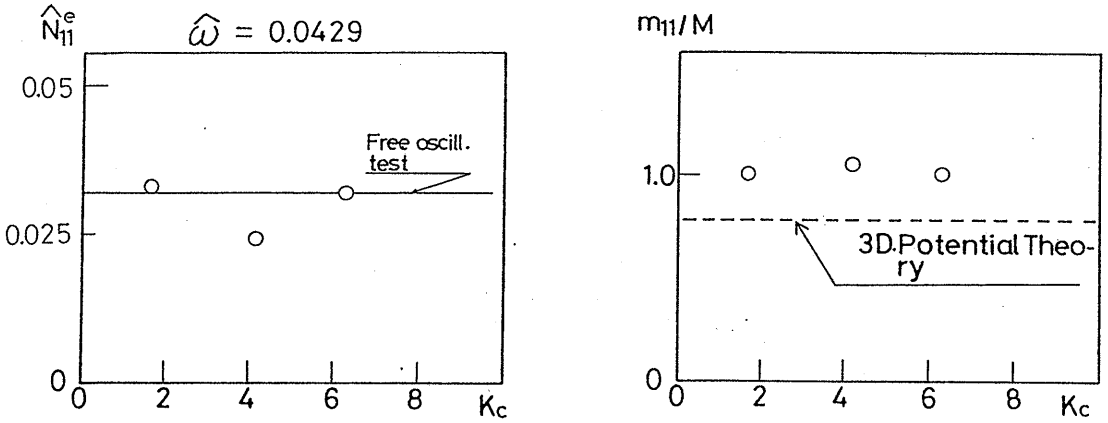

Figure 3.7 Added mass and damping coefficients ($K_c$number base)

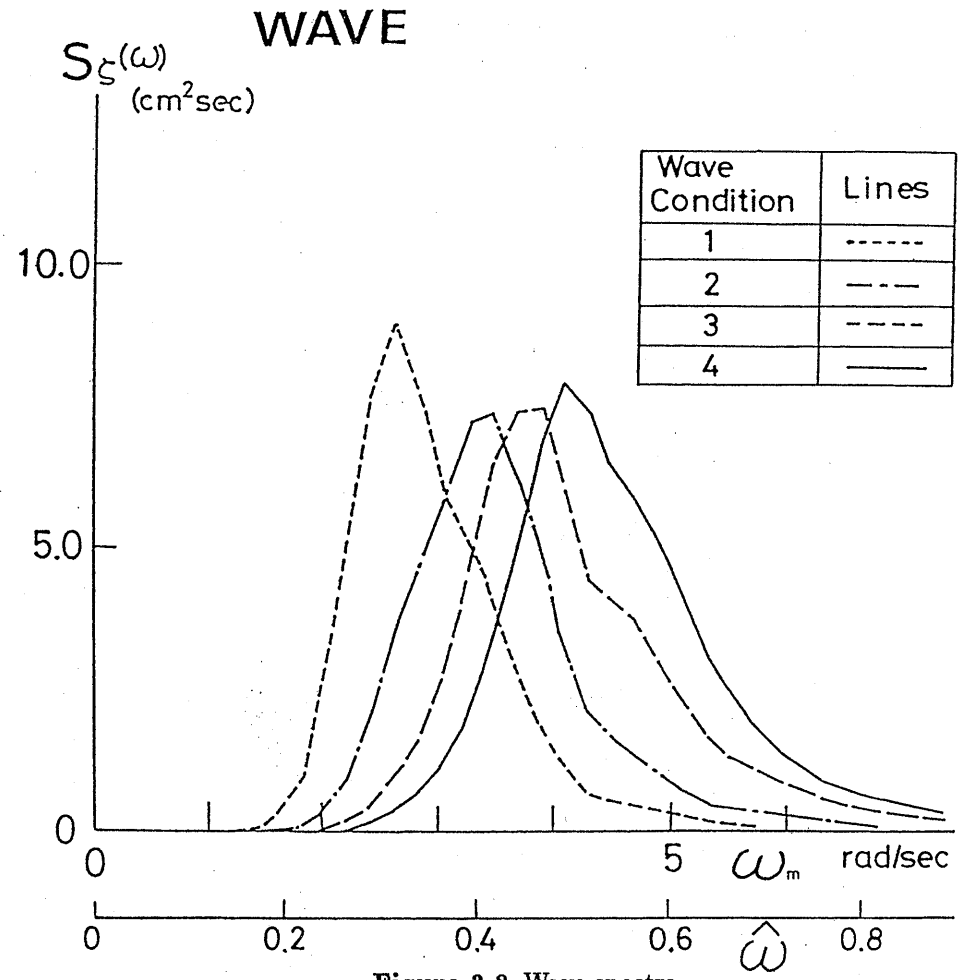

Figure 3.8 Wave spectra

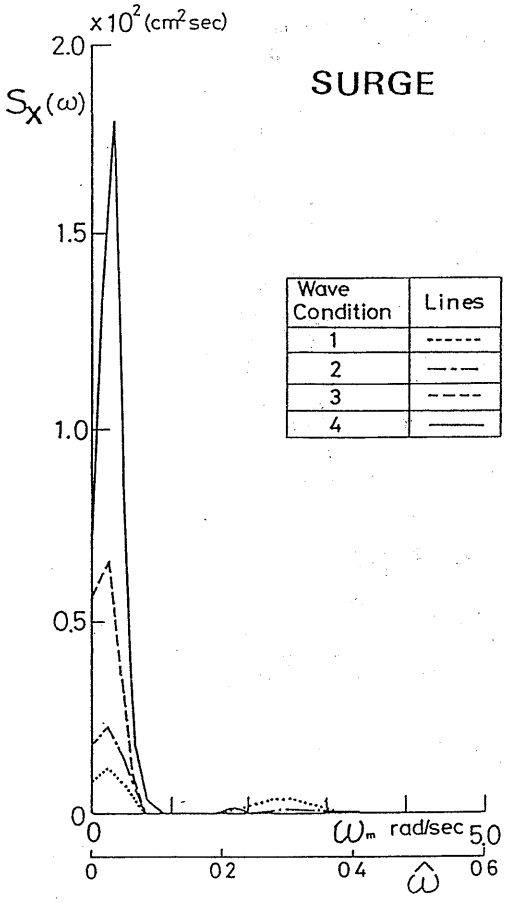

Figure 3.9 Surge response spectra

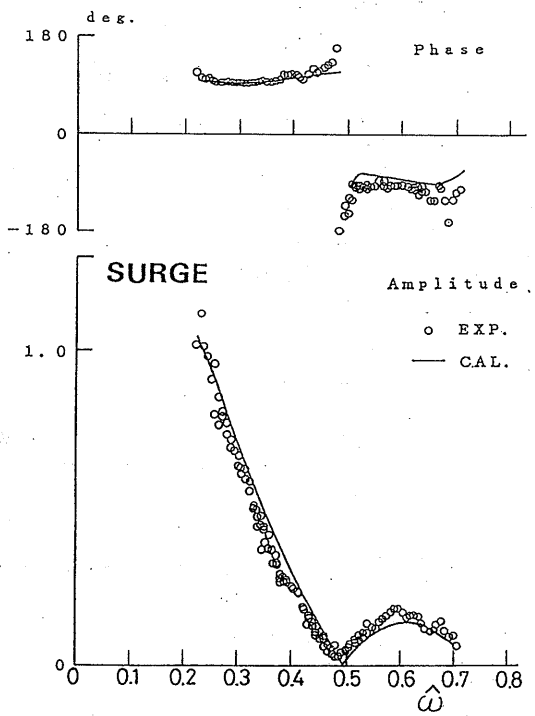

Figure 3.10 Linear transfer function $G_1(\omega)$ of surge motion

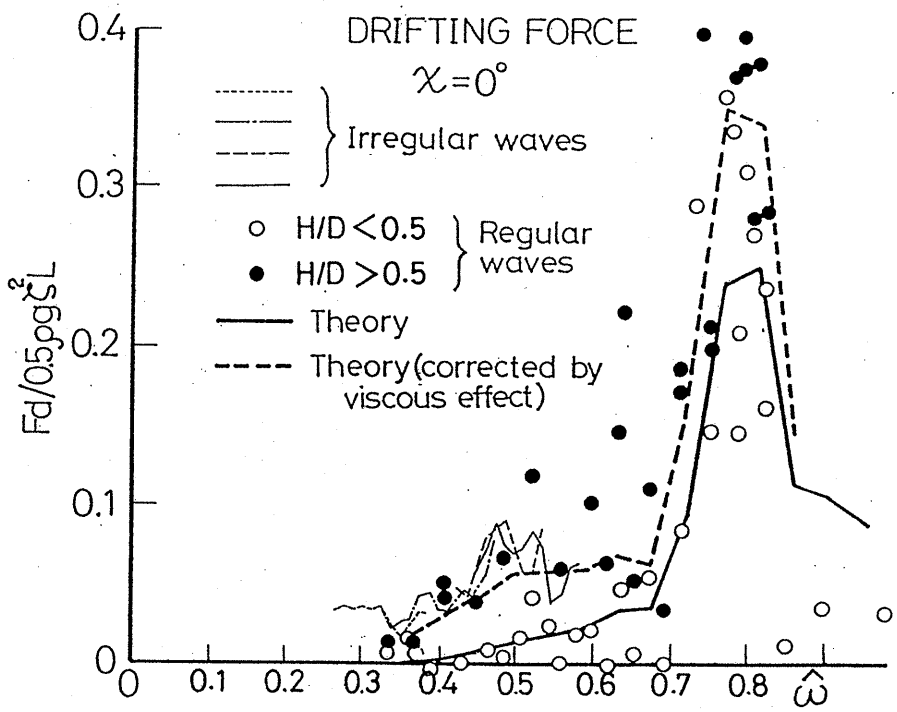

Figure 3.11 Longitudinal steady drift force in head waves

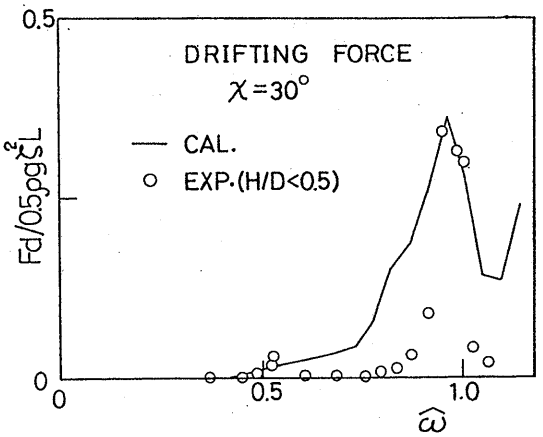

Figure 3.12 Longitudinal steafy drift force in oblique waves ($\chi = 30°$)

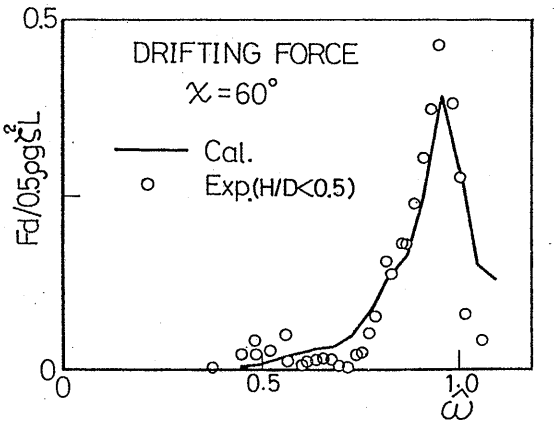

Figure 3.13 Longitudinal steady drift force in oblique waves ($\chi = 60°$)

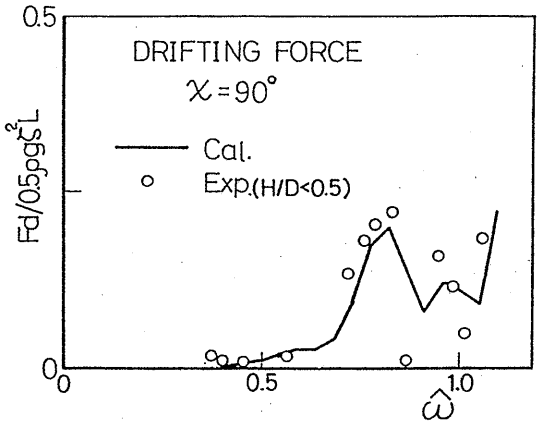

Figure 3.14 Longitudinal steady drift force in beam waves ($\chi = 90°$)

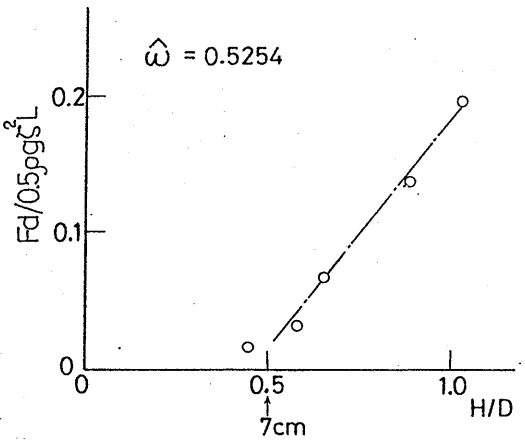

Figure 3.15 a) An example of wave height effect to steady drift force in head waves ($\hat{\omega} = 0.5254$)

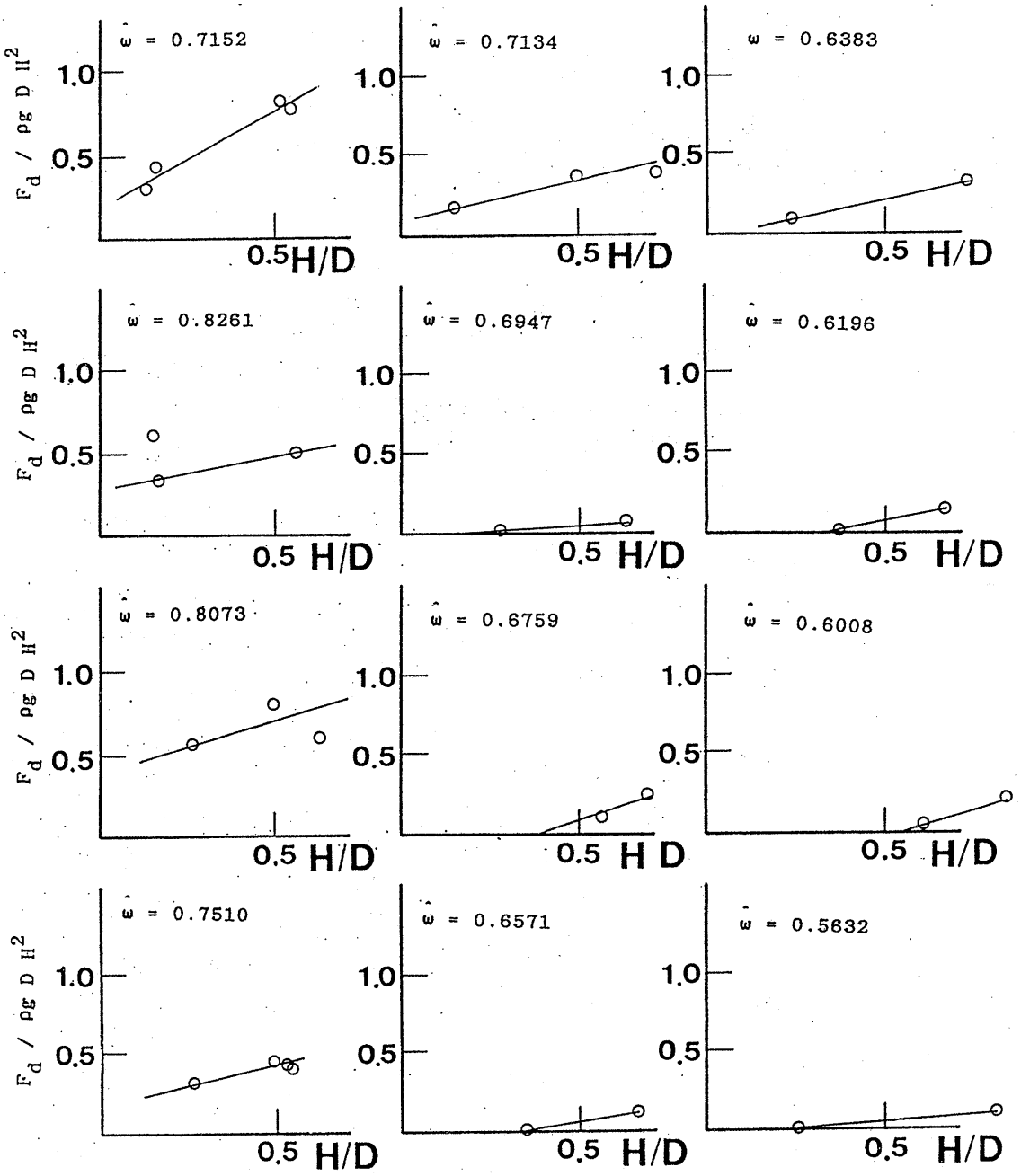

Figure 3.15 b) Wave height effects to steady drift force in head waves

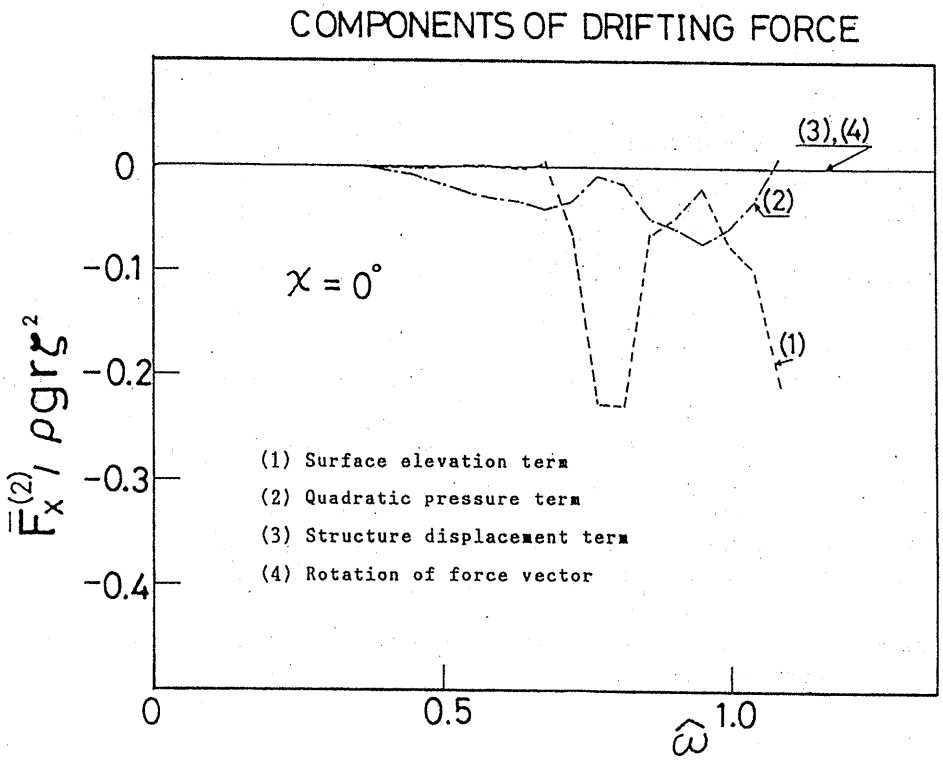

Figure 3.16 Components of steady drift force in head waves where r is half of the length L

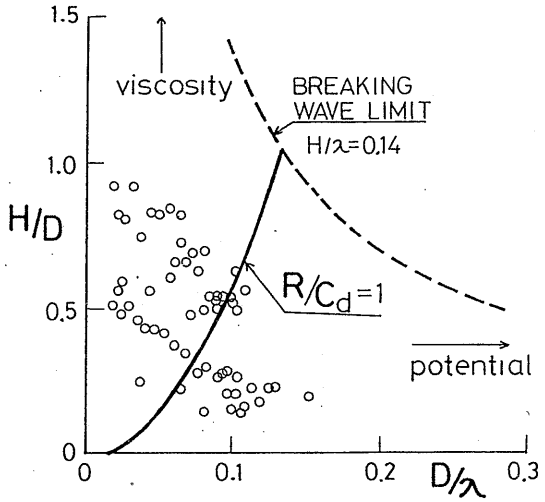

Figure 3.17 Comparison with viscous and potential components of drift forces to a vertical cylinder

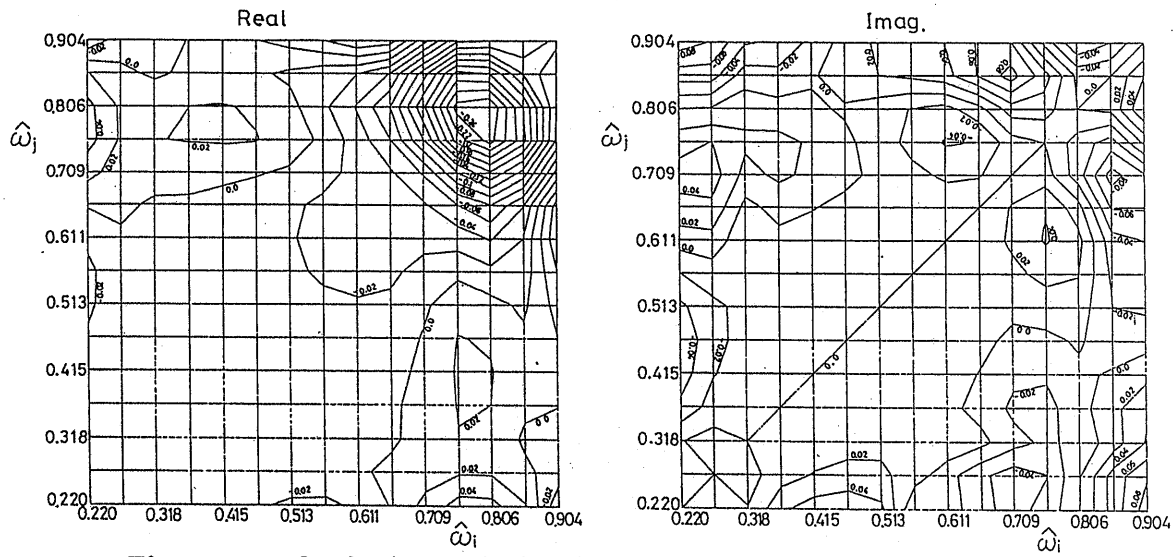

Figure 3.18 Quadratic transfer function of slowly varying drift force obtained from numerical calculation

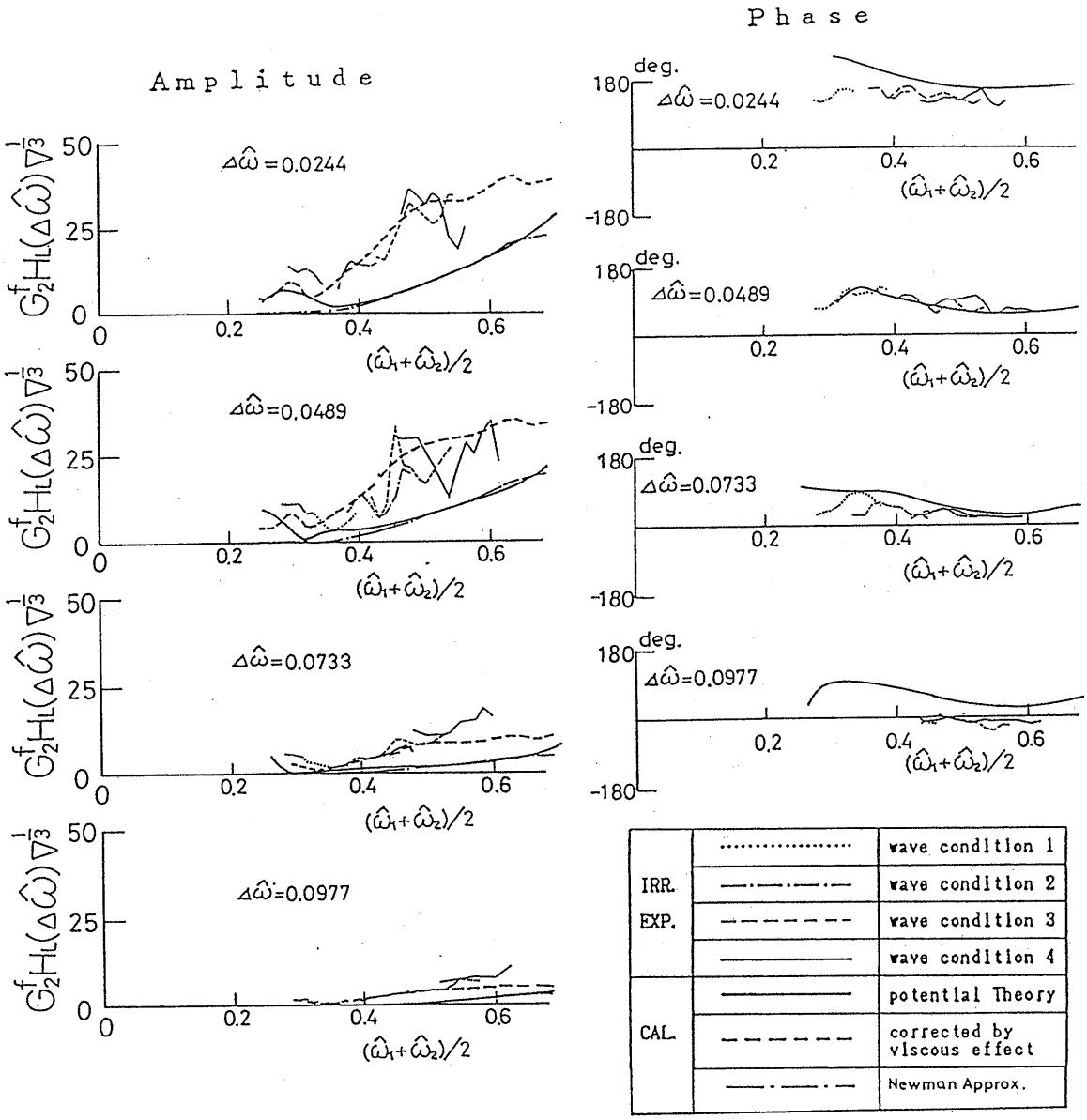

Figure 3.19 Comparison with experimental and numerical results on the quadratic transfer function of slowly varying drift force

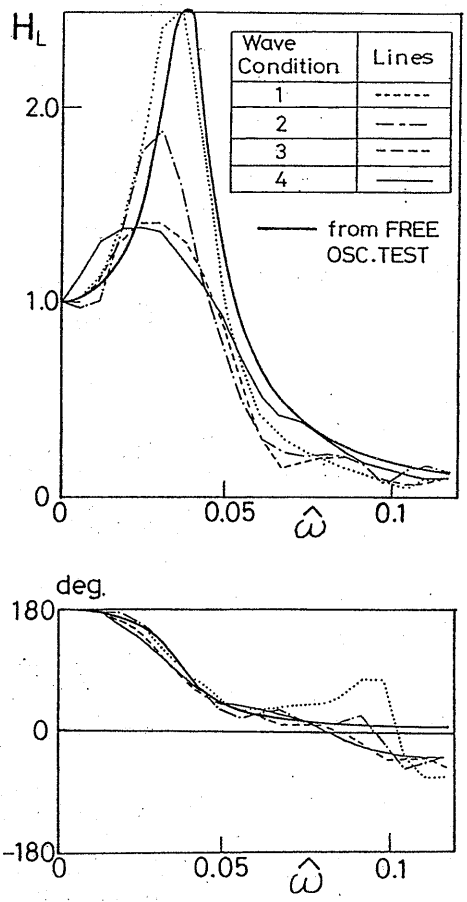

Figure 3.20 Frequency response function $H_L(\omega)$ of surge motion to external forces

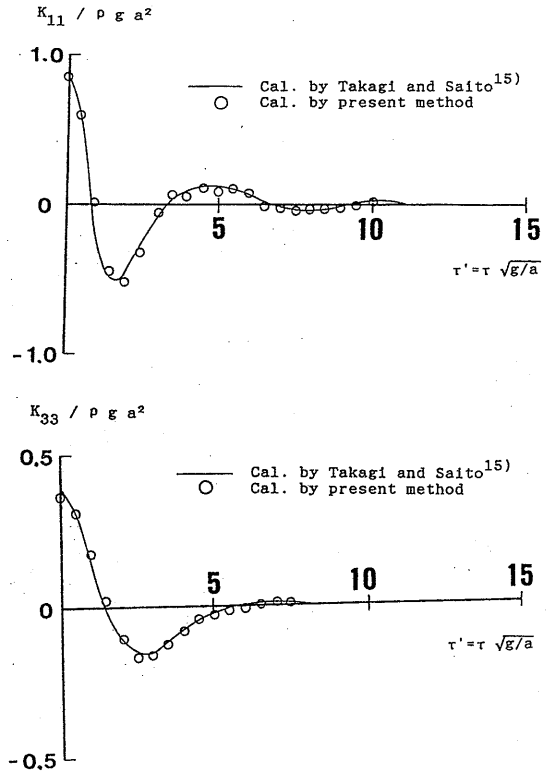

Figure 3.21 Memory effect functions of a half submerged sphere

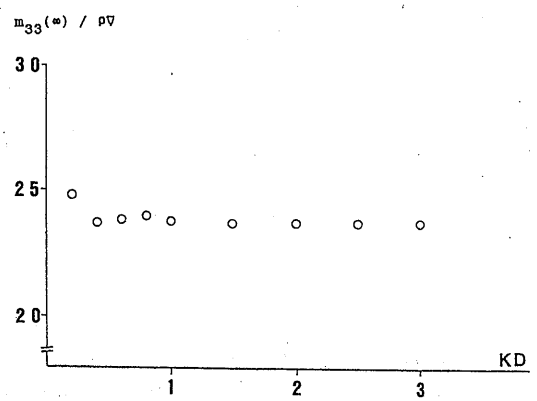

Figure 3.22 Heaving added mass at $\omega = \infty$ of a half submerged rectangular cylinder

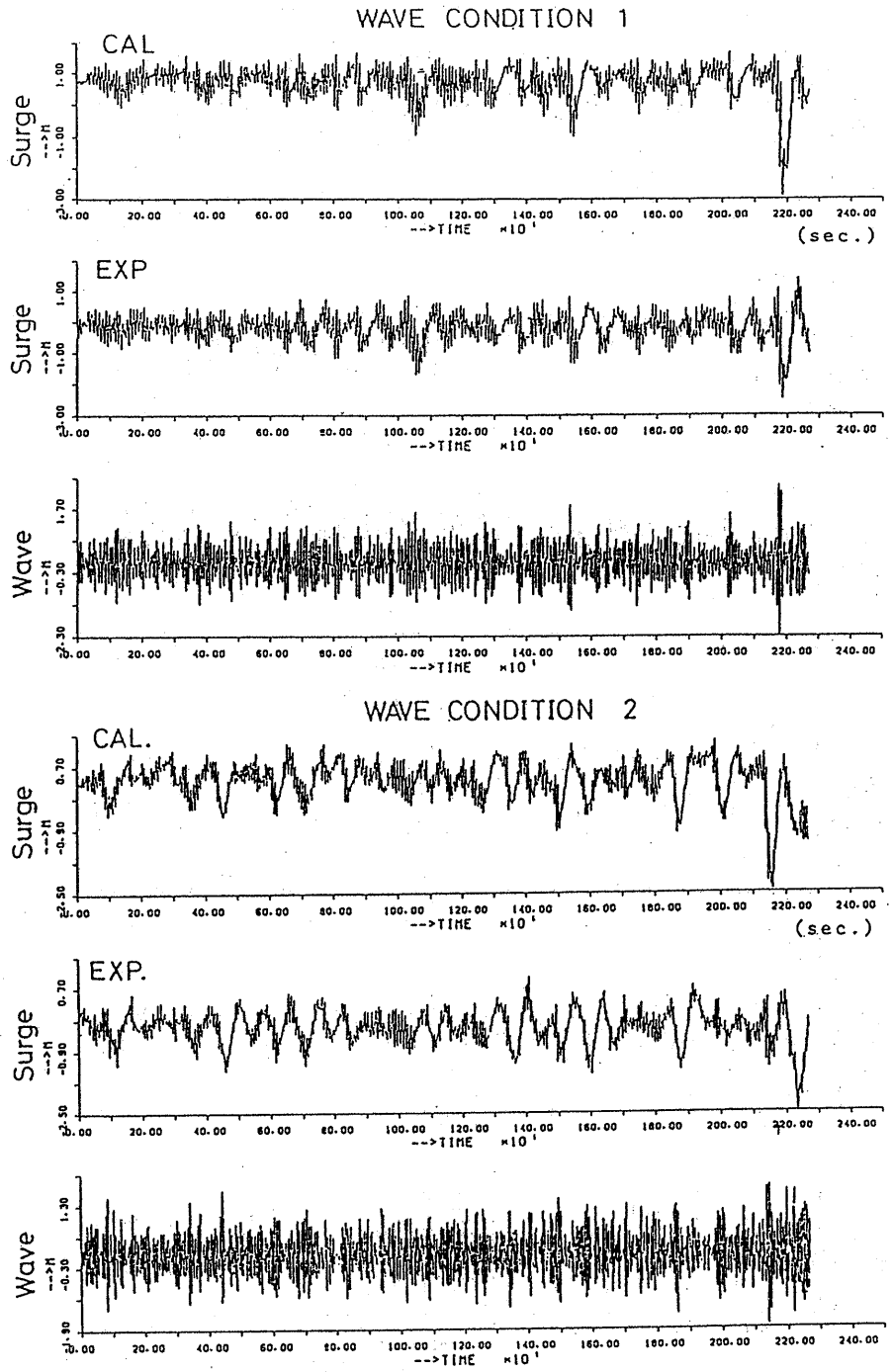

Figure 3.23 Comparisons between surge simulation results and measured ones on the floating body which is moored by linear springs (Wave conditions No1. and No2.)

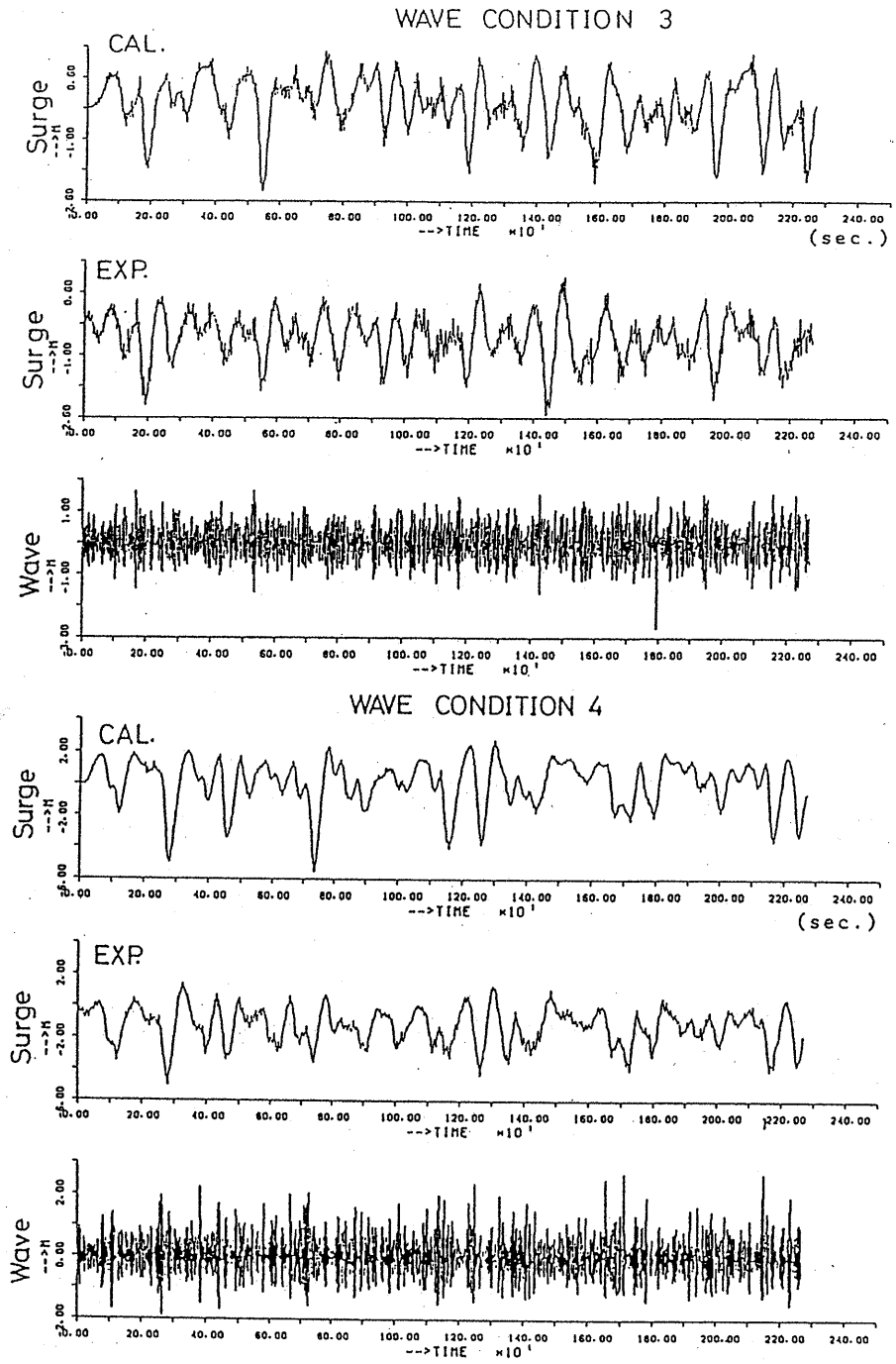

Figure 3.24 Comparisons between surge simulation results and measured ones on the floating body which is moored by linear springs (Wave conditions No3. and No4.)

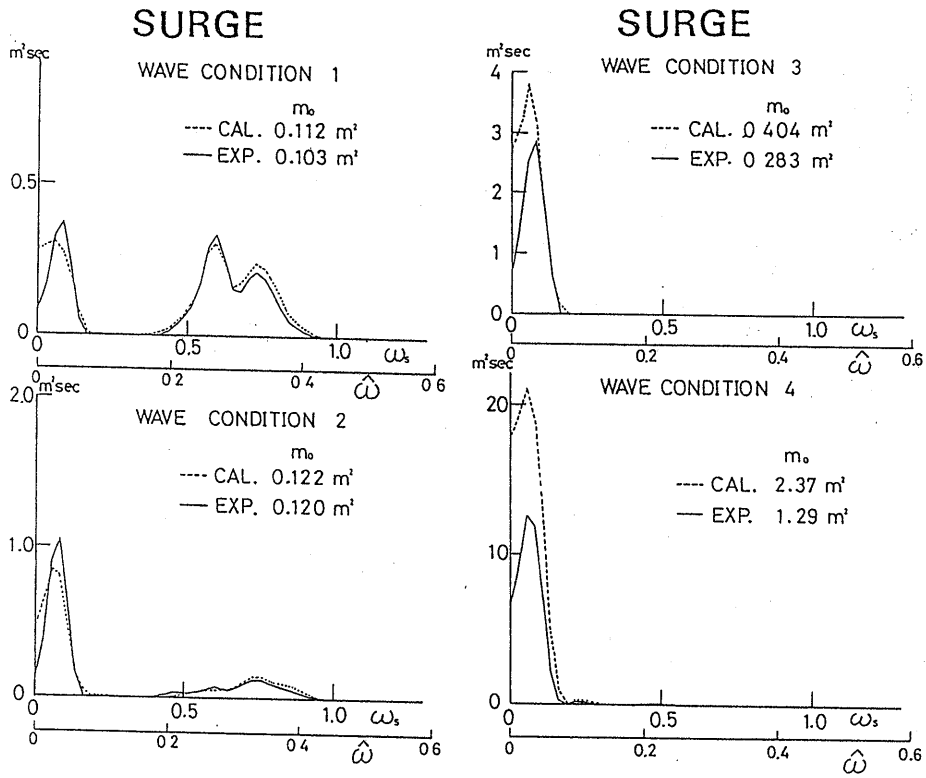

Figure 3.25 Comparisons with surge spectra of simulations and experiments

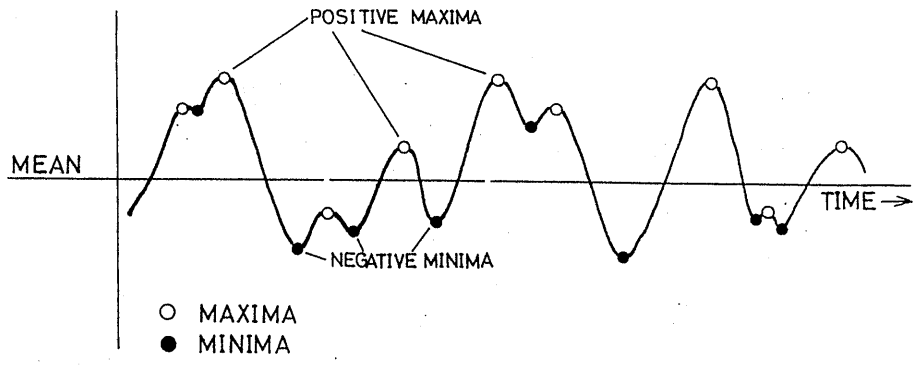

Figure 4.1 Explanatory sketch of a random process $X(t)$

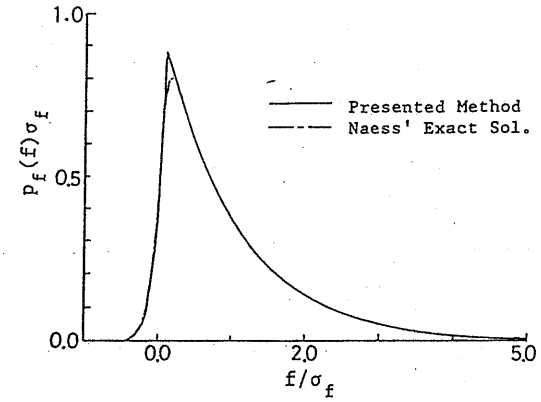

(a) Circular Structure

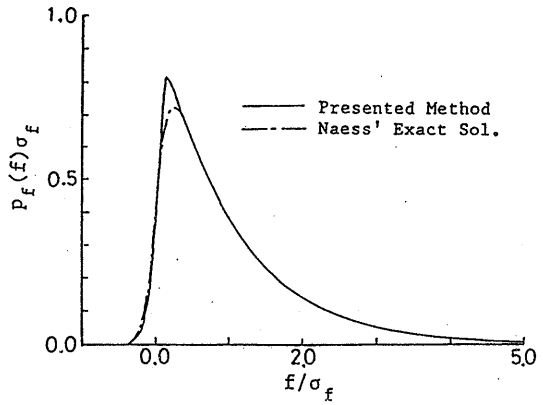

(b) Rectangular Structure

Figure 4.2 Instantaneous p.d.f. of pure second order forces

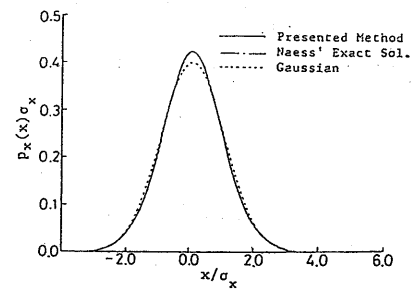

(a) P.D.F. of the Slowly Varying Sway Motion

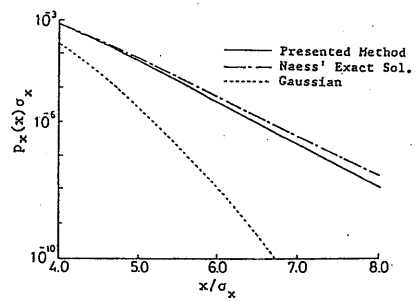

(b) P.D.F. Tail Behaviour

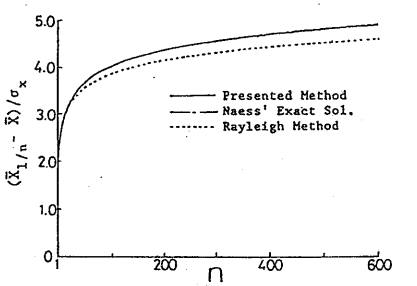

(c) 1/n th Highest Expected Amplitude

Figure 4.3 Instantaneous p.d.f. and 1/n th highest mean amplitude of pure second order responses(Case 1 - circular cylinder)

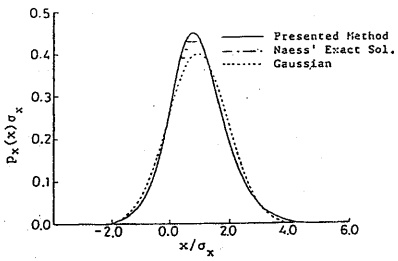

(a) P.D.F. of the Slowly Varying Sway Motion

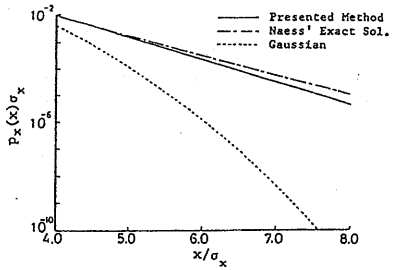

(b) P.D.F. Tail Behaviour

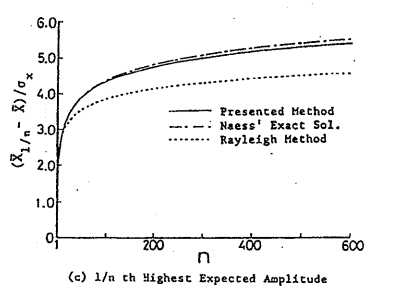

(c) 1/n th Highest Expected Amplitude

Figure 4.4 Instantaneous p.d.f. and 1/n th highest mean amplitude of pure second order responses(Case 2 - circular cylinder)

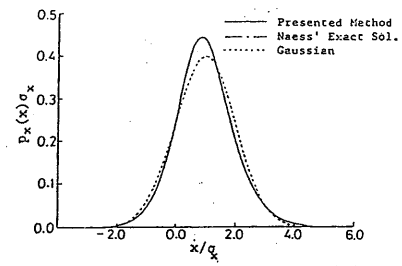

(a) P.D.F. of the Slowly Varying Sway Motion

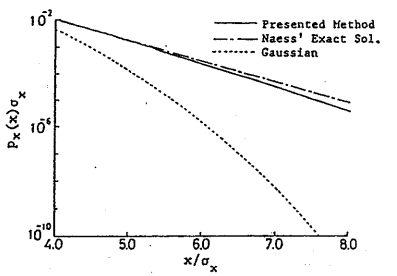

(b) P.D.F. Tail Behaviour

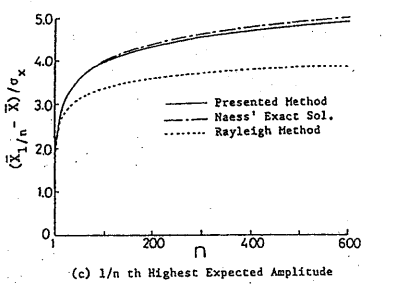

(c) 1/n th Highest Expected Amplitude

Figure 4.5 Instantaneous p.d.f. and 1/n th highest mean amplitude of pure second order responses(Case 3 - rectangular cylinder)

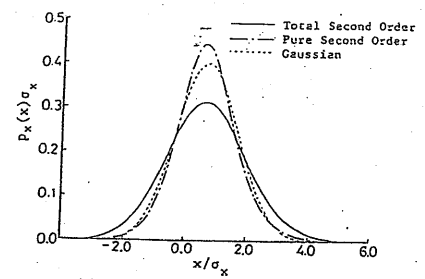

(a) P:D.F. of the Slowly Varying Sway Motion

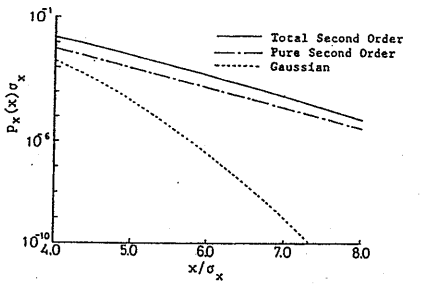

(b) P:D.F. Tail Behaviour

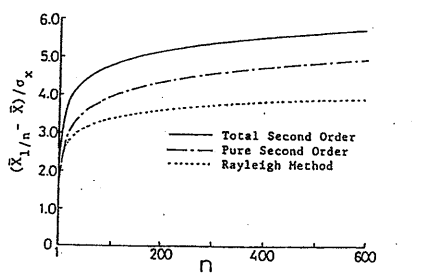

(c) 1/n th Highest Expected Amplitude

Figure 4.6 Statistical interference between first and second order responses for heavy damping($\frac{\sigma_1}{\sigma_2} = 1.36$ and $\kappa = 0.1$)

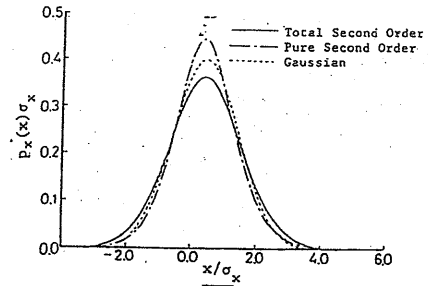

(a) P.D.F. of the Slowly Varying Sway Motion

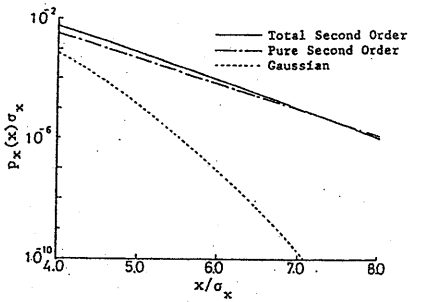

(b) P.D.F. Tail Behaviour

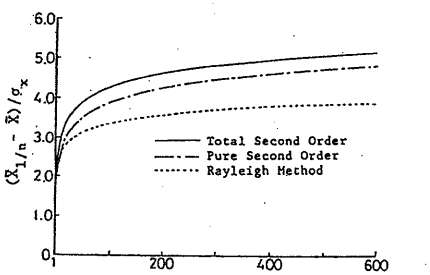

(c) 1/n th Highest Expected Amplitude

Figure 4.7 Statistical interference between first and second order responses for medium damping($\frac{\sigma_1}{\sigma_2} = 2.9$ and $\kappa = 0.006$)

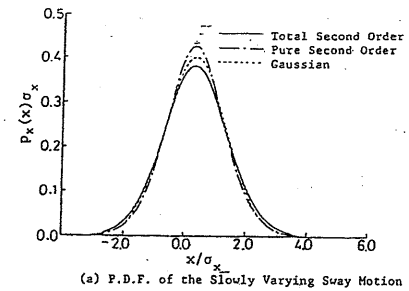

(a) P.D.F. of the Slowly Varying Sway Motion

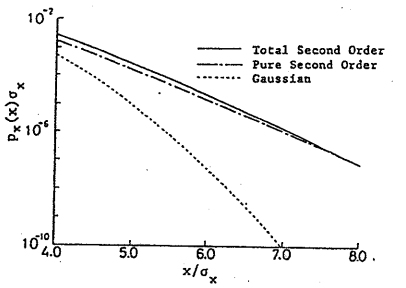

(b) P:D.F. Tail Behaviour

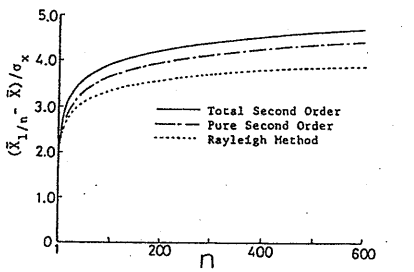

(c) 1/n th Highest Expected Amplitude

Figure 4.8 Statistical interference between first and second order responses for light damping($\frac{\sigma_1}{\sigma_2} = 4.96$ and $\kappa = 0.0001$)

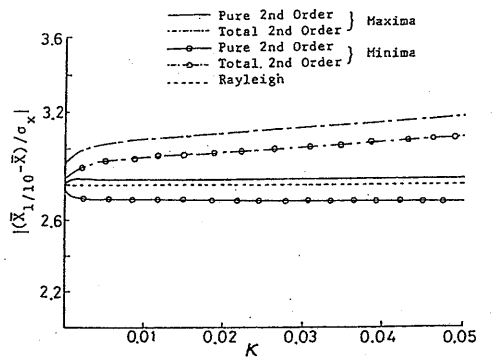

(a) 1/10th Highest Expected Amplitude VS. Damping Coefficient(ω_0=0.1 rad/sec.)

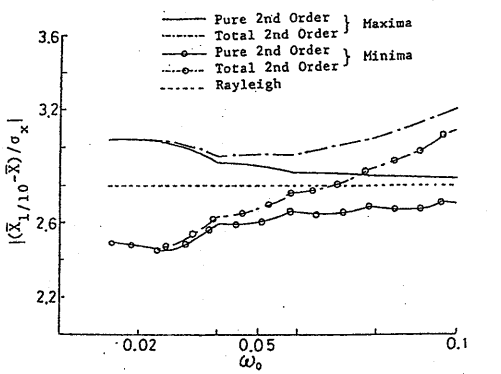

(b) 1/10th Highest Expected Amplitude VS. Natural Frequency(κ=0.06)

Figure 4.9 1/10 th highest mean amplitudes VS. damping coefficient and natural frequency

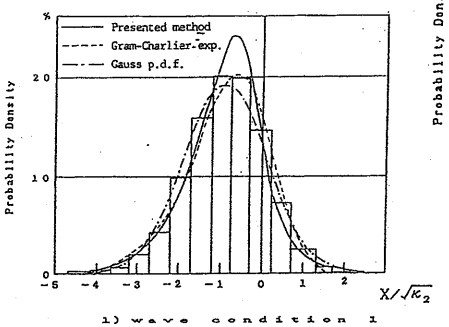

1) wave condition 1

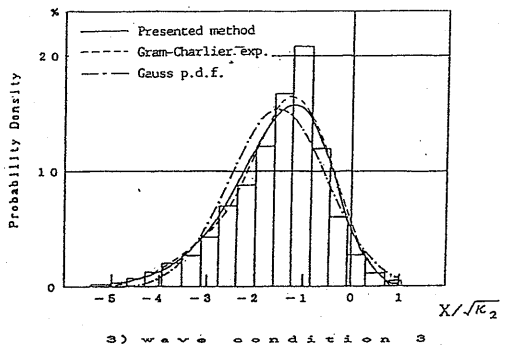

3) wave condition 3

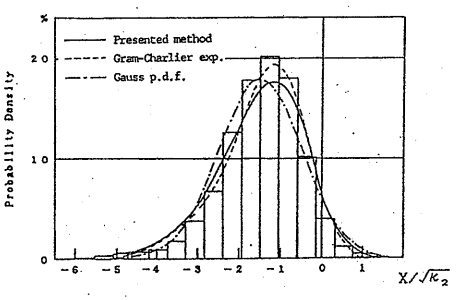

2) wave condition 2

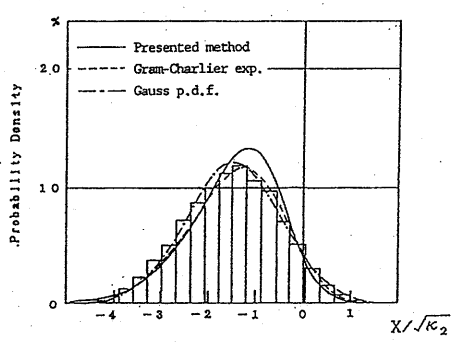

4) wave condition 4

Figure 4.10 Comparisons between observed histograms and estimated instantaneous probability density functions of surge motion (Wave conditions 1 and 2)

Figure 4.11 Comparisons between observed histograms and estimated instantaneous probability density functions of surge motion (Wave conditions 3

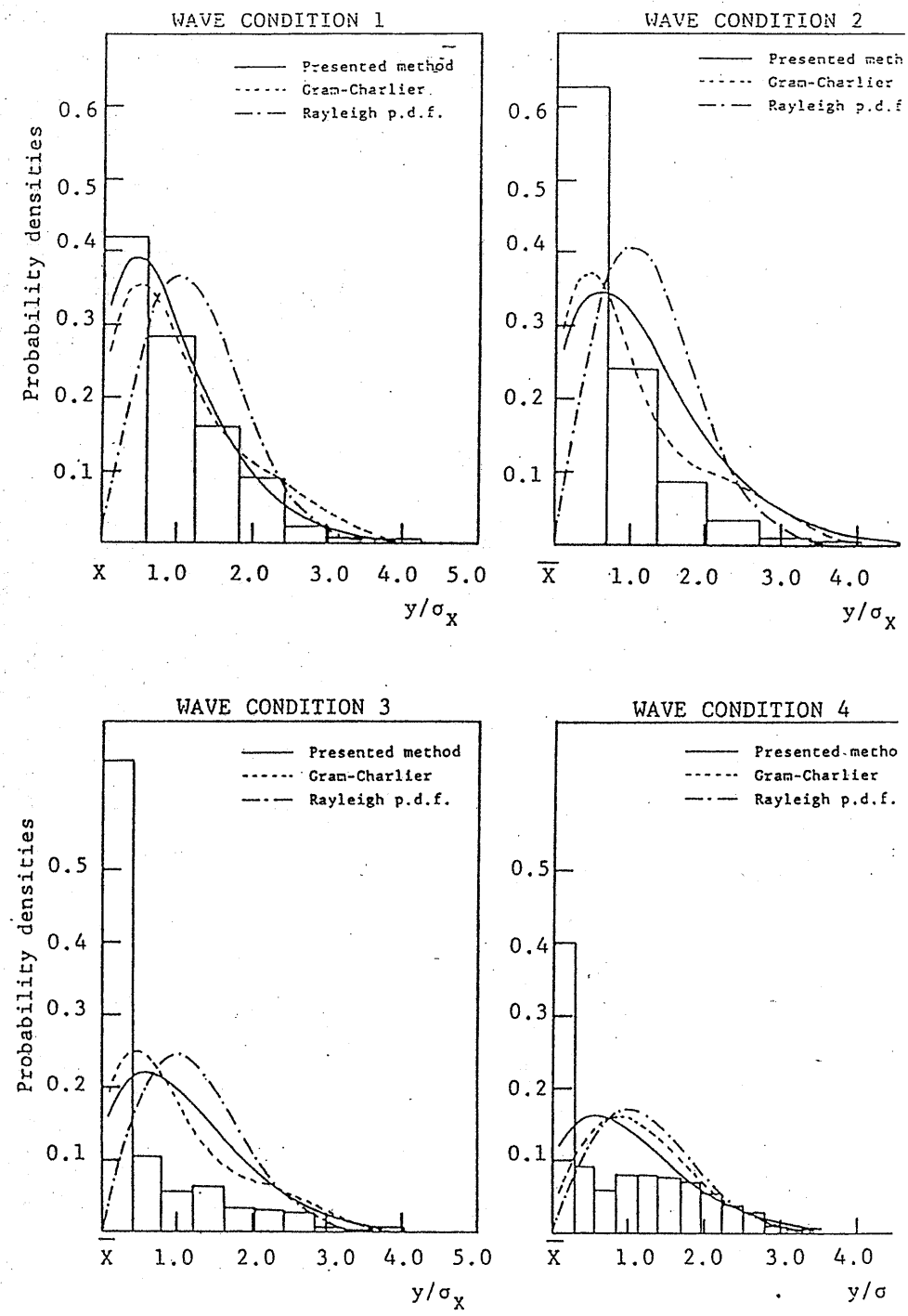

Figure 4.12 Comparisons between observed histograms and estimated maxima probability density functions of surge motion

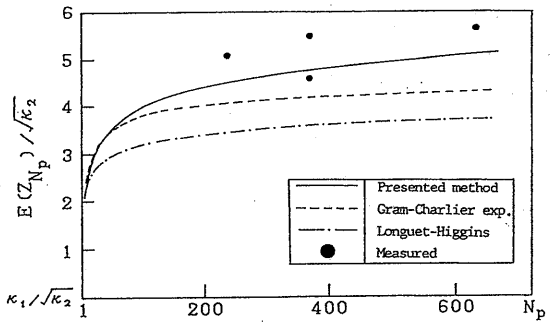

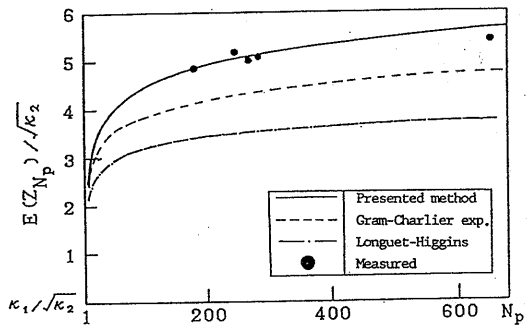

Figure 4.13 Comparisons between observed extreme responses and estimated ones (Wave conditions 1 and 2)

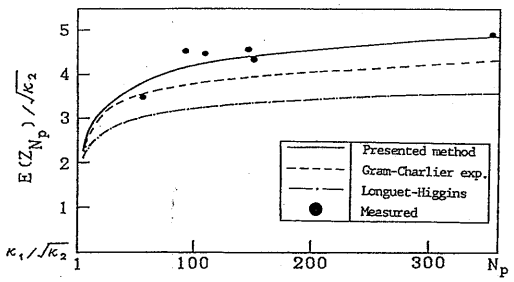

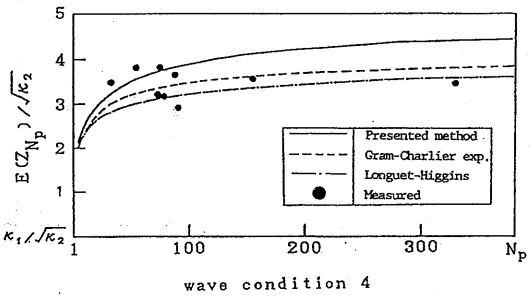

Figure 4.14 Comparisons between observed extreme responses and estimated ones (Wave conditions 3 and 4)

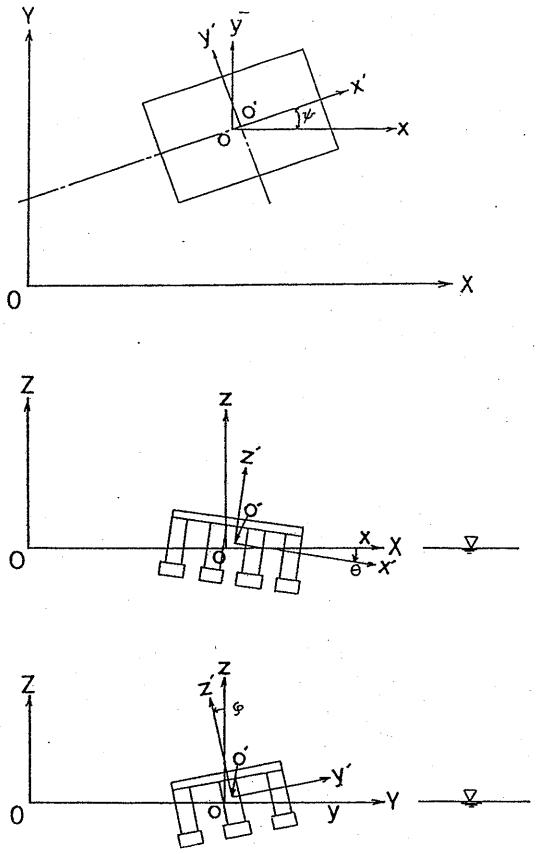

Figure A.1 System of coordinates

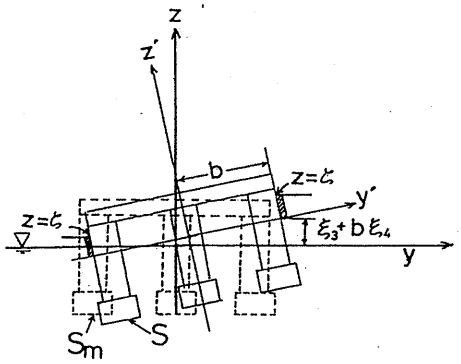

Figure A.2 Relationship between S and S_m

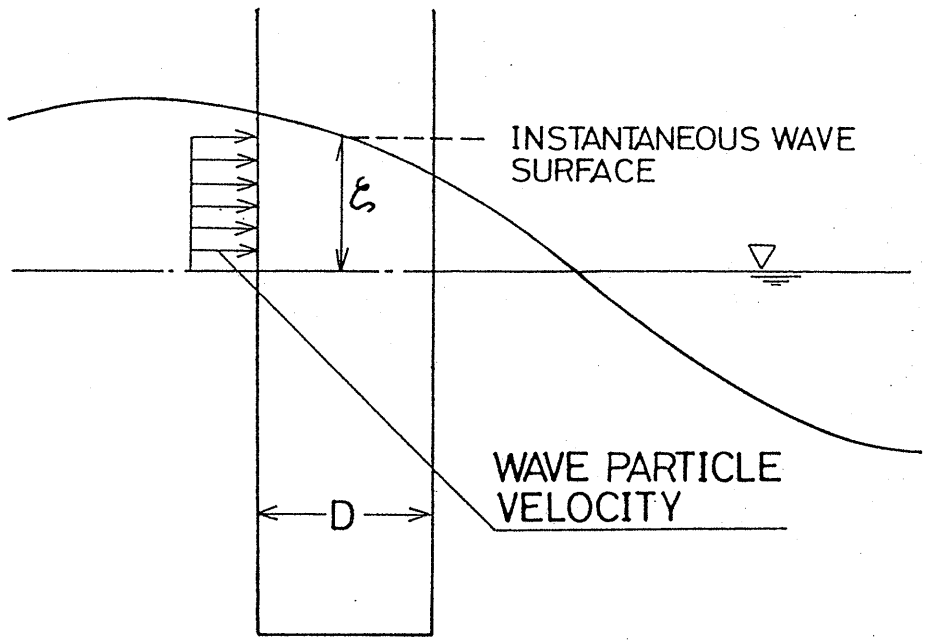

Figure C.1 Contribution to mean force from portion of wave between mean and instantaneous free surface

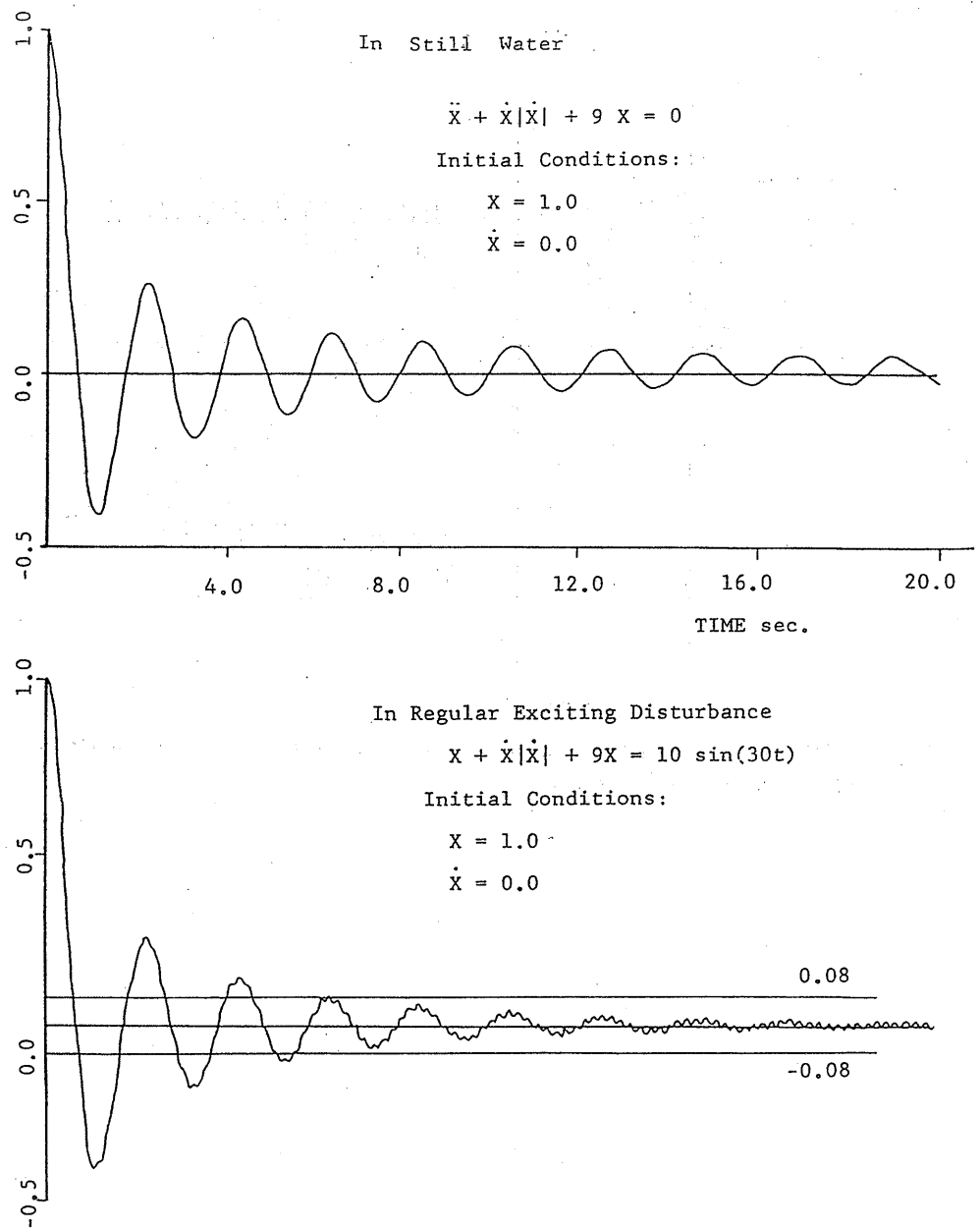

Figure D.1 Free oscillations in still water and in regular exciting disturbance

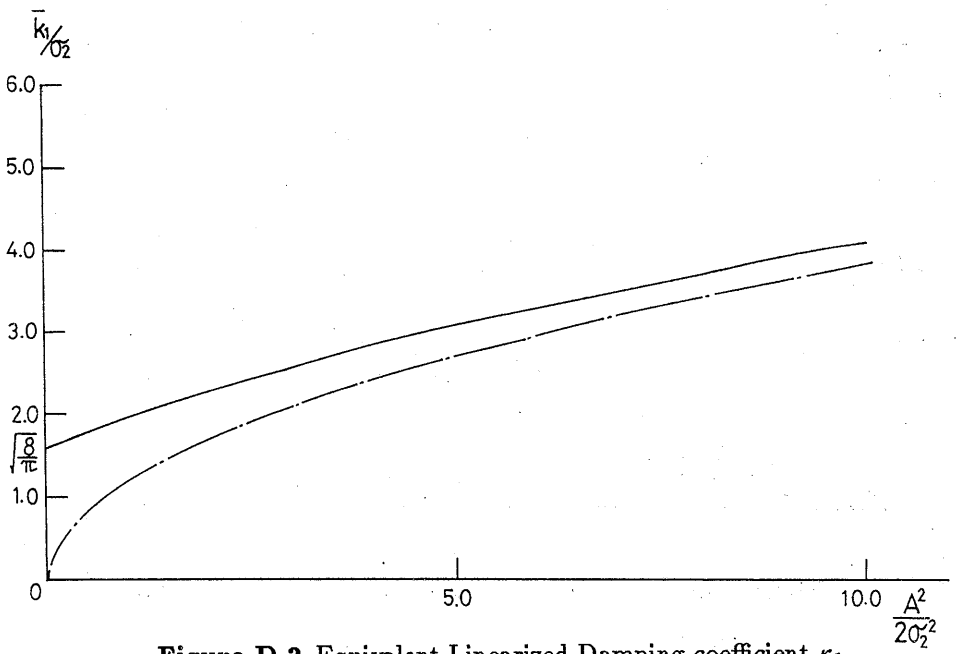

Figure D.2 Equivalent Linearized Damping coefficient κ_1

$(-\cdot-\cdot-;\frac{8}{3\pi}\sqrt{\frac{A}{\sigma_2}},\text{——};\frac{\kappa_1}{\sigma_2})$

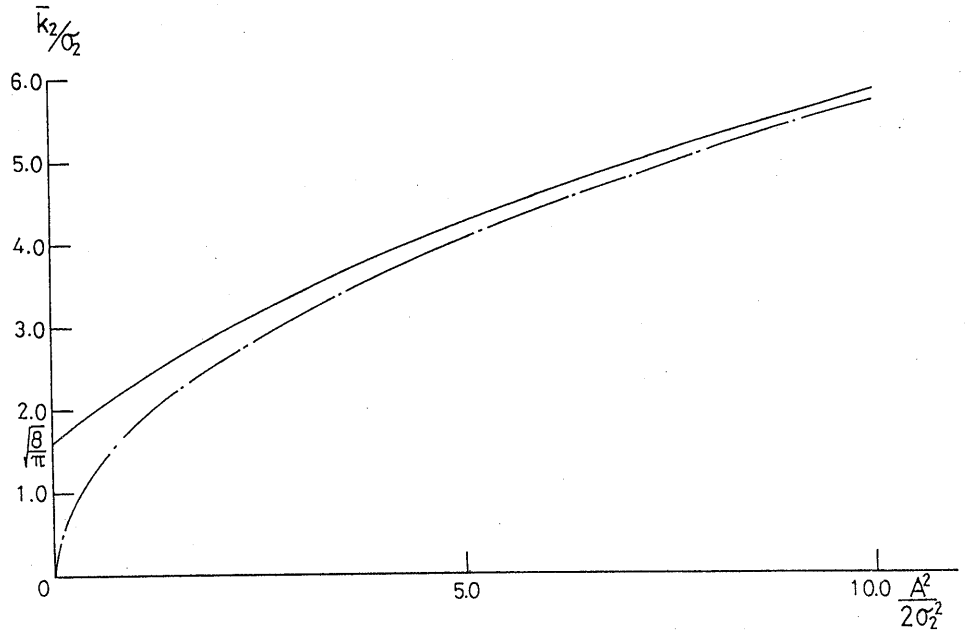

Figure D.3 Equivalent Linearized Damping coefficient κ_2

$(-\cdot-\cdot-;\frac{4}{\pi}\sqrt{\frac{A}{\sigma_2}},\text{——};\frac{\kappa_2}{\sigma_2})$

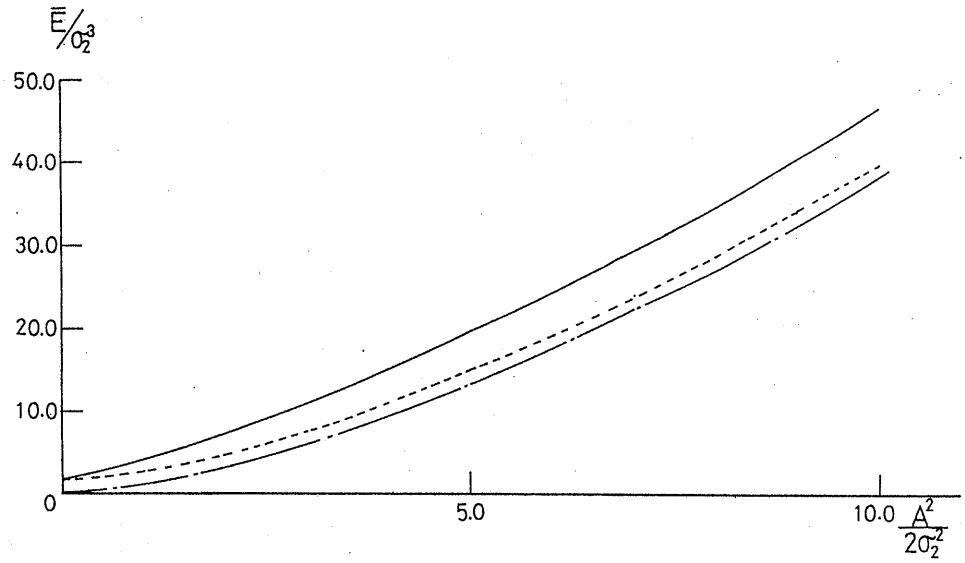

Figure D.4 Energy dissipation due to nonlinear damping $\dot{X}|\dot{X}|$ (– – –; $\frac{8}{3\pi}\frac{A}{\sigma_2}^3$, ——; $\bar{E}$)

Table 3.1 Principal dimensions

ITEMS	ACTUAL	MODEL
Length(m)	30.0	2.10
Breadth(m)	20.0	1.40
Displacement(t)	527.5 in sea water	0.168 in water
Draft(m)	5.5	0.385
KG(m)	6.8	0.33
κ_{yy}	43.7%L	44.0%L
GM_t(m)	4.8	0.269
Scale ratio	1.0	$\frac{1}{14.3}$
Mooring system	Chain catenary	Linear spring

Table 3.2 Experimental results of free damping oscillation tests

Spring Coefficient(kg/m)	1.683×2	5.09×2
Natural Period(sec.)	21.0	10.6
Virtual Mass(kg·sec^2/m)	37.6	28.97
Equivalent damping force(kgsec/m)	4.6	8.325

Table 3.3 Statistical values of irregular waves

WAVE	STATISTICAL			SPECTRAL			DURATION
COND. No.	*Variance* (m^2)	$H_{1/3}$ (m)	T_{xcr} (sec)	m_0 (m^2)	$4\sqrt{m_0}$ (m)	T_{01} (sec)	TIME (hour)
1	0.2527	1.954	7.888	0.2396	1.958	8.038	2.84
	(0.00124)	(0.1366)	(2.086)	(0.00172)	(0.1369)	(2.126)	(0.75)
2	0.2311	1.869	6.562	0.238	1.952	6.628	2.84
	(0.00113)	(0.1307)	(1.735)	(0.00116)	(0.1365)	(1.753)	(0.75)
3	0.2502	1.957	5.477	0.2568	2.027	5.606	2.84
	(0.00122)	(0.1368)	(1.448)	(0.00126)	(0.1417)	(1.482)	(0.75)
4	0.3047	2.219	5.006	0.3104	2.229	5.045	5.67
	(0.00149)	(0.1552)	(1.324)	(0.00152)	(0.1559)	(1.334)	(1.5)

( ) in Model Scale

Table 3.4 Numerical tables of the quadratic transfer function of slowly varying drift force where $\hat{\omega} = \omega\sqrt{D/g}$ and D is the diameter of a column

$$\Re\{G_2^f(\omega_i, -\omega_j)\}$$

$\hat{\omega}_i$	$\hat{\omega}_j$														
	0.2199	.2687	.3176	.3665	.4154	.4543	.5131	.5620	.6109	.6597	.7086	.7575	.8064	.8553	.9041
.2199	-.000293	-.000633	-.002154	-.00465	-.00988	-.01737	-.024	-.0246	-.0154	.00238	.02738	.049	.0464	.0211	-.0362
.2687	-.000633	-.000266	-.000565	-.001045	-.00224	-.00426	-.00636	-.00625	-.00214	.00357	.01016	.0178	.01684	.00456	-.01048
.3176	-.002154	-.000565	-.000509	-.000801	-.001504	-.00278	-.00416	-.00471	-.00441	-.00237	.0065	.01941	.01547	-.003691	-.01318
.3665	-.00465	-.001045	-.000801	-.00167	-.002967	-.004986	-.00702	-.00742	-.00578	-.00279	.00626	.021	.01995	.00399	.00101
.4154	-.00988	-.00224	-.001504	-.002967	-.00475	-.007324	-.0098	-.01046	-.00928	-.00646	.0045	.02227	.0212	.00558	.0107
.4643	-.01737	-.00426	-.00278	-.004986	-.007324	-.0105	-.01341	-.0144	-.0138	-.01102	.00184	.02086	.01793	.00356	.01918
.5131	-.024	-.00636	-.00416	-.00702	-.0098	-.01341	-.01667	-.01826	-.01878	-.0165	-.00328	.013	.00625	-.00375	.02668
.562	-.0246	-.00625	-.00471	-.00742	-.01046	-.0144	-.01826	-.02142	-.02442	-.0239	-.01319	-.00455	-.01516	-.01295	.03931
.6109	-.0154	-.00214	-.00441	-.00578	-.00928	-.0138	-.01878	-.02442	-.0305	-.03184	-.0257	-.0288	-.4171	-.01964	.05657
.6597	.00238	.00357	-.00237	-.00279	-.00646	-.01102	-.01649	-.0239	-.03184	-.03461	-.03711	-.0594	-.07921	-.0408	.0504
.7086	.02738	.01016	.0065	.00626	.0045	.00184	-.00328	-.01319	-.0257	-.03711	-.06273	-.1191	-.1559	-.111	-.0111
.7575	.049	.0178	.01941	.021	.02227	.02086	.013	-.00455	-.0288	-.0594	-.1191	-.20833	-.2479	-.1881	-.07609
.8064	.0464	.01684	.01547	.01995	.0212	.01793	.00625	-.01516	-.04171	-.07921	-.1559	-.2479	-.26064	-.181	-.08084
.8553	.0211	.00456	-.003691	.00399	.00558	.00356	-.00375	-.01295	-.01964	-.0408	-.111	-.1881	-.181	-.12043	-.0795
.9041	-.0362	-.01048	-.01318	.00101	.0107	.1918	.02668	.03931	.05657	.0504	-.0111	-.07609	-.08084	-.0795	-.1059

$$\Im\{G_2^f(\omega_i, -\omega_j)\}$$

$\hat{\omega}_i$	$\hat{\omega}_j$														
	0.2199	.2687	.3176	.3665	.4154	.4543	.5131	.5620	.6109	.6597	.7086	.7575	.8064	.8553	.9041
.2199	.0	-.01886	-.00080	-.03595	-.05041	-.05470	-.0444	-.02034	,00966	.03532	.04695	.0322	-.00137	-.04963	-.0915
.2687	.01886	.0	.00782	-.0112	-.02149	-.0274	-.0244	-.00965	.01334	.03638	.05063	.04024	.00129	-.05029	-.07833
.3176	.00080	-.00782	.00	-.00771	-.00946	-.01153	-.01430	-.01685	-.01596	-.00576	.01377	.02379	.01342	-.01031	-.04245
.3665	.03595	.0112	.00771	.00	-.00656	-.01214	-.01468	-.01261	-.00572	.00718	.02416	.02634	.00751	-.01437	-.03581
.4154	.05041	.02149	.00946	.00656	.00	-.00626	-.01014	-.01083	-.00801	.00104	.01575	.01727	.00365	-.00250	-.01466
.4643	.05470	.02740	.01153	.01214	.00626	.00	-.00497	-.00845	-.01006	-.00552	.00525	.00477	-.00229	.01013	.0075
.5131	.0444	.0244	.0143	.01468	.01014	.00497	.00	-.00523	-.01011	-.00980	-.00492	-.00964	-.01034	.01973	.02361
.562	-.02034	.00965	.01685	.01261	.01083	.00845	.00523	.00	-.00648	-.0104	-.01454	-.02629	-.02103	.02381	.03055
.6109	-.00966	-.01334	.01596	.00572	.00801	.01006	.01011	.00648	.00	-.00807	-.02354	-.04198	-.02724	.03224	.04023
.6597	-.03532	-.03638	.00576	-.00718	-.00104	.00552	.00980	.0104	.00807	.00	-.02226	-.03937	-.00892	.06155	.06197
.7086	-.04695	-.05063	-.01377	-.02416	-.01575	-.00525	.00492	.01454	.02354	.0226	.00	-.00971	.02979	.08913	.06230
.7575	-.03220	-.04024	-.02379	-.02634	-.01727	-.00477	.00964	.02629	.04198	.03937	.00971	.00	.02936	.0500	-.00436
.8064	.00137	-.00129	-.01342	-.00751	-.00365	.00229	.01031	.02103	.02724	.00892	-.02979	-.02936	.00	-.00417	-.0589
.8553	.04963	.05029	.01031	.01437	.00250	-.01013	-.01973	-.02381	-.03224	-.06155	-.08913	-.0500	.00417	.00	-.0399
.9041	.09150	.07833	.04245	.03581	.01466	-.0075	-.02361	-.03055	-.04023	-.06197	-.06230	.00436	.0589	.0399	.00

Table 3.5 Comparisons with hydrodynamic coefficients in still water and in slow drift oscillations

Wave cond.	$\widetilde{M_1 + m_{11}}/M_1 + m_{11}$	$\widetilde{N_{11}^e}/N_{11}^e$
2	1.0	1.39
3	0.89	1.67
4	0.87	1.65

Table 4.1 Principal dimensions of 2-D structures

Items	Case No.		
	No.1	No.2	No.3
Structure type	Circular	Circular	Rectangular
Beam or Diameter	20m	20m	20m
Draft (d)	10m	10m	10m
Total Mass ($M_1 + m_{11}$)	3.21×10^5 kg/m	3.21×10^5 kg/m	3.21×10^5 kg/m
Undamped natural freq. (ω_0)	0.06 rad/sec	0.06 rad/sec	0.06 rad/sec
Relative damping coef. (κ)	3.0×10^{-5}	0.1	0.1

Table 4.2 Quadratic transfer function for circular cylinder in beam sea where $\hat{\omega} = \omega\sqrt{d/g}$ and d is the draft

Numerical Calculation of $\Re\{\frac{G_2^{f*}(\omega_i,-\omega_j)}{2\rho g}\}$

$\hat{\omega}_i$	$\hat{\omega}_j$							
	1.25	1.18	1.12	1.06	0.95	0.89	0.84	0.65
1.25	0.308	0.285	0.259	0.25	0.24	0.24	0.233	0.256
1.18	0.285	0.314	0.308	0.292	0.277	0.246	0.234	0.254
1.12	0.239	0.308	0.338	0.34	0.324	0.267	0.234	0.247
1.06	0.25	0.292	0.34	0.368	0.367	0.301	0.245	0.243
0.95	0.25	0.277	0.324	0.367	0.383	0.329	0.257	0.241
0.89	0.24	0.246	0.267	0.301	0.329	0.303	0.227	0.195
0.84	0.233	0.234	0.234	0.245	0.257	0.277	0.147	0.105
0.65	0.256	0.234	0.247	0.243	0.241	0.195	0.105	0.051

Numerical Calculation of $\Im\{\frac{G_2^{f*}(\omega_i,-\omega_j)}{2\rho g}\}$

$\hat{\omega}_i$	$\hat{\omega}_j$							
	1.25	1.18	1.12	1.06	0.95	0.89	0.84	0.65
1.25	0.0	0.043	0.059	0.061	0.059	0.069	0.112	0.16
1.18	-0.043	0.0	0.030	0.038	0.032	0.028	0.066	0.112
1.12	-0.059	-0.030	0.0	0.015	0.013	0.004	0.041	0.087
1.06	-0.061	-0.038	-0.015	0.0	0.0	-0.006	0.033	0.082
0.95	-0.059	-0.032	-0.013	0.0	0.0	-0.004	0.04	0.094
0.89	-0.069	-0.028	-0.004	0.006	0.004	0.0	0.056	0.129
0.84	-0.11	-0.066	-0.041	-0.033	-0.04	-0.056	0.0	0.09
0.65	-0.16	-0.112	-0.087	-0.082	-0.094	-0.129	-0.09	0.0

Table 4.3 Quadratic transfer function for rectangular cylinder in beam sea
where $\hat{\omega} = \omega\sqrt{d/g}$ and d is the draft

Numerical Calculation of $\Re\{\frac{G_2^{f^*}(\omega_i,-\omega_j)}{2\rho g}\}$

$\hat{\omega}_i$	$\hat{\omega}_j$							
	1.25	1.18	1.12	0.89	0.84	0.79	0.76	0.69
1.25	0.363	0.317	0.272	0.270	0.286	0.302	0.330	0.406
1.18	0.317	0.336	0.305	0.260	0.269	0.264	0.261	0.321
1.12	0.272	0.305	0.315	0.245	0.255	0.248	0.228	0.258
0.89	0.270	0.260	0.245	0.326	0.339	0.313	0.236	0.172
0.84	0.286	0.269	0.355	0.339	0.384	0.380	0.300	0.208
0.79	0.302	0.264	0.248	0.313	0.380	0.405	0.337	0.234
0.76	0.330	0.261	0.228	0.236	0.300	0.337	0.280	0.175
0.69	0.406	0.321	0.258	0.172	0.208	0.234	0.175	0.059

Numerical Calculation of $\Im\{\frac{G_2^{f^*}(\omega_i,-\omega_j)}{2\rho g}\}$

$\hat{\omega}_i$	$\hat{\omega}_j$							
	1.25	1.18	1.12	0.89	0.84	0.79	0.76	0.69
1.25	0.0	0.045	0.059	0.050	0.034	0.031	0.049	0.075
1.18	-0.045	0.0	0.034	0.024	0.002	-0.021	-0.014	0.009
1.12	-0.059	-0.034	0.0	0.009	-0.017	-0.047	-0.048	-0.021
0.89	-0.050	-0.024	-0.009	0.0	-0.026	-0.086	-0.115	-0.067
0.84	-0.034	-0.001	0.017	0.026	0.0	-0.068	-0.111	-0.052
0.79	-0.031	0.021	0.047	0.086	0.068	0.0	-0.053	0.008
0.76	-0.049	0.014	0.048	0.113	0.111	0.053	0.0	0.068
0.69	-0.075	-0.009	0.021	0.067	0.052	-0.008	-0.068	0.0

Table 4.4 Linear transfer function for circular structure in beam sea where $\hat{\omega} = \omega\sqrt{d/g}$ and d is the draft

$\hat{\omega}_i$	$\Re\{\frac{G_1^I(\omega_i)}{\rho g d^2}\}$	$\Im\{\frac{G_1^I(\omega_i)}{\rho g d^2}\}$
1.25	0.0495	0.0
1.18	0.0543	0.0085
1.12	0.0570	0.0168
0.89	0.0621	0.0432
0.84	0.0631	0.0463
0.79	0.0645	0.0490
0.76	0.0662	0.0498
0.69	0.0705	0.0459

Table 4.5 Eigenvalues

Eigenvalues No.	Wave condition No. 1 (m)	2 (m)	3 (m)	4 (m)
1	-0.117	-0.2068	-0.3028	-0.3751
2	0.0455	-0.1391	-0.1749	-0.2494
3	-0.0636	-0.0810	-0.1409	-0.2273
4	0.0253	0.0796	-0.0963	-0.1251
5	-0.0319	-0.0528	0.1137	0.1379
6	0.0127	0.0373	0.0657	0.0978
7	-0.0184	-0.0323	0.0558	0.0853
8	-0.017	-0.0254	-0.0576	-0.0816
9	-0.0142	-0.0249	0.0368	0.0456
10	-0.0105	0.0218	-0.0379	0.0313
11	0.0072	0.0206	-0.0341	-0.0483
12	0.0067	0.0114	0.0214	-0.042
13	0.0061	0.009	0.014	-0.0307
14	0.0042	0.007	0.0117	-0.0279
15	-0.0075	-0.0115	-0.0218	-0.0243
16	-0.0068	-0.0104	-0.0193	0.0188
17	0.0026	0.0043	-0.0166	0.0152
18	-0.0041	-0.0063	0.0069	0.0094
19	-0.0036	-0.0059	-0.0114	-0.016
20	-0.0024	-0.0054	-0.0109	-0.0147
21	-0.0021	-0.0032	-0.0072	0.0058
22	-0.0019	-0.0027	-0.0059	-0.0102
23	0.0016	0.0021	0.0043	-0.0064
24	0.0009	0.0019	0.0028	0.0027

Table 4.6 Comparisons of statistical values between estimations and experimental results

WAVE COND. No.	Sample $\lvert E[X]\rvert$ (m)	$V[X]$ (m^2)	estimated $\lvert k_1\rvert$ (m)	k_2 (m^2)	Parameters of Gamma p.d.f. $\tilde{\theta}_1$ (m)	$\tilde{\theta}_2$ (m)	$\tilde{\nu}_1$	$\tilde{\nu}_2$
1	0.291~0.477	0.162~0.198	0.380	0.1831	0.03	0.061	8.554	9.307
2	0.409~0.57	0.173~0.275	0.746	0.2919	0.0472	0.1132	8.655	10.112
3	0.607~0.844	0.269~0.719	1.220	0.7254	0.0672	0.1627	10.012	11.276
4	1.183~1.327	1.173~1.558	1.675	1.294	0.09	0.215	10.3	11.71